



Master's thesis

Geoinformatics

ASSESSING AND MINIMIZING PEDESTRIANS' EXPOSURE TO TRAFFIC NOISE WITH  
SPATIAL ANALYSIS AND WEB GIS

Joose Helle

2019

Supervisors:

Tuuli Toivonen

Henrikki Tenkanen?

University of Helsinki

Faculty of Science

Department of Geosciences and Geography

PL 64 (Gustaf Hällströmin katu 2)

00014 University of Helsinki



Tiedekunta/Osasto Fakultet/Sektion – Faculty	Laitos/Institution– Department	
Faculty of science	Department of Geosciences and Geography	
Tekijä/Författare – Author		
Joose Helle		
Työn nimi / Arbetets titel – Title		
<del>Assessing pedestrians' exposure to traffic noise with spatial analysis: the effects of home location and route choice</del>		
Assessing and minimizing pedestrians' exposure to traffic noise with spatial analysis and Web GIS		
Oppainaine /Läroämne – Subject		
Geography, geoinformatics		
Työn laji/Arbetets art – Level	Aika/Datum – Month and year	Sivumäärä/ Sidoantal – Number of pages
Master's thesis	August 2019	
Tiivistelmä/Referat – Abstract		
Avainsanat – Nyckelord – Keywords		
Säilytyspaikka – Förvaringsställe – Where deposited		
HELDА		
Muita tietoja – Övriga uppgifter – Additional information		



Tiedekunta/Osasto Fakultet/Sektion – Faculty  Matemaattis-luonnontieteellinen tiedekunta	Laitos/Institution– Department  Geotieteiden ja maantieteen laitos	
Tekijä/Författare – Author  Joose Helle		
Työn nimi / Arbetets titel – Title		
Oppaine /Läroämne – Subject  Maantiede, geoinformatiikka		
Työn laji/Arbetets art – Level  Pro gradu -tutkielma	Aika/Datum – Month and year  Elokuu 2019	Sivumäärä/ Sidoantal – Number of pages
Tiliviselmä/Referat – Abstract		
Avainsanat – Nyckelord – Keywords		
Säilytyspaikka – Förvaringställe – Where deposited  HELDA		
Muuta tietoja – Övriga uppgifter – Additional information		

## TABLE OF CONTENTS

1 Introduction .....	1
2 Background .....	3
2.1 Noise definition and measurement.....	3
2.2 Traffic noise and health.....	4
2.3 Traffic noise modeling .....	5
2.4 Concepts and approaches in assessing dynamic exposure.....	6
2.5 Graph-based least cost path analysis.....	8
2.6 Exposure-based impedances in routing.....	10
2.7 Web GIS concepts and developments.....	12
3 Material & Methods .....	15
3.1 Overview of the methods .....	15
3.2 Study area.....	15
3.3 Materials.....	16
3.3.1 Modelled traffic noise data .....	17
3.3.2 OpenStreetMap data.....	21
3.3.3 Register based origin-destination (OD) commuting data .....	22
3.3.4 Routing service of the local public transport authority.....	23
3.4 Technical framework and architecture.....	23
3.5 Quiet path routing method .....	25
3.5.1 Environmental impedance function .....	25
3.5.2 Network acquisition and manipulation .....	27
3.5.3 Quiet path routing application .....	30
3.5.4 Noise exposure assessment of short and quiet paths .....	33
3.6 Web-based quiet path route planner.....	35
3.7 Assessment of pedestrians' exposure to traffic noise at a neighborhood level.....	37
3.7.1 Overview of the analysis.....	37
3.7.2 Estimation of local walks by commutes .....	39

3.7.3 Least cost path calculations: short and quiet paths .....	43
3.7.4 Assessment of exposures to traffic noise on the paths.....	44
3.7.5 Assessment of achievable reductions in exposure to traffic noise.....	45
<b>4 Results .....</b>	<b>47</b>
4.1 Pedestrians' exposure to traffic noise .....	47
4.2 Spatial patterns in pedestrians' exposures to traffic noise .....	48
4.3 Quiet path routing API.....	52
4.4 Quiet path route planner.....	52
4.5 Achievable reductions in exposure to traffic noise.....	54
4.6 Sharing of the methods and results .....	59
<b>5 Discussion .....</b>	<b>60</b>
5.1 Technical assessment – quality of the shortest paths.....	60
5.2 Indirect large-scale assessment of pedestrians' exposures to traffic noise can reveal unequal walking conditions .....	63
5.3 Significant but varying reductions in traffic noise exposure can be achieved with quiet path routing .....	65
5.4 Alternative quiet paths need to be calculated to suit different situations and users with varying preferences .....	66
5.5 Uncertainties in exposure-response relationships challenge the environmental impedance function .....	67
5.6 Exposure-based routing should be developed as a concept to consider multiple pollutants ...	68
5.7 Publishing a green path routing application online can facilitate citizens to choose healthier paths .....	69
<b>6 References .....</b>	<b>71</b>
<b>ACKNOWLEDGEMENTS .....</b>	<b>76</b>
<b>APPENDICES .....</b>	<b>76</b>

## LIST OF FIGURES

Figure 1. Equal loudness contours by ISO 226 ( <i>Acoustics – normal equal-loudness contours. International Standard ISO 226</i> , n.d.) .....	3
Figure 2. Composed scatterplot between $L_{den}$ and percentage of highly annoyed (HA%) for several studies on road traffic noise and annoyance (by (Guski et al., 2017)).....	5
Figure 3. Exposure to traffic noise on a path as distances (left) and durations (right) of different traffic noise levels.....	7
Figure 4. Example of steps in Dijkstra's algorithm by (Jasika et al., 2012).....	9
Figure 5. "Interacting web services feeding into apps within application workflows." by (Veenendaal et al., 2017).....	13
Figure 6. "Focus and trends in increasing web mapping functionality" by (Veenendaal et al., 2017). .....	14
Figure 7. Illustration of the internal methodological dependencies of the study.....	15
Figure 8. Map of the study area; extent of the city of Helsinki excluding the southern islands.....	16
Figure 9. Modelled daytime traffic noise levels (dB) in Helsinki. ....	19
Figure 10. Modelled daytime traffic noise levels (dB) in Viikki.....	20
Figure 11. Modelled daytime traffic noise levels (dB) in more central location in Helsinki. ....	21
Figure 12. Technical framework of the study: internal (blue) and external (grey) technical dependencies (* = Python library). The numerous external dependencies of the used Python libraries are not included in the graph.....	24
Figure 13. Noise cost coefficients for dB range 45–75 dB calculated with both equations (3 & 4) presented in this chapter.....	27
Figure 14. Workflow of network (graph) acquisition and construction. ....	28
Figure 15. Workflow of extracting exposures to traffic noise (contaminated distances) to the edges of the graph.....	29
Figure 16. Workflow of calculating and adding noise sensitivity specific edge costs as new edge attributes.....	31
Figure 17. The sequence of high-level actions included in solving one short and quiet path routing problem. ....	33
Figure 18. Technical architecture of the quiet path route planner web application.....	36
Figure 19. Workflow of the analysis for identifying origin – PT stop (or commuting destination) walks and estimating of their utilization rates based on commuter flows. ....	38

Figure 20. Workflow of the analysis for 1) calculating short and quiet paths by ODs of the local walks, 2) assessing exposures to traffic noise on the paths and 3) assessing achievable reductions in traffic noise exposure by taking quiet paths. ....	39
Figure 21. An example of local walks (and utilization ratios) from one origin as a result of the routing analysis. Most of the destinations of the walks are public transport stops. ....	41
Figure 22. Inclusion (%) of commutes per origin in the analysis for finding local PT stops and walks. ....	42
Figure 23. Number of commutes vs. commutes included in the routing analysis (%) per origin. ....	43
Figure 24. All shortest paths visualized with feature blending method: overlapping paths show darker on the map.....	44
Figure 25. The average walking distance from homes to public transport (PT) stops. The averages are weighted with the estimated utilization rates of the walks based on the total flow of commutes utilizing each PT stop.....	50
Figure 26. The mean dB on walks from homes to PT stops. The averages are weighted with the estimated utilization rates of the walks based on the total flow of commutes utilizing each PT stop.	50
Figure 27. The average walking distance in +65 dB traffic noise level on walks from homes to public transport (PT) stops. The averages are weighted with the estimated utilization rates of the walks based on the total flow of commutes utilizing each PT stop.....	51
Figure 28. The average walking distance in +70 dB traffic noise level on walks from homes to public transport (PT) stops. The averages are weighted with the estimated utilization rates of the walks based on the total flow of commutes utilizing each PT stop.....	52
Figure 29. Regression analysis between the reductions in exposures to traffic noise on quiet paths and the traffic noise indexes of the respective shortest paths. Shortest paths within the length range of 300 m to 600 m were selected in the analysis (as well as the respective quiet paths). The red lines represent the regression lines of the regression analysis and the green lines show the theoretical maximum reductions in the noise exposure indexes.....	56
Figure 30. Regression analysis between the reductions in exposures to traffic noise on quiet paths and the traffic noise indexes of the respective shortest paths. Shortest paths within the length range of 700 m to 1300 m were selected in the analysis (as well as the respective quiet paths). The red lines represent the regression lines of the regression analysis and the green lines show the theoretical maximum reductions in the noise exposure indexes.....	57

Figure 31. A typical user story demonstrating the basic functionality of the quiet path route planner. (Blue / green = user's actions; grey = actions of the user interface; white = components of the quiet path routing service).....	53
Figure 32. Landing page of the quiet path route planner. ....	53
Figure 33. Display of path options and exposures to noise along the alternative paths. ....	54
Figure 34. Display of path alternatives. ....	54
Figure 35. Display of the route planner in a situation where no alternative quiet paths were found. ....	54
Figure 36. Path length differences (m) to reference path lengths as a function of path length. ....	63
Figure 37. Differences in lengths of the paths (%) to the reference paths as a function of path length. ....	63

## LIST OF TABLES

Table 1. Materials that were used in the study.....	16
Table 2. Query strings for street network data downloads using OSM Overpass API via OSMnx python library.....	22
Table 2. Noise cost coefficients for dB range 45–75 dB calculated with both equations presented in this chapter (3 & 4). .....	27
Table 4. Indexes describing exposure to traffic noise on a path and reduction in exposure to traffic noise on a quiet path.....	35
Table 5. Parameters used in routing with Digitransit routing API.....	40
Table 6. Descriptive statistics of the length of the shortest paths to PT stops and workplaces (n=31291).....	43
Table 7. Descriptive statistics of exposure to traffic noise on the first walks of public transport itineraries to workplaces and on direct walks to nearby workplaces (n=31291). ....	47
Table 8. Descriptive statistics of exposure to traffic noise on the first walks of public transport itineraries to workplaces (direct walks to nearby workplaces are filtered out, n=18716). ....	48
Table 9. Descriptive statistics of the achievable reductions in noise exposure index $ER_{+65dB}$ on different subsets of the paths. The subsets were defined by 1) the length of the shortest path, 2) the length difference of the quiet path and 3) the initial $ER_{+65dB}$ .....	58
Table 10. Descriptive statistics of the achievable reductions in noise exposure index $dB_{mean}$ on different subsets of the paths. The subsets were defined by 1) the length of the shortest path, 2) the length difference of the quiet path and 3) the initial $dB_{mean}$ .....	59

Table 11. Differences in path lengths between the calculated shortest paths and the reference paths (n=31228).....	61
Table 12. Statistics of offsets (distances) between the origin and destination points of the paths and the origin and destination points of the reference paths.....	62

# 1 Introduction

Active transport modes are getting increasing attention among policy makers and urban planners. The term active transport usually refers to walking and cycling but also other active transport modes such as E-scooters and even city rowboats are emerging in urban context. Undoubtedly, walking remains the most popular mode of active transport since it doesn't require any accessories and is essential part of all itineraries made by public transport.

It has been shown that active transport modes provide health benefits to their users (Pucher & Buehler, 2010) and also to others since they can help to reduce congestion. Hence, cities often have a strong willingness to facilitate and promote active transport modes for urban mobility. In encouraging people to e.g. walking, it is essential for the cities to provide sufficient infrastructure and comfortable environments to make walking pleasant and practical.

Multiple factors affect the ease with which active transport is applicable in different urban environments. While infrastructure for cycling is predominantly defined by the more or less exclusive network of cycleways and bike lanes, the one for walking (footpaths, sidewalks etc.), in the other hand, is denser and more evenly distributed. However, not only the physical properties of the walking network define its applicability and desirability (walkability), but also multiple more or less subjective factors need to be considered (Maghelal & Capp, 2011). These include variables such as safety, building design, openness of spaces, proximity to opportunities, air quality and green spaces.

Many of the factors limiting walkability and other active transport modes are often caused by (or at least related to) other, “non-human”, users of the urban space. Evidently, one of the most significant of these is vehicular traffic and the infrastructures supporting it. Vehicular traffic affects walkability and bikeability by introducing large and typically unpleasant structures to urban spaces. From the active transport point of view, these structures act as barriers fragmenting the active transportation networks and thus reduce the opportunities for walking and cycling.

Furthermore, vehicular traffic consumes the opportunities for active transport with at least two “invisible” ways. Firstly, since most of the traffic is powered by gasoline engines, it has a strong negative impact on air quality due to the exhaust gases. According to numerous studies, these urban air pollutions can cause or worsen many lung diseases such as asthma or even cancer. Secondly, both the engines and the wheels of the vehicles cause noise. According to several studies, pedestrians' exposure to traffic noise has implications on their health, namely stress levels and problems related to blood circulation (Babisch et al., 2005; Ising et al., 1980; Passchier-Vermeer W & Passchier W F,

2000). The list of potential negative health effects is even longer but missing strong enough scientific evidence. Since many of the potential health effects are not instant but accumulative over the years, assessing children's health effects from exposure to noise is particularly important. Due to increasing traffic flows and numbers of daily commuters, the negative effects of traffic noise on public health are likely to get amplified in the fast urbanizing world (Passchier-Vermeer W & Passchier W F, 2000).

In this study, the broad and comprehensive definition of walkability is not trying to be addressed per se. Instead, from the perspective of walkability research, this study can be seen as an attempt to capture one narrow but important component of walkability; exposures to traffic noises have the potential to offer relevant spatial information of routes and areas of low walkability.

It is anticipated, yet not explicitly verified in the study, that traffic noise levels are spatially correlated with also other negative impacts of traffic such as air pollution and presence of large unwalkable (and unpleasant) infrastructures. With respect to this assumption, the methods developed in the study are suitable for identifying areas where improvements to walking conditions are most needed.

Given this context, the aims of the study were defined as follows:

- 1) Develop a routing method that can optimize quiet paths by estimating and minimizing exposure to traffic noise pollution.
- 2) Discover spatial patterns and possible inequalities in pedestrians' exposure to traffic noise.
- 3) Assess pedestrians' opportunities to reduce exposure to traffic noise by choosing quiet paths.
- 4) Create a mobile-friendly web-based route planner application on the quiet path routing method.

By these aims, the study intends to facilitate both 1) city planners to discover areas of problematic walking conditions (with respect to traffic noise) and 2) citizens to choose healthier (quieter) walking routes for their daily walks (via the "quiet route planner" web application). The first can be seen as a long-term and the latter as a short-term solution to mitigating the negative effects of exposure to traffic noise on pedestrians' health.

## 2 Background

### 2.1 Noise definition and measurement

Noise, in general, can be defined simply as unpleasant sound. Other defining words unwanted, loud and disruptive reflect the subjective nature of the term. The lack of explicit definition of noise derives from noise being indistinguishable from sound in physics; both are fundamentally just vibrations in the air (or other transmission medium). Yet, the concept of noise is central in assessing health effects from exposure to high or unpleasant sounds.

A common measure of noise has been sound pressure level (SPL) measured in decibels. The decibel (dB) is a logarithmic unit that works well for measuring sound level and difference in sound level. However, since human ear is unequally sensitive to different frequencies, SPL does not reflect perceived loudness well as such. Thus, so-called A-weighting is often used to balance out these unequal (perceived) responses to different frequencies. A-weighting method utilizes standardized equal loudness contours, where loudness-SPA (phon-dB) relationships are modelled for a range of frequencies starting at different SPAs (Figure 1).

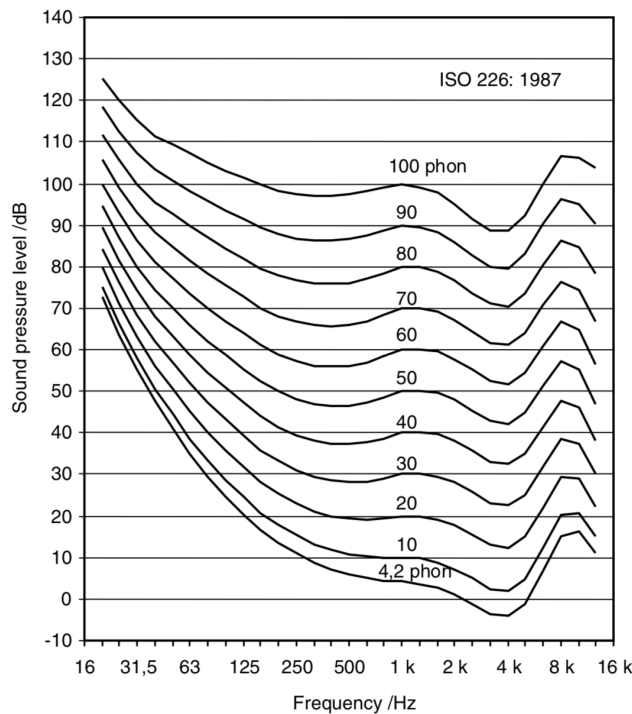


Figure 1. Equal loudness contours by ISO 226 (*Acoustics – normal equal-loudness contours. International Standard ISO 226*, n.d.).

## 2.2 Traffic noise and health

In urban areas, vehicular traffic is usually one of the major sources of noise. Level of noise is affected by the flow and speed of the traffic and the type of the road surface. Increased but also varying traffic noise levels are typical to highways and other major roads.

A variety of metrics have been developed to measure level of traffic noise. They aim to consider the perceived loudness of the noise in time, which can be challenging for the type of noises that change considerably over short periods of time. Also, different vehicles and road surfaces cause noise of different frequencies which affect the perceived loudness due to human ears varying sensitivity to different frequencies. A widely used approach to measure and compare traffic noise levels is to use the A-weighted sound pressure level averaged to certain hours of a day. According to Torija & Flindell (2015), A-weighting may be particularly suitable for modeling the loudness of traffic noise, due to the appropriate weighting of the low-frequency sounds.

The environmental noise guidelines by (WHO Europe, 2018) as well as the research on traffic noise commonly utilize metrics based on “equivalent continuous sound pressure levels” averaged to different times of the day (e.g.  $L_{day}$ ,  $L_{evening}$  and  $L_{night}$ ). One of the standard metrics of community noise considers day, evening and night-time noise levels together ( $L_{den}$ ) and features additional weightings for evening and night-time noise levels (WHO Europe, 2018). These metrics are heavily compressed, and thus lose information about fluctuations in SPA in time. Nevertheless, standardized metrics are needed in order to efficiently compare different noise environments in space and time.

Several studies have aimed to evaluate the relationship between noise level and annoyance by statistical means. A common way to attempt this has been to study the percentages of the highly annoyed people (HA%) living in certain noise environments by  $L_{den}$  or  $L_{Aeq}$ . An important notice on these assessments is that they use a static approach where exposures to noise are considered only at home locations. (Guski et al., 2017) reviewed many of the studies and plotted the reviewed HA% values against  $L_{den}$  (Figure 2). Both somewhat linear and non-linear relationships can be seen in the scatterplot, indicating an unclear and case-specific statistical relationship between noise exposures and annoyance.

According to several literature reviews on traffic noise and annoyance (e.g. Brown & Van Kamp, 2017; Guski et al., 2017) and a report based on those reviews by WHO Europe (WHO Europe, 2018), longer exposure to noise levels above 53 dB can cause negative health effects and should therefore be avoided. Accurate assessment of different health effects (from traffic noise) is challenging due to

different temporal realizations of the effects and overlapping exposure-response -relationships of multiple pollutants. Moreover, the net health effect and perception of noise is likely affected by various “nonacoustic factors” such as gender, age, education and subjective noise sensitivity (WHO Europe, 2018: 14).

It is likely that many of the effects from exposure to pollutants are developed over years or decades of cumulative exposure while some are perceived from the exposure in the present time. Accordingly, the potential longer-term effects from exposure to traffic noise include e.g. respiratory infections, cardiovascular disease and stress (Recio et al., 2016; Van Kempen et al., 2018) whereas the short-term effects can be e.g. annoyance or stress.

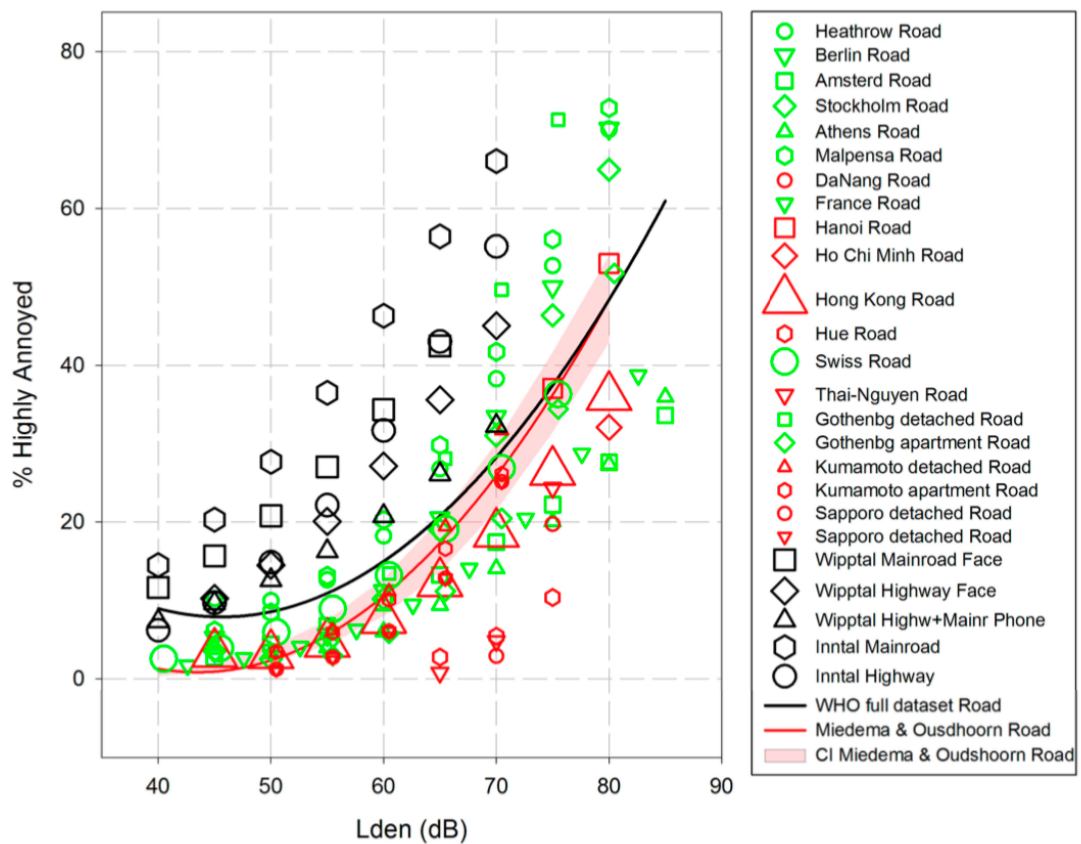


Figure 2. Composed scatterplot between L<sub>den</sub> and percentage of highly annoyed (HA%) for several studies on road traffic noise and annoyance (by (Guski et al., 2017)).

### 2.3 Traffic noise modeling

While air pollution is often challenging to quantify, measure and model (and tends to be rather dynamic with respect to weather conditions), then traffic noise can be measured and modelled in a

more straightforward manner. Vehicular traffic noise levels have been spatially modelled in many cities with fairly high spatial resolution - not only due to technical possibilities and national legislation, but also as required by the EU (*Directive 2002/49/EC*, 2002).

Advanced software is nowadays available to perform the noise ever more complex modelling. The noise models are usually standardized by either national or international policies. In the Nordics, a commonly used noise model is Nord2000 (Jonasson & Storeheier, 2001). Also, the EU has recently established a technical noise modeling framework “Common noise assessment methods in Europe” (CNOSSOS-EU) (Kephalaopoulos et al., 2012) that is being employed at EU-wide policies and assessments.

Many environmental features can be considered in the noise models for calculating the noise surfaces. Typically, two kinds of input data are needed to run the models: 1) spatial data of the noise sources and 2) spatial data on features that affect the pathways and absorption of noise. Noise sources can be e.g. measured or modelled traffic flow data whereas the latter category can include e.g. 3D surface model of the landscape, buildings, noise barriers and even weather conditions.

## **2.4 Concepts and approaches in assessing dynamic exposure**

In this chapter, literature on assessing dynamic exposure to both air pollution and noise are reviewed, as only few studies have focused solely on exposure to noise. Also, the concept and spatial analysis methods for assessing dynamic exposures to different pollutants are more or less analogous if not the same.

According to e.g. (Tainio et al., 2016), negative health impacts of vehicular traffic can compromise the potential health benefits of walking. Thus, means for assessing pedestrians’ exposure to the pollutants produced by traffic are required in estimating the net health effect. (Davies & Whyatt, 2009) use the concept “journey-time exposure” to emphasize the relative importance of it as a component in individual’s total exposure. Journey-time exposure takes place in space and time, where both an individual and environmental conditions are (spatiotemporally) dynamic. This poses a technical challenge in implementing assessments for journey-time exposures: the used data needs to have both high spatial and temporal resolution.

Significant share of the studies on journey-time exposure have focused on air quality and exposure to air pollution, since many health effects from air pollution are well known and backed by medical research. Exposure to a pollutant (e.g. traffic noise or air pollution) is commonly measured simply as either duration or distance of exposure to certain concentrations or levels of the pollutant (e.g. Figure

3). Specific to research of pedestrians' exposure, distance and duration of exposure are often used interchangeably. If the pollutant is in the air, the exposure can be quantified as the total inhaled dose of the pollutant. If travel time and distance are considered proportional, a simple but useful metric on exposure can be calculated by multiplying the distance travelled by the level of concentration of the pollutant (e.g. (Hasenfratz et al., 2015)). Depending on the study setting, exposures can finally be aggregated by calculating total exposures to certain concentration/level ranges on a street, walk or route.

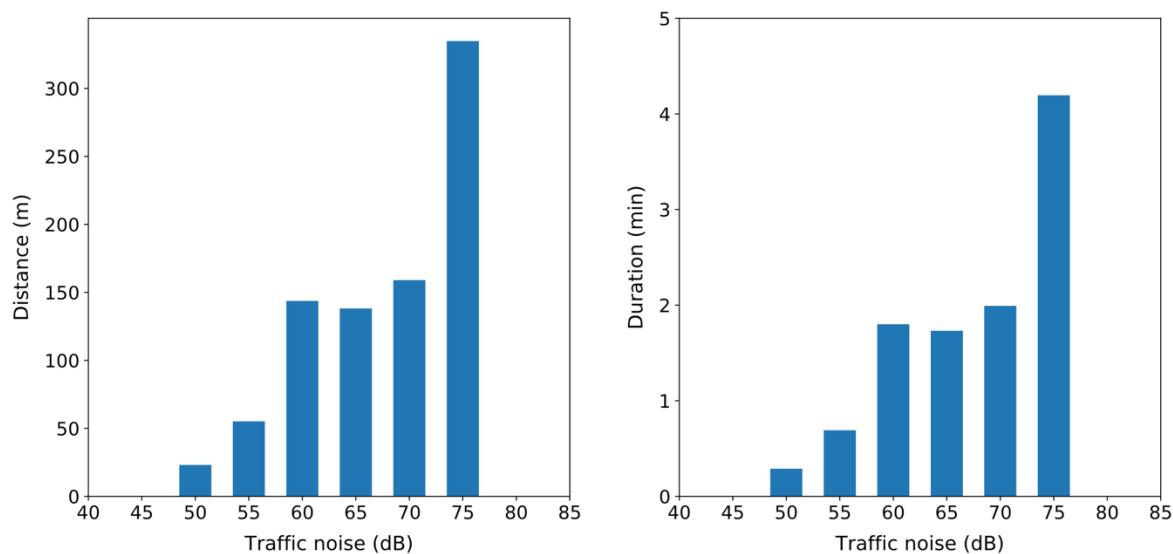


Figure 3. Exposure to traffic noise on a path as distances (left) and durations (right) of different traffic noise levels.

Based on a literature review, several alternative approaches exist for assessing pedestrians' or cyclists' dynamic exposure to traffic noise (or air pollution):

- 1) Direct way: using measurement instruments (e.g. air quality or volume sensor) attached to members of a study group and tracking them temporally and spatially with GPS (e.g. Apparicio, Carrier, Gelb, Séguin, & Kingham, 2016; Cole-Hunter, Morawska, Stewart, Jayaratne, & Solomon, 2012).
- 2) Indirect way: using measured and modelled pollutant surfaces and spatial analysis to assess exposure to pollution on e.g. GPS-tracked routes of people (Whyatt et al., 2007).
- 3) Indirect way: using measured and modelled pollutant surfaces and spatial analysis to assess exposure to pollution on modelled routes of people by e.g. OD data.

However, due to different technical and data availability related constraints and urban contexts, studies of pedestrians' exposure to pollutants have usually been rather case-specific in their methodologies and study questions. Hence, along with the three approaches listed above, many alternative or mixed methodologies have been used to study dynamic exposure to noise.

Different approaches are suitable for different spatial and temporal scales. Where the entirely direct way (measured and tracked routes and pollutants) can provide accurate exposure data for a small subset of the population, spatial analysis on modelled routes and pollutants can reveal more broader patterns in commuters' exposures. The latter approach is needed in order to estimate population or district level health effects of exposure to pollutants. An example of another type of spatial approximation of dynamic exposures to noise is the study by (Sheng & Tang, 2011), where pedestrian exposure to noise was not studied by commutes or walks but in terms of relative significance and length of the sidewalks and respective traffic noise levels.

GIS, as a technical framework, has been widely utilized in processing and analyzing the data for dynamic exposure analysis. Its advantage has been the ability to spatially and temporally compare data on both pollutants and individuals' movements. One common step for most of the dynamic exposure assessments has been the spatial join between pollutant surfaces and GPS-trajectories (or modelled routes). It is a key step in determining either the durations or distances of exposures to different concentrations or levels of the pollutant. Technicalities of the spatial join have varied depending on the type of the pollutant data (raster/vector), route data, software and (in some cases) programming environment.

Furthermore, exposure-based routing is enabled by the concepts and methods for calculating journey-time exposures. In the following two chapters, assessing and minimizing exposures to pollutants using routing methods is reviewed.

## 2.5 Graph-based least cost path analysis

Graph is a data structure that enables modeling of connected phenomena or object structure, such as social network, decision tree (abstract phenomena) or transport network (physical phenomena). Essentially, graphs consist of nodes and edges. Edges are connections between nodes and allow "travelling" from one point (node) in a graph to another given that a connection between the nodes exist. Furthermore, graphs enable assessing e.g. centrality of certain element. To support the context of this thesis, the focus will be on street network graphs.

Graphs provide many useful functionalities for modeling and analyzing street network graphs. Usually, intersections are modelled as nodes and streets as edges. Both can have arbitrary number of attributes. Numerical edge attributes enable routing analysis between nodes. Namely, a widely utilized application of graph theory is the least cost path (LCP) problem. If length of the edges is used as the cost attribute (weight), a least cost path becomes the same as the shortest path. However, any numerical but non-negative edge attribute can be used as the cost, allowing variety of routing problems to be addressed.

Several algorithms exist for least cost path routing. One of the most well-known of them is Dijkstra's algorithm. According to e.g. Noto & Sato (2000), the other two main methods for the least cost path problem are the A\* algorithm and genetic algorithms. Dijkstra's algorithm finds the optimal least cost paths between nodes in a graph by finding the shortest path from an origin node to all other nodes in a graph (Figure 4). If the shortest path is needed for only one origin-destination (OD) pair, pathfinding is stopped once the path to the destination node has been found.

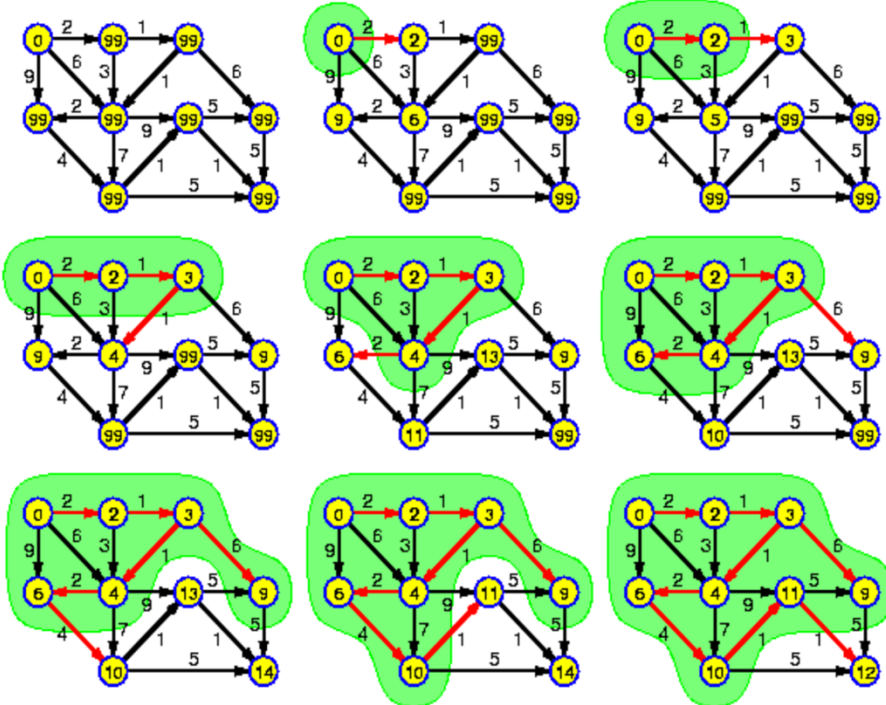


Figure 4. An example of a sequence of steps in executing Dijkstra's algorithm by (Jasika et al., 2012).

When the size of the graph grows, the traditional form of Dijkstra's algorithm becomes computationally increasingly demanding. Thus, considerable share of the research on path optimization problems has focused on optimizing the least cost path analysis itself e.g. (Ahuja et al., 1990; Goldberg & Harrelson, 2005; Noto & Sato, 2000). Generally speaking, many of the proposed

ways of making the shortest path finding faster have utilized the following idea: reduce the total number of shortest paths that need to be optimized before the path in question. In A\* algorithm, this can be achieved by using Euclidean bounds around the origin and destination nodes to select only a subset of nodes that need to be visited (with Dijkstra's algorithm). As (Noto & Sato, 2000) put it: “[A\* algorithm] eliminates fruitless searches by considering the distance to the destination”.

## 2.6 Exposure-based impedances in routing

In accessibility research, travel time is often used as the main measure of accessibility; how many minutes it takes to get from an origin to a destination? Likewise, in routing, travel time is most often the only or at least mostly optimized variable. However, also other types of costs have been incorporated in routing to find more favorable routes by varying terms. In route planners for walking and cycling, also environmental exposure-based costs have been incorporated in LCP analysis to take the perceived impedance and potentially health into account in pathfinding. Moreover, routing analysis seems to have a potential to combine assessment of journey-time exposure, provided that speed and the considered environmental conditions can be either measured, modelled or assumed. This is an essential feature in routing, as it enables comparison of different route alternatives with respect to total exposure and length.

Many of the exposure-based routing methods (and applications) focus on air pollution. Minimizing total exposure to e.g. PM<sub>2.5</sub> or PM<sub>10</sub> particles by routing have been demonstrated or at least addressed in several studies (Davies & Whyatt, 2009; Hertel et al., 2008). In these studies, considerable achievable decreases (%) in the total exposure to the pollutants were found, indicating a potential for green path route planners.

Both raster (surface) -based and graph-based methods have been used to optimize impedance-based LCPs. Many studies have utilized graph-based LCP analysis as it is well suited for modeling urban street networks. In the graph-based method, streets can be efficiently modelled as edges between nodes of a graph. Then, using customized edge costs, LCP analysis can be used to solve various subtypes of LCP problems. Many studies have demonstrated how graph-based LCP routing can be used to minimize exposure to pollutants (Alam et al., 2018; Hasenfratz et al., 2015; Hertel et al., 2008; Sharker et al., 2012; Su et al., 2010).

Based on a non-systematic literature review, the use of raster-based LCP analysis (for minimizing journey time exposure) have been demonstrated only in few studies. For example, (Davies & Whyatt, 2009) utilized pollution surfaces (PM<sub>10</sub>) and spatial data on traversable and non-traversable features

of the study area to enable common raster-based LCP functions. The decision to use raster-based method enabled them to incorporate continuous areas (e.g. parks) in the routing. Their method worked well for a relatively small study area but required careful data preparations to mask out all unwalkable features.

In the previous studies on graph-based LCP, distance and travel time were often considered as proportional. This allowed calculation of exposure-based costs simply by multiplying the concentration of a pollutant by distance of the road segment. Where exposure to multiple pollutants needed to be addressed at the same time, also additional cost coefficient was included in the cost function. While all the exposure-based costs aimed to account for the health effect of the exposure, the formulas of the cost functions varied considerably between studies. For example, (Ribeiro & Mendes, 2013) used the concept “contamination of distances” to model exposure-based impedance from noise and PM<sub>10</sub> at different parts of the network. They assigned noise-based costs to edges of a graph according to contaminated distances to different noise levels, using predefined thresholds (dB) to decide whether a noise cost should be assigned or not.

Common to most of the prior studies on exposure-based routing, the alternative routes were presented with relevant statistics allowing comparison of reductions in journey-time exposure and route length or travel time. Varying and vivid names have been introduced to conceptualize different kinds of least-exposure paths. These names include e.g. green, healthy, sustainable, safe and quiet paths. Since the number of studies addressing least-exposure path routing is still limited, most of them were only case specifically defined and hence not well-established or generic concepts. In the context of this study, the concept quiet path is used to refer to routes of less noise exposure.

Some of the exposure-based LCP methods were developed further as route planner web services (e.g. (Hasenfratz et al., 2015; Su et al., 2010)). This required focusing also on the efficiency of the LCP analysis to provide reactive enough user experience. Also, special attention was then paid on the visualization of the different route alternatives as well as showing descriptive statistics on the total exposures to pollutants and achievable reductions in them. (Hasenfratz et al., 2015) demonstrated how using static pollution maps and loading the LCP analysis application into the memory of a smartphone can provide very fast responses to user's routing requests. On the other hand, (Su et al., 2010) implemented their route planner as a service based application, where the user interface communicates with a dedicated (remote) exposure-based LCP service via asynchronous requests. Varying technical implementations for such services seem to be available due to increased opportunities that modern Web GIS technologies provide (2.7.).

## 2.7 Web GIS concepts and developments

In this chapter, concepts and developments in Web GIS are reviewed with a focus on the latest technological advancements that enable highly interactive web map applications. According to (Agrawal & Gupta, 2017; Veenendaal et al., 2017), developments in Web GIS technologies and their applications have happened in the context of both emerging new paradigms in web technologies and increasing numbers of users. Apart from the number of users, also the ways of *using* web applications have shifted towards mobile use, creating demand and new opportunities for mobile-friendly web map applications.

Some of the advances in Web GIS are enabled by the increased computational capabilities of devices. Modern web browsers have access to increased computing power and graphics processing capabilities needed for running ever more versatile web applications. Therefore, web mapping libraries (e.g. OpenLayers) can provide also increasingly extensive toolkits for geospatial analysis right in the web browser.

Moreover, emerging service-oriented architecture (SOA) in Web GIS have allowed distributing the most expensive data processing and analysis operations in dedicated machines. SOA-based Web GIS systems can thus allow an uninterrupted user-interface layer and scalable services for varying numbers of clients (users). This development can be seen as an adoption of a larger scale paradigm shift from independent applications to service-oriented architectures in Web GIS (Agrawal & Gupta, 2017). As per (Lu, 2005), “The service-oriented architecture is a very promising architecture for practical implementation of the next generation geographical information systems”. Development of SOA-based Web GIS solutions is facilitated by the emergence of cloud-based computing platforms and hosted virtual machines. These services allow deployment of custom GIS applications to appropriate infrastructure. In this way, distributed GIS services and data sources can be utilized via application programming interfaces (APIs) in similar manner as other distributed web services. Furthermore, complex but efficient GIS systems can be composed by combining a desired set of separate services and data sources, as illustrated by (Veenendaal et al., 2017) (Figure 5).

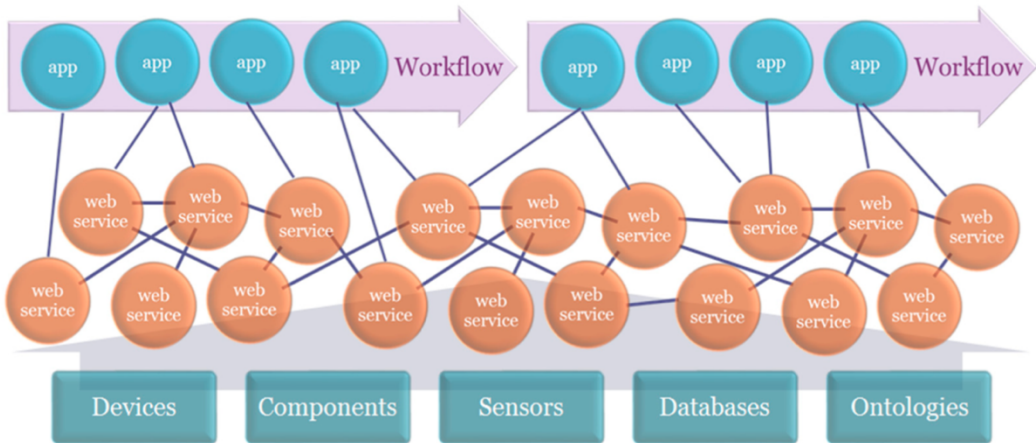


Figure 5. “Interacting web services feeding into apps within application workflows.” by (Veenendaal et al., 2017)

The advantages of using SOA in Web GIS also includes the ability to utilize open APIs and services provided by public authorities and governments. This is made possible by standardized geographical data transfer protocols such as web map service (WMS) and web feature service (WFS) along with the traditional data interchange protocols such as representational state transfer (REST). In the service-based Web GIS architecture, the user-interface can communicate with the supporting GIS services asynchronously (as demonstrated by (Su et al., 2010), leaving user-interface layer always reactive to new user inputs. This can be seen as an important factor improving the user experience of the application: meanwhile the service processes the request in the background, user can do something else with the web map application at the same time.

Another aspect that has supported the fast advancements of modern Web GIS is the extensive utilization and development of open source data formats and source code for geospatial analysis and web-based visualization (e.g. web map libraries, spatial databases and libraries for geospatial analysis). Many of these formats and software are being developed by active open source communities and in some cases also supported by private companies (e.g. (*Leaflet*, n.d.; *OpenLayers*, n.d.; *PostGIS*, n.d.)).

A critical component of Web GIS systems is the user interface, typically a web map. Essentially, web map libraries enable building customized interactive web map applications that run in web browsers. Web map libraries usually run as JavaScript applications as JavaScript is one of the few programming languages that is natively supported by most web browsers. While most of all web maps used to be based on displaying tiled raster maps, also alternative web map technologies started emerging

(Gaffuri, 2012; Lienert et al., 2012). HTML5, the latest major revision of HTML (hypertext markup language), has brought capabilities for drawing increasingly rich interactive visualizations. It has been demonstrated that HTML5-based technologies can be used to implement web map applications with vivid vector graphics (Boulos et al., 2010). The other advantage of this advancement is the ability to draw rich map canvas without additional plugins such as Adobe Flash Player. A promising example of these, among others, is WebGL, a vector graphics technology supported by HTML5 that can be utilized to display interactive web maps composed of rich vector graphics (e.g. (Qiu & Chen, 2018)).

Apart from the technical advancements of the modern web-mapping components, the bigger picture of contemporary Web GIS can be studied with respect to various parallel developments, trends and opportunities. (Veenendaal et al., 2017) illustrated this larger conceptual and technical framework (around developing Web GIS) with a labelled Data, Information, Knowledge, Intelligence and Wisdom (DIKIW) pyramid (Figure 6). According to a review by (Veenendaal et al., 2017), the advanced technical frameworks of Web GIS can facilitate providing users with both more personal and deeper geospatial information.

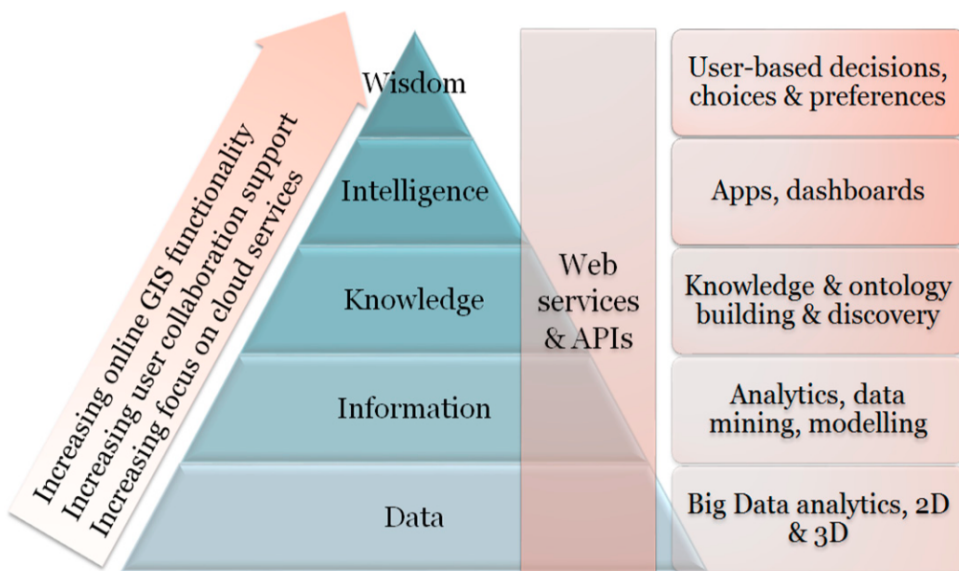


Figure 6. "Focus and trends in increasing web mapping functionality" by (Veenendaal et al., 2017).

### 3 Material & Methods

#### 3.1 Overview of the methods

Overview of the methods and their internal dependencies is illustrated in Figure 7. As shown in the figure, all outcomes of the thesis depend on the routing application that optimizes both shortest and quiet paths. Assessments of pedestrians' exposure to traffic noise and potential to reduce exposure to traffic noise are linked to each other, as the achievable reductions are calculated with respect to exposures on the shortest paths.

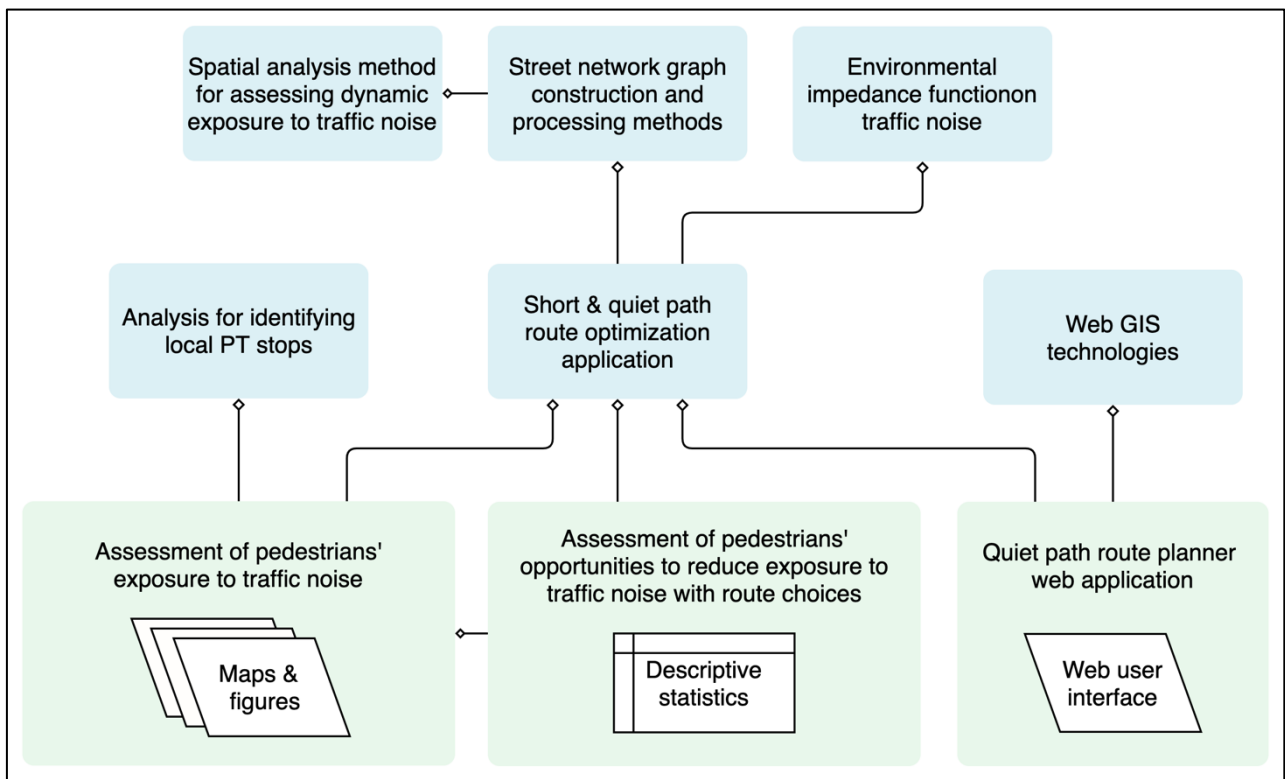


Figure 7. Illustration of the internal methodological dependencies of the study.

#### 3.2 Study area

The study area of the thesis is defined by the extent of the Traffic noise zones in Helsinki, i.e. the adjusted municipal boundaries of the city (Figure 8). Some of the islands in southern Helsinki were excluded since the traffic noise data did not cover them. Despite the defined study area, the concepts and methods of the quiet path routing method were developed as applicable to any area for which both modelled traffic noise surfaces and OpenStreetMap (OSM) data are available; the coverage of noise mapping campaigns includes for example most of the major urban areas in Europe, since traffic

noise assessments are required by EU legislation (*Directive 2002/49/EC*, 2002) and OSM features (almost) global coverage.

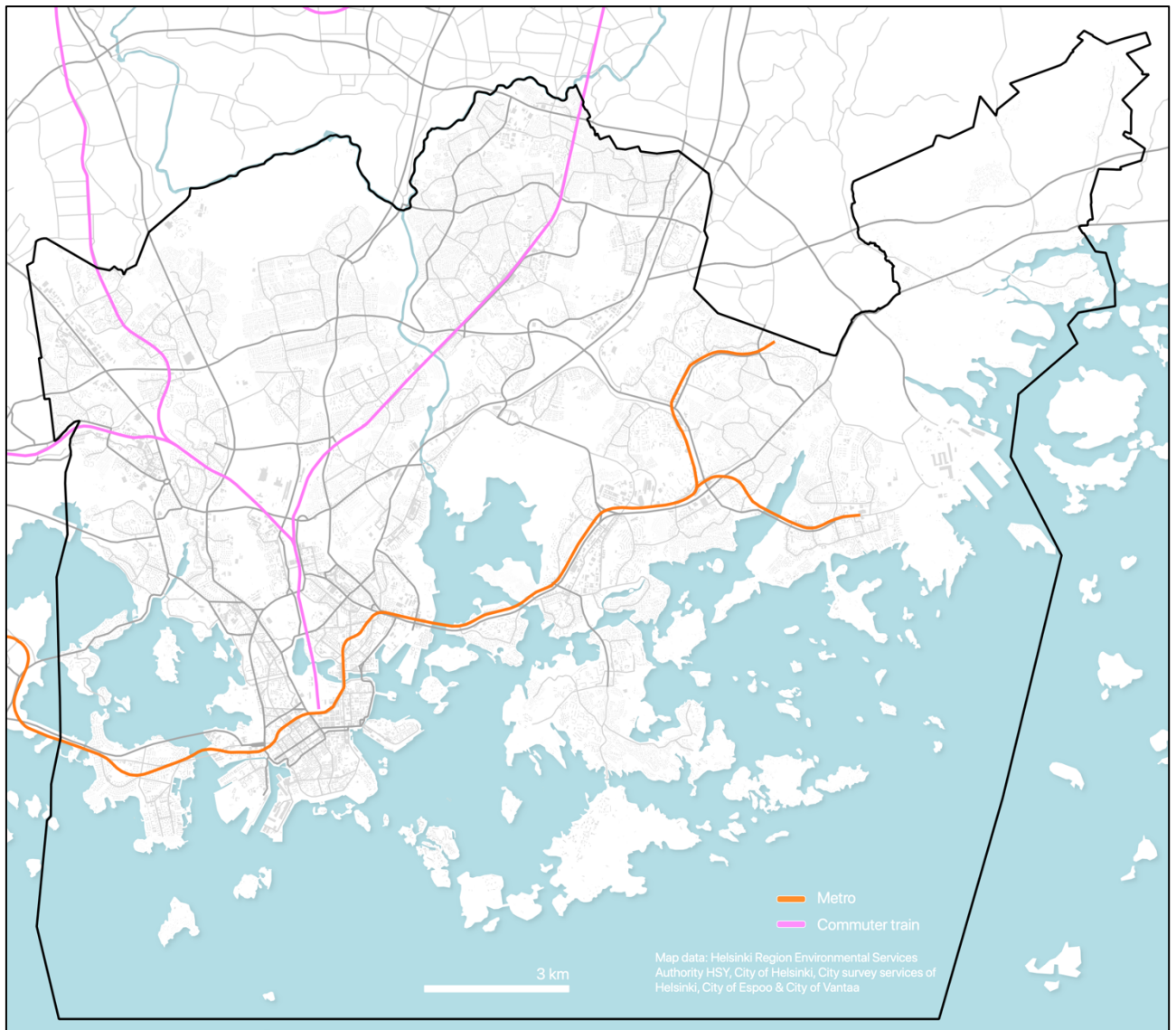


Figure 8. Map of the study area; extent of the city of Helsinki excluding the southern islands.

### 3.3 Materials

Table 1. Materials that were used in the study.

Name	Source	Description	Use in the study
Traffic noise zones in Helsinki 2017	Urban Environment Division of city of Helsinki (Helsingin)	Modelled traffic noise surfaces as polygon layer covering the city of Helsinki. Minimum and	Traffic noise exposures are based on the traffic noise surfaces (zones) of this dataset.

	kaupunkiympäristön toimiala)	maximum noise levels are stored as attribute information.	
250m statistical grid	Statistics Finland	250m * 250m polygon grid layer that is related to YKR- commuting data.	Center points of the grid layer were used as origins and destinations in the routing analysis. Grid cell polygons were used in visualizing the results.
YKR-commuting data (T06_tma_e_TOL2008_2016_hel)	Finnish Environment Institute (SYKE) / Statistics Finland	Commutes between 250m statistical grid cells as table. One row in the table represents the total number of commutes between two grid cells.	Utilization rates of local PT stops were calculated based on PT itineraries planned for the commutes.
City districts in the Helsinki Metropolitan Area	Helsinki Region Environmental Services Authority HSY	City districts as polygons.	Centers of the city districts were used as the destinations to distant workplaces in routing analysis.
OpenStreetMap: highways	© OpenStreetMap contributors	All walkable highways and paths as network segments.	A network graph suitable for routing was constructed from the data.
Digitransit Routing API	Helsinki Region Transport (HRT)	Routing service for planning public transport itineraries as an application programming interface (API).	Local PT stops were identified by requesting PT itineraries for the commutes from Digitransit routing API.

### 3.3.1 Modelled traffic noise data

Pedestrians' exposure to traffic noise was assessed with respect to modeled traffic noise zones for Helsinki (*City of Helsinki: strategic noise mapping*, 2017). The dataset contained two parallel noise surfaces for the area produced with two different noise models: 1) CNOSSOS-EU (Jarno Kokkonen et al., 2016; Kephhalopoulos et al., 2012) and 2) joint-Nordic traffic noise estimation model (Jonasson & Storeheier, 2001; Nielsen, 1997). The latter was chosen for the study since its modeling height (2 m from the ground) was arguably closer to the walking altitude of pedestrians than in the other model (4 m from the ground). However, since CNOSSOS-EU model is described to have higher level of detail in both noise source and noise diffusion modeling (*City of Helsinki: strategic noise mapping*, 2017), choosing it instead would have been justified as well. In the implementation of the noise model, a wide range of factors affecting the paths and levels of noise were taken into account. These included input data on modelled traffic flows and speeds on different roads, the three-dimensional surface model of the city, buildings, sound barriers and acoustic properties of different surfaces (*City*

*of Helsinki: strategic noise mapping*, 2017). The modelling was conducted by Sito Oy as a commission from the city of Helsinki (*City of Helsinki: strategic noise mapping*, 2017). Noise modelling software Datakustik CadnaA 2017 was utilized in the modelling.

A few alternative noise indexes were available in the dataset. Noise index  $L_{Aeq}$  for daytime (7am – 22pm) noise levels was chosen as the primary noise index used in the thesis (layer: *2017\_alue\_01\_tielikenne\_L\_Aeq\_paiva*). In this thesis, the abbreviation dB is used to refer to the modelled sound level  $L_{Aeq}$  unless otherwise specified in the text.  $L_{Aeq}$  is composed of A-weighted equivalent continuous sound level and measured in decibels. A-weighting is used to consider the human ear's ability to hear different frequencies in calculating the sound pressure level at range from 20 Hz to 20 kHz, whereas “Equivalent continuous (A-weighted) sound level is defined as the steady sound level that transmits to the receiver the same amount of acoustic energy as the actual time varying sound over the prescribed time period.“, as per (Kumar et al., 2014). According to (Guski et al., 2017; Van Kempen et al., 2018), both of these metrics (A-weighting and equivalent continuous sound level) have been extensively utilized in studies on traffic noise and annoyance.

The traffic noise data includes modelled traffic noise surfaces with specified minimum and maximum traffic noise level ( $L_{Aeq}$ ), each covering a 5-dB range. The traffic noise levels in the data range from 45 dB to 80 dB, the highest 5-dB range ranging from 75 dB to 80 dB. Three maps of different spatial scales were made to illustrate the high spatial precision of the modelling (Figure 9, Figure 10 & Figure 11). Also, the effect of buildings as effective noise barriers can be seen when comparing the noise surfaces between Figure 10 and Figure 11; in the first map the +60 dB noise surfaces extend hundreds of meters from the highways whereas in the latter they are more concentrated between the buildings.

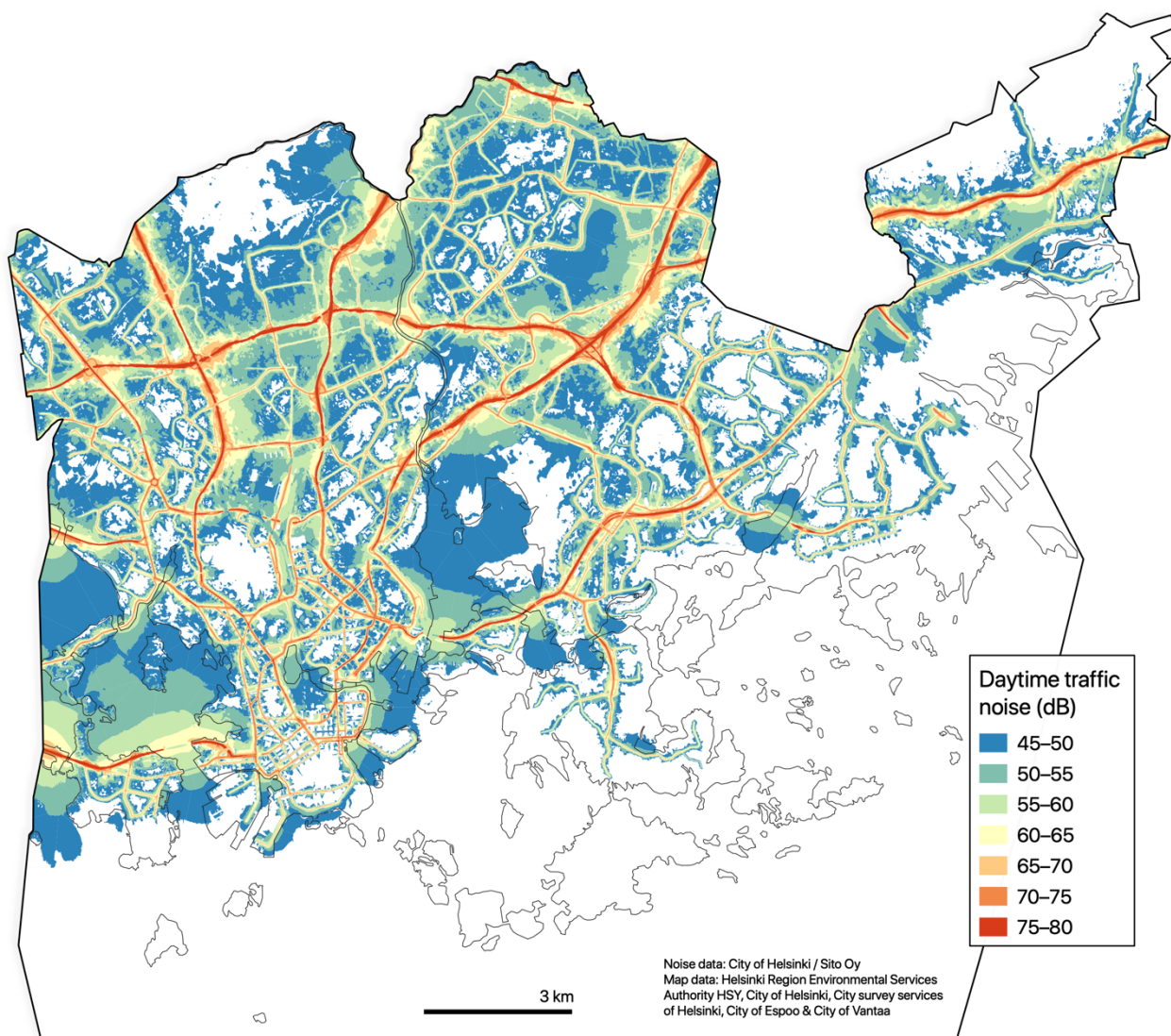


Figure 9. Modelled daytime traffic noise levels (dB) in Helsinki.

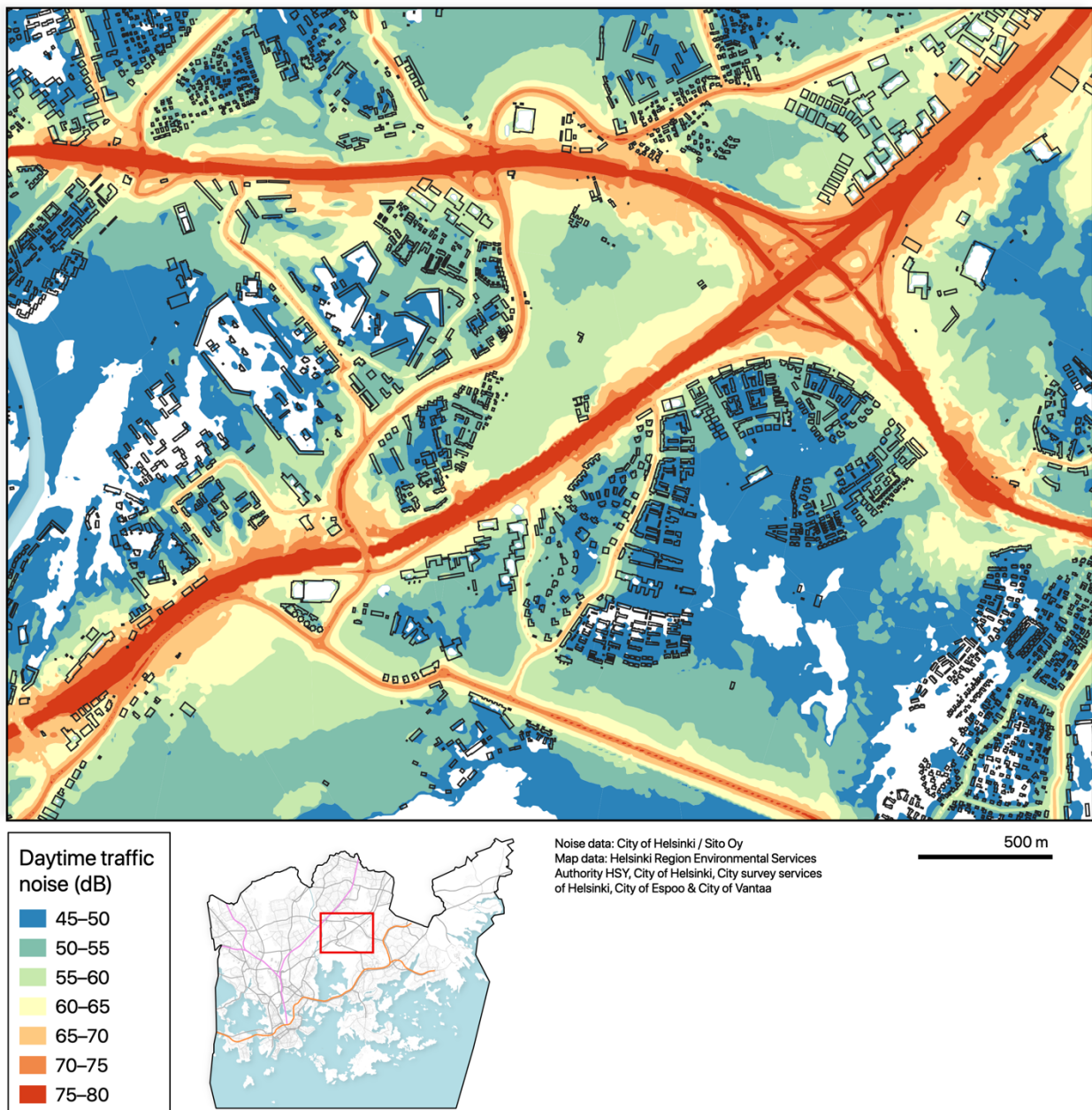


Figure 10. Modelled daytime traffic noise levels (dB) in Viikki.

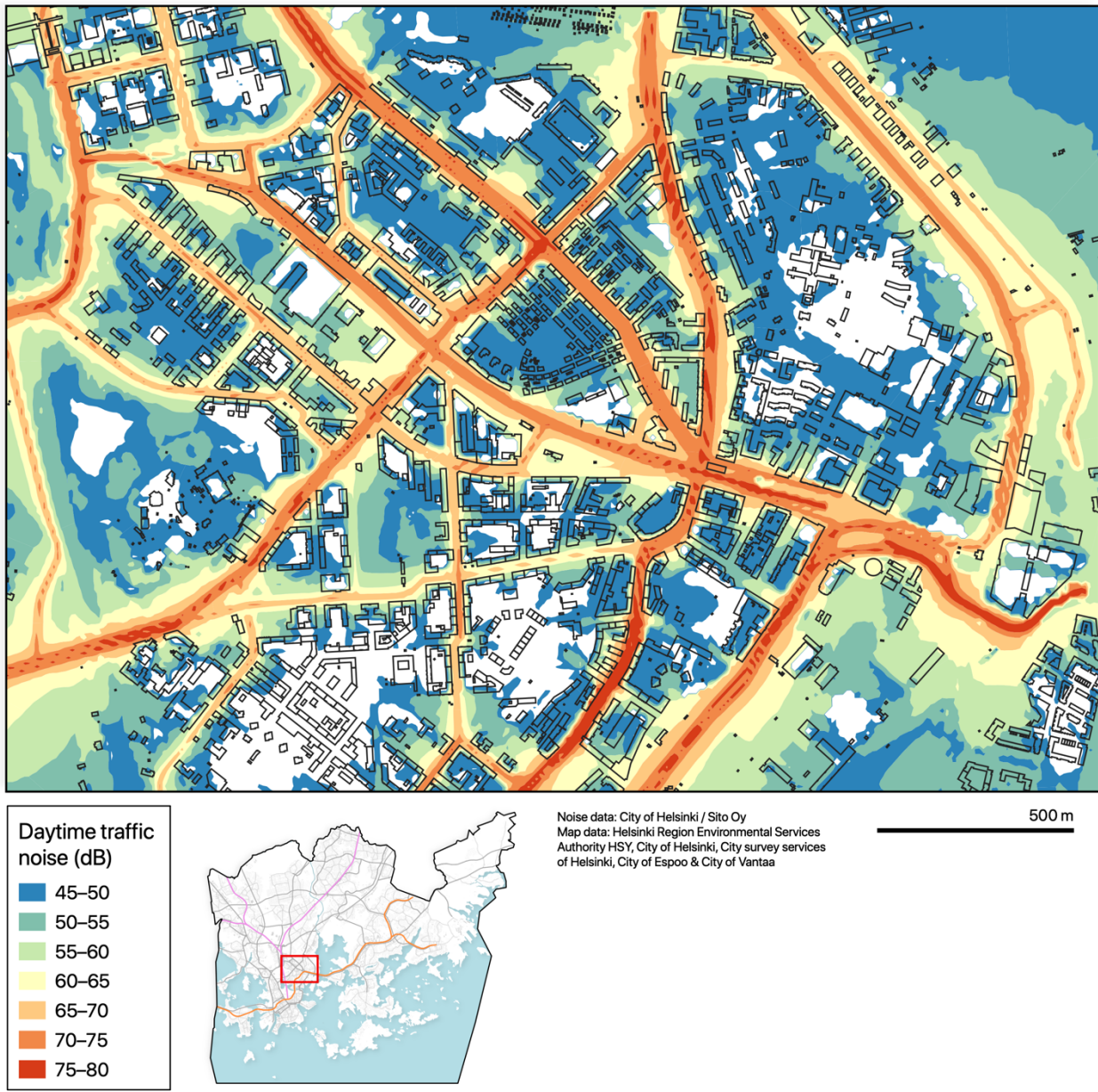


Figure 11. Modelled daytime traffic noise levels (dB) in more central location in Helsinki.

### 3.3.2 OpenStreetMap data

A large set of street feature data was downloaded from OpenStreetMap (OSM) for walkable street network graph construction. The OSM highway features were selected and queried from Overpass API which allowed using a custom query consisting of OSM key-value pairs (tags) to request only the appropriate features. The python library OSMnx (ref.) provided a practical way for accessing the API and defining the customized query string. The query string was edited from the default query string of OSMnx for walkable street feature download (Table 2).

Some unwalkable street features were needed to be filtered out from the graph only after creating the graph due to limitations in the querying capabilities of OSMnx. Hence, a subsequent download of unwalkable street network data was required.

Choosing OSM data as the basis of the walkable street network graph could be justified with several arguments:

- OSM data is often rich in walkable street features (especially in urban areas), since walkable streets and paths are frequently updated by active local OSM communities.
- OSM data is used by the official route planner application of Helsinki Region Transport (HRT/HSL) and hence kept up to date by also professionals.
- Use of OSM data allows easier adopting of the methodology in other study areas and contexts.

Table 2. Query strings for street network data downloads using OSM Overpass API via OSMnx python library.

Graph	Query string
Walkable street network graph	<code>["area"!~"yes"]["highway"!~"trunk_link motor proposed construction abandoned platform raceway"]["foot"!~"no"]["service"!~"private"]["access"!~"private"]</code>
Graph of problematic unwalkable street segments (e.g. service tunnels)	<code>["area"!~"yes"]["highway"!~"trunk_link motor proposed construction abandoned platform raceway"]["foot"!~"no"]["service"!~"private"]["access"!~"private"]["highway"~"service"]["layer"~-1 -2 -3 -4 -5 -6 -7"]</code>
-	-

### 3.3.3 Register based origin-destination (OD) commuting data

A census-based commuting data (T06\_tma\_e\_TOL2008\_2016\_hel) was acquired for the study to allow obtaining realistic routes from homes to workplaces in the assessment. The data was collected and produced by Statistics Finland and processed by the Finnish Environment Institute (Syke) (ref.). In the data, commutes are reported by aggregated origin-destination (OD) flows between 250 m statistical grid cells covering the whole country. Essentially, one OD flow is described with one row with various statistics. Since the data aims to cover all commutes, it can also be used to assess the

number of residents at each grid cell. Before using the data in the analysis, it was filtered down to cover only commutes of having the origin in the study area (Helsinki).

### **3.3.4 Routing service of the local public transport authority**

A route planner web service of Helsinki Region Transport (HRT/HSL) was utilized to obtain realistic itineraries made with public transport for the OD-pairs of the commutes. The service was accessed via its application programming interface (API) to enable fast and reproducible method. Essentially, the routing service was needed for two purposes:

- 1) To be able to identify local public transport stops that would work as the destinations of the local walks.
- 2) To be able to assess the quality of the shortest paths calculated with the quiet path routing method in comparison to the reference paths (returned from the API).

## **3.4 Technical framework and architecture**

The technical framework of the study consists of several internal and external dependencies (Figure 12). Majority of the programming for data analysis and quiet path routing method was done in Python programming language. Thus, the main external dependencies consist of Python libraries for utilizing and analyzing scientific, geospatial and graph data (e.g. Pandas, GeoPandas, NetworkX and OSMnx). Also the used libraries and packages have several external dependencies which are now shown in the figure.

A modular design was applied in developing the methods, enabling creation of common utilities needed at different parts of the analysis and also by the quiet path routing application. Functions were divided into (Python) modules with descriptive names in order to make finding, combining and using them practical. A single Conda-environment was created to provide the needed libraries for all functions of the study from graph processing to running the server-based quiet path routing application. The environment was described with an explicit environment file (Appendix 1) to facilitate running the analysis and quiet path routing application easily on any computer.

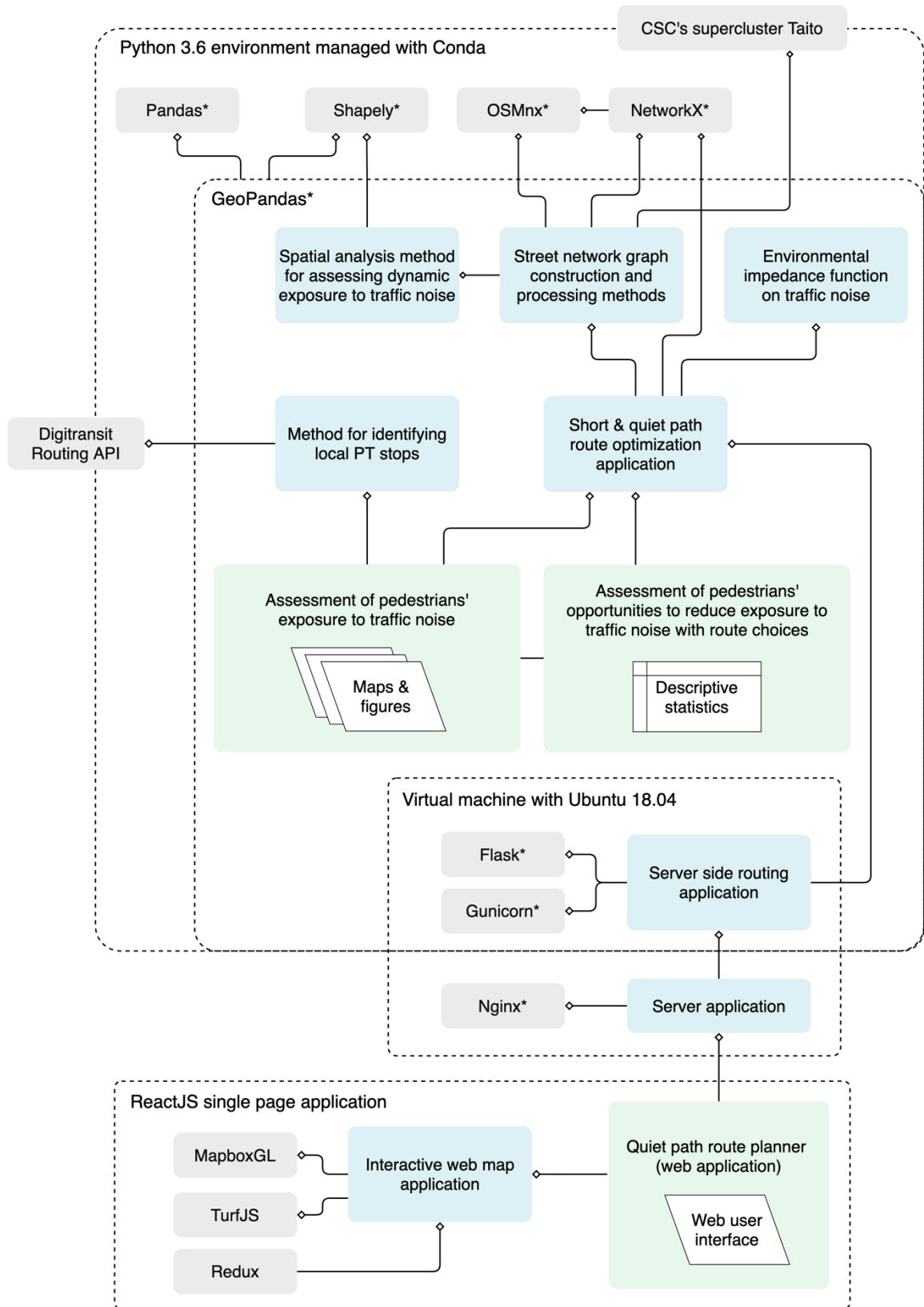


Figure 12. Technical framework of the study: internal (blue) and external (grey) technical dependencies (\* = Python library). The numerous external dependencies of the used Python libraries are not included in the graph.

### 3.5 Quiet path routing method

#### 3.5.1 Environmental impedance function

An environmental impedance function (EIF) on noise needed to be defined to allow noise exposure - based routing analysis. The equation for calculating adjusted, noise-based edge costs (i.e. EIF) was defined as:

$$C_e = d_e + C_{en} \quad (1)$$

where  $C_e$  is the total composite cost of the edge;  $d_e$  is the length of the edge (i.e. base cost) and  $C_{en}$  is an additional noise exposure -based cost of the edge. From now on, the noise exposure -based cost is referred to as noise cost. The concept of contaminated distances was applied in calculating the noise cost for an edge (as in)(Ribeiro & Mendes, 2013). However, instead of using few fixed SPAs (dB) as thresholds in assigning the noise costs (Ribeiro & Mendes, 2013), the following formula was developed to calculate them on a continuous scale:

$$C_{en} = \sum_{i=db_{min}}^{db_{max}} d_{dB_i} \times a_{dB_i} \times s \quad (2)$$

where  $dB_i$  refers to a 5 dB range from  $dB_i$  to  $dB_i + 5$  dB (e.g.  $dB_{55}$  refers to the dB-range: 55–60 dB),  $d_{dB_i}$  is the total contaminated distance (m) with the dB-range  $dB_i$  (e.g. 14 m of 55–60 dB) on the edge geometry;  $a_{dB_i}$  is a dB-specific noise cost coefficient and  $s$  is an arbitrary noise sensitivity coefficient (e.g. 0.1–40).

Arguably, the critical, yet conceptually most challenging, component of the EIF is the dB-specific noise cost coefficient ( $a_{dB_i}$ ). Ideally, the noise cost coefficient should reflect the perceived loudness and annoyance of a given  $L_{Aeq}$ . According to the literature review by (Guski et al., 2017), assessing exposure to A-weighted equivalent continuous sound level (e.g.  $L_{Aeq}$ ) has been the standard metric in the studies on noise and annoyance. Based on the review, no widely accepted linear or non-linear relationship between A-weighted sound pressure level (SPL) and perceived loudness seem to exist, regardless of the sound attempts to find one by (Miedema & Oudshoorn, 2001). Furthermore, these papers focus on static exposure (e.g.  $L_{Aeq}$  at home location), which further limits their applicability to asses traffic noise - annoyance (or loudness) relationship for dynamic exposure.

Given the previously described uncertainty on deriving loudness or annoyance metrics based on  $L_{Aeq}$ , two alternative functions were created for calculating  $L_{Ae}$ -based noise cost coefficients. First (0) of the functions assumes a linear relationship between loudness and  $L_{Ae}$  and sets the noise costs on range 0.0–1.0 from 40 to 75 dB:

$$a_{dB_i} = \frac{dB_i - 40 \text{ dB}}{75 \text{ dB} - 40 \text{ dB}} \quad (3)$$

The second function (4) utilizes the power law between loudness and sound intensity that Parmanen (2007: 60) reformatted from widely used Stevens' power law (Stevens, 1960):

$$a_{dB_i} = 10^{\frac{0.3 * dB_i}{10}} \quad (4)$$

where  $dB_i$  is the lower limit of a 5-dB interval and the minimum  $dB_i$  is 40. Respective noise cost coefficients for  $dB_i$  values from 45 dB to 75 dB are presented in **Error! Not a valid bookmark self-reference.** and in Figure 13. Applicability of the Stevens' power law is limited in this context due to varying tone (and frequency distribution) of traffic noise at different distances from the sources as well as the related fact that it was not designed to work with A-weighted sound pressure levels (but with simple intensity metrics).

Equation (4) was selected for calculating the noise cost coefficients. The power law doubles the cost (loudness) roughly at every 10-dB increase, hence giving significantly higher costs to the highest noise levels. This is the most desired feature of the function, as the highest noise levels (> 65 dB) are known to be the most harmful to people. The power function may also be partially supported by interpretation of the nonlinear HA%/ $L_{den}$  curves in Figure 2 (Guski et al., 2017): a majority of the annoyance/SPL curves took the form “J” instead of a straight line, suggesting that an increase in SPL at a higher noise level may have a bigger effect on the perceived annoyance (and possibly loudness) compared to an equivalent increase in SPL at a lower noise level.

However, when both functions for noise cost coefficient were tested in developing the quiet path routing application, almost identical quiet paths were got in most cases. It may be that the sensitivity index and overall availability of quiet path options (between an OD-pair) override the effect of the small differences between the noise cost functions. The uncertainties in noise/annoyance/loudness relationships are considered further in the discussion (chapter 5.2).

Table 3. Noise cost coefficients for dB range 45–75 dB calculated with both equations presented in this chapter (( & (4).

Traffic noise level (dB)	Noise cost coefficient ( $a_{dB_i}$ )	
	$\frac{dB_i - 40 \text{ dB}}{75 \text{ dB} - 40 \text{ dB}}$ (Eq. (0))	$a_{dB_i} = 10^{\frac{0.3 * dB_i}{10}}$ (Eq. (4))
45–50	0.14	0.22
50–55	0.29	0.32
55–60	0.43	0.45
60–65	0.57	0.63
65–70	0.71	0.89
70–75	0.86	1.26
75–80	1.00	1.78

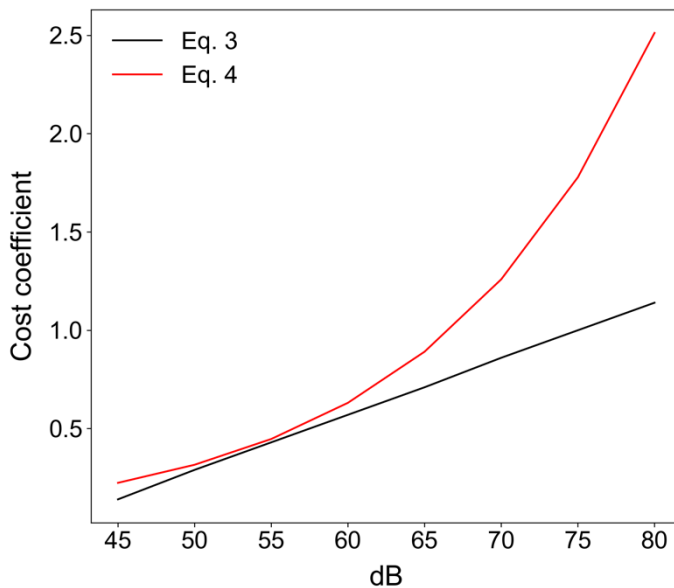


Figure 13. Noise cost coefficients for dB range 45–75 dB calculated with both equations ( & (4) presented in this chapter.

### 3.5.2 Network acquisition and manipulation

The following three steps were required to acquire and process street network data to a graph suitable for optimizing quiet paths:

- 1) Walkable street network data acquisition and graph construction (Figure 14).

- 2) Determining contaminated distances with different noise levels: spatially joining noise surface data to edges (Figure 15).
- 3) Calculating new noise sensitivity -specific edge costs to edge attributes: implementing the environmental impedance function on noise attributes of the edges of the graph (Figure 16).

The Python library OSMnx was used to download walkable street network data from OSM and to build a graph from it in NetworkX format (as described in chapter 3.3.2). OSMnx was also used to convert the directed graph to an undirected one, as walkable street segments should be walkable to both directions. Also, undirected graphs require less computing power and memory for processing. After initial graph construction, straight line geometries were added to edges missing them, based on locations of the origin and destination nodes of the edges.

A temporary graph of unwalkable edges (e.g. service tunnels) was constructed in similar manner as the main graph but by using an edited query string (Table 2). The unwalkable edges were matched with the edges of the main graph by both osm\_id and geometrical overlay analysis. Both matching methods were needed since osm\_id is not guaranteed to be fully unique in all cases. The edges that were matched and identified as unwalkable were then removed from the graph. Finally, it was made sure that no isolated edges or nodes were left in the graph (due to removed connections between nodes).

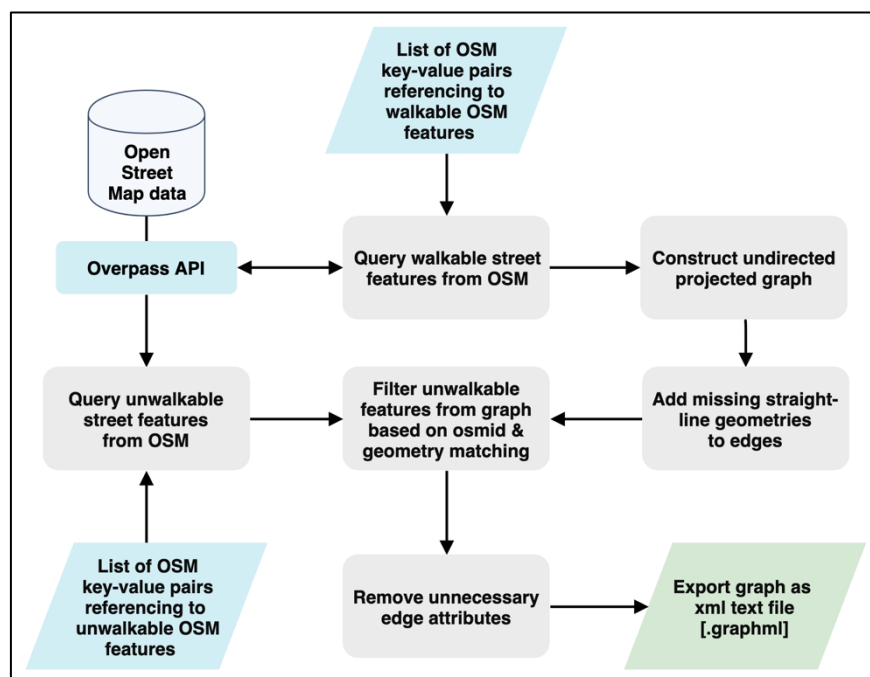


Figure 14. Workflow of network (graph) acquisition and construction.

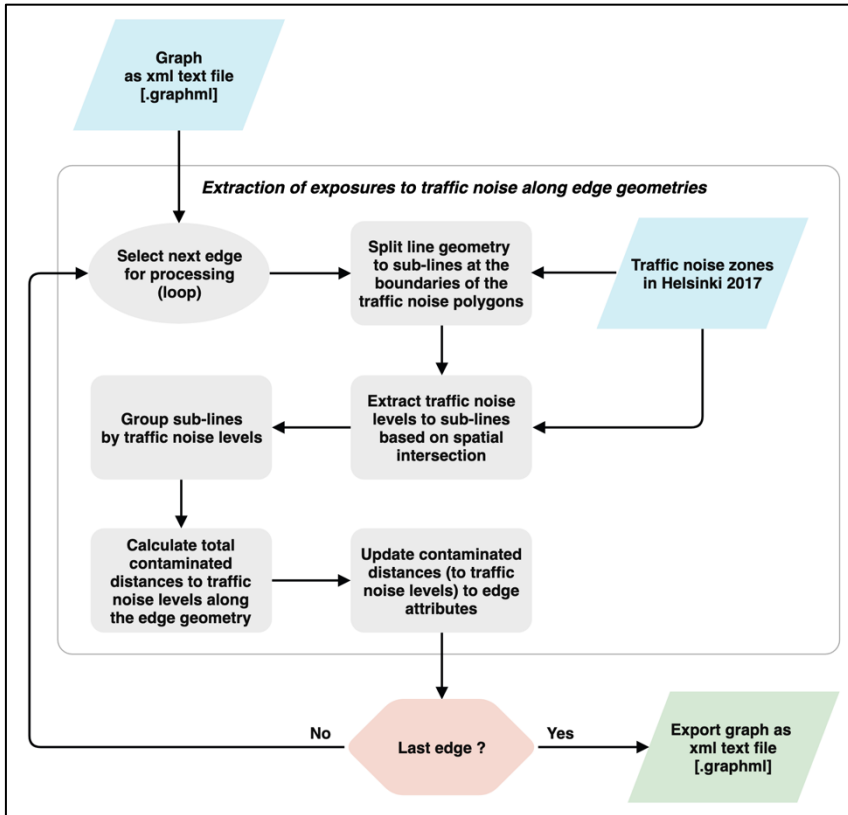


Figure 15. Workflow of extracting exposures to traffic noise (contaminated distances) to the edges of the graph.

A lossless spatial join of noise data ( $L_{Aeq}$ ) to the edges of the graph was implemented to add information of contaminated distances with different noise levels to edge attributes (Figure 15). The edge geometries were first split at the boundaries of the traffic noise surfaces. Then, underlying traffic noise data was extracted to the split edge geometries by their center point using vector-based point sampling in GeoPandas. Finally, the split edges were aggregated and grouped by the original edge id and contaminated distances with different noise levels were added up for each edge. The result of the spatial join was validated by checking that the sum of the contaminated distances to different noise levels never exceeded the total length of the edge.

Due to the high number of edges in the graph (180647), the main challenge of the spatial join was its high demand for computing power and high memory consumption. Hence, the first iteration of the analysis was run in CSC's supercluster Taito (ref.). The reserved +20 processing cores and plenty of memory were utilized with the standard multiprocessing library of Python, enabling running the spatial join of edges in parallel. However, the Python script for the spatial join was further optimized to enable running it also on a typical computer; by organizing the edges as list of GeoDataFrames (edge-chunks), it was possible to process of multiple sets of hundreds of edge geometries in parallel.

(simultaneously) with the standard multiprocessing library of Python. The outcome of the script optimization was desired: the lossless spatial join could be made accurately but also fast.

### 3.5.3 Quiet path routing application

In this chapter, the main functions of the short and quiet path routing application are described. The operation of the application is described by explaining the sequence of actions that are executed in solving a typical short and quiet path routing problem.

Essentially, the application has three distinct responsibilities:

- 1) It optimizes shortest paths (least cost paths by length).
- 2) It optimizes quiet paths (least cost paths by noise exposure -based costs).
- 3) It assesses dynamic exposure to noise on paths to make them comparable.

The application first loads the processed graph file to a NetworkX graph object and then calculates noise exposure -based costs to attributes of the edges. The environmental impedance function (chapter 3.5.1) is used to calculate the noise costs from contaminated distances with different noise levels (Figure 16). This process is not computationally demanding and could hence be set to run at runtime of the application as opposed to saving and loading the costs as edge attributes. Calculating and assigning the costs at runtime facilitated testing the effects of the different versions of the environmental impedance function and different sets of noise sensitivity indexes.

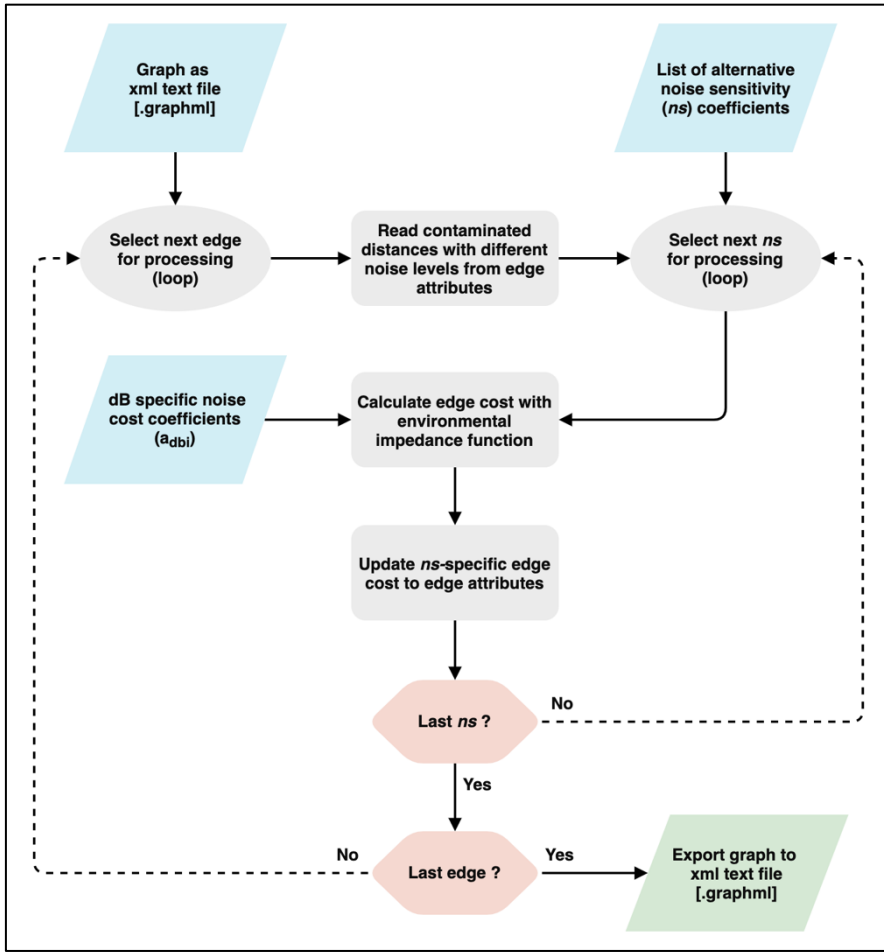


Figure 16. Workflow of calculating and adding noise sensitivity specific edge costs as new edge attributes.

To enable fast finding of origin and destination nodes for a given OD-pair, geometries of both feature types are collected to GeoPandas GeoDataFrames. Hence, the spatial indexes of the GeoDataFrames help to quickly narrow down the candidates for nearest edge and node at a given location. In most cases, the distance to the nearest edge is smaller than to the nearest node. Thus, a new node needs to be created to the graph at the nearest point on the nearest edge. Subsequently, two linking edges need to be created to the graph to connect the newly created node to the origin and destination nodes of the nearest edge. The geometrical operations for splitting the edge at the nearest point were implemented by utilizing the geometrical functions from Shapely package. Contaminated distances with different noise levels are then estimated for the linking edges as fractions of the respective contaminated distances of the nearest edge, based on the ratio of the length of the linking edge to the length of the nearest edge. Then, noise exposure -based costs (by different noise sensitivity coefficients) are calculated and updated to the edge attributes of the linking edges, allowing them to be used in the LCP analysis in the same way as all other edges.

The complete sequence of higher-level actions included in solving one quiet path routing problem is illustrated in Figure 17. As illustrated, a set of noise sensitivity coefficients is iterated in routing to calculate a set of alternative quiet paths, resulting a list of paths represented by sequences of node ids. At this stage, the number of paths is equal to the number of noise sensitivity indexes. Then, the respective edges of the paths are fetched from the graph object by the node ids of the paths (based on origin and destination nodes of the edges). Subsequently, the attributes of the edges are aggregated for each path. The line geometry of each path is constructed from the individual line geometries of its edges. Also, total length and contaminated distances with different noise levels and statistics on dynamic noise exposure are calculated from the aggregated edge attributes. The definitions of the indexes on dynamic noise exposure are in the following chapter (3.5.4).

Finally, paths having unique geometry are filtered out from the full set of (quiet) paths. The filtering is done in two phases. First, the paths having exactly same length are filtered out. Then, a simple overlay analysis is executed to filter out paths with nearly identical geometries. For each path, all paths that fall completely within a 30 m radius (buffer) around the path are collected. The collected paths must also have a length difference of less than 25 m. Then, the best path of the collection is determined by the normalized noise exposure index, which is defined in the following chapter (3.5.4). Only the best path of each collection is retained, resulting a set of fewer but geometrically more unique paths. One of the desired outcomes of this filtering step is to lose one of the two paths that take the same road but use different sidewalks by it. Another reason is posed by an issue with the OSM-based street network graph: some of the edge geometries are located in the middle of a road. Again, only the nearly similar path that uses the sidewalk by the road should be retained, if found. The shortest path is also included in this filtering process, and hence may be replaced with an overlapping quiet path.

Once the paths are fully processed, they are returned either as a GeoPandas GeoDataFrame or GeoJSON. The first format was appropriate in the assessment of pedestrians' exposure to traffic noise and the second one for the web-based quiet path application programming interface (quiet path API). The attributes and schema of the returned paths are described further in the next chapter (3.5.4) and in the documentation of the quiet path API (see x.x.).

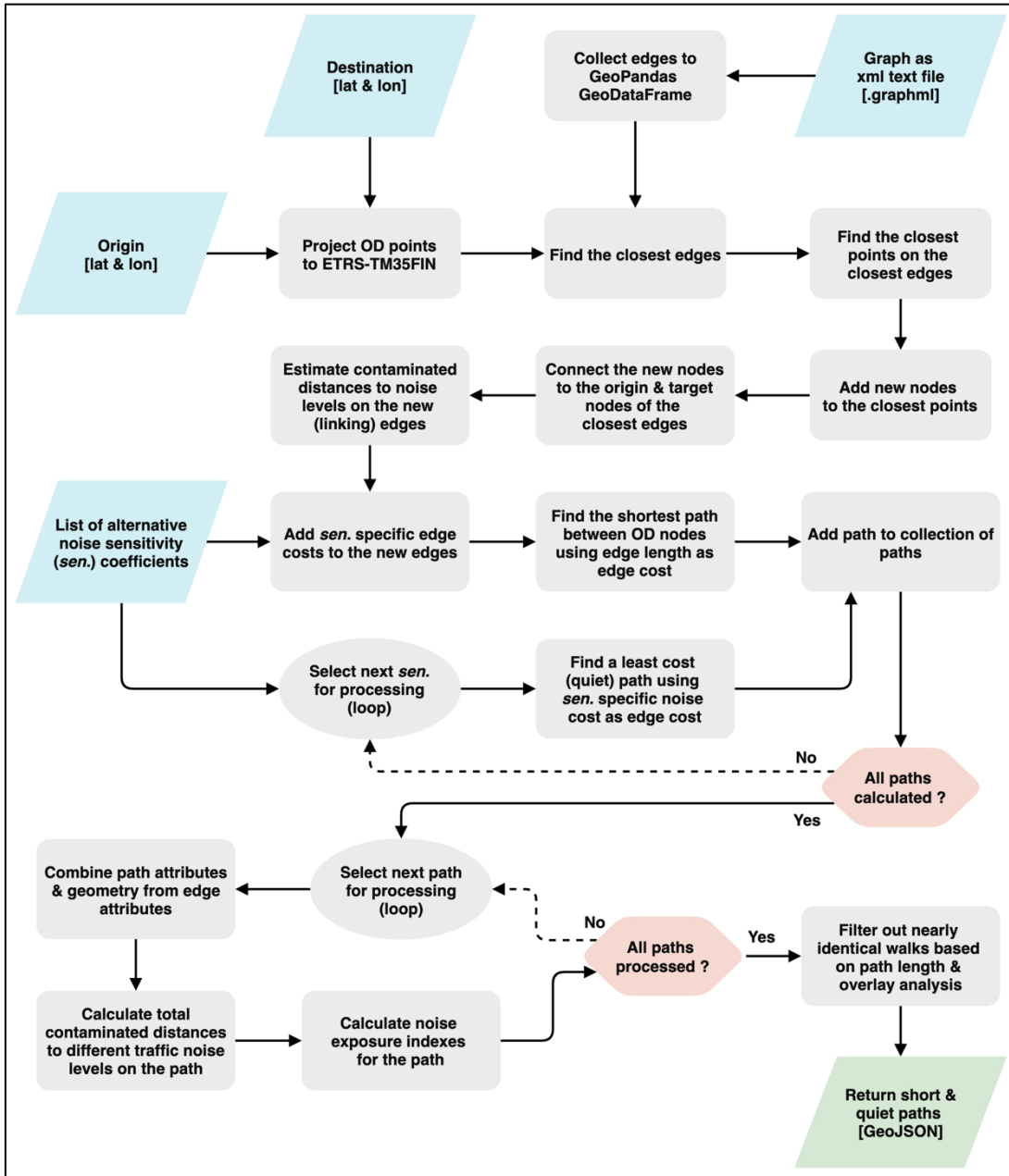


Figure 17. The sequence of high-level actions included in solving one short and quiet path routing problem.

### 3.5.4 Noise exposure assessment of short and quiet paths

A set of metrics and indexes was developed for assessing dynamic exposure to traffic noise on the paths optimized by the short and quiet path routing application. The indexes defined in this chapter (

Table 4) play a key role in comparing alternative quiet and short paths both in the web-based quiet path route planner and in the analysis of pedestrians' opportunities to reduce exposure to traffic noise. The key challenge in developing such indexes was compressing the information from contaminated distances with different traffic noise levels ( $ED_{dB_i}$ ) to simple but descriptive indexes of traffic noise exposure.

The simplest of the indexes ( $ED_{+dB_i}$  - Equation (6) describes the total cumulative contaminated distance (i.e. distance of exposure) with noise levels higher than a fixed threshold (e.g. exposure to traffic noise levels higher than 65 dB on a path). Then, a ratio of  $ED_{dB_i}$  to total length of the path can be calculated as a *dB-specific exposure ratio* ( $ER_{+dB_i}$  - Equation (7)). The exposure ratio can already be used to compare paths of different lengths, as it is distance normalized. The mean noise level ( $dB_{mean}$ ) of a path is calculated simply by adding up the products of its contaminated distances and the respective noise levels and dividing the sum with the total length (Equation (8)).

The noise cost equation of the environmental impedance function (2) was applied to define a *traffic noise exposure index* which aims to model the total noise-based environmental impedance of a path (EI - Equation (9)). Only a simple form of the noise cost equation was needed, excluding the base-cost (length) and the noise sensitivity coefficient ( $s = 1$ ). Also, a distance normalized version of the index was defined; the *distance normalized traffic noise exposure index* ( $EI_n$  - Equation (11)) varies between 0.0 and 1.0, as it is calculated by dividing the traffic noise exposure index of a path with the theoretical maximum traffic noise exposure index of a path of same length. Furthermore, the difference in EI can be calculated for a quiet path to measure the reduction in EI compared to the EI of the shortest path.

Table 4. Indexes describing exposure to traffic noise on a path and reduction in exposure to traffic noise on a quiet path.

Metric	Equation	Description
Contaminated distance with traffic noise level $dB_i$ (m)	$ED_{dB_i} = d_{dB_i}$	(5) The total (cumulative) exposure to traffic noise level $dB_i$ on the path
Total contaminated distance with traffic noise levels higher than $dB_i$ (m)	$ED_{+dB_i} = \sum_{i=+dB_i}^{dB_{max}} ED_{dB_i}$	(6)
Percentage of total contaminated distance with traffic noise levels higher than $dB_i$ of the total path length (%)	$ER_{+dB_i} = \frac{\sum_{i=+dB_i}^{dB_{max}} ED_{dB_i}}{d} * 100$	(7)
Mean dB on the path	$dB_{mean} = \frac{\sum_{i=dB_{min}}^{dB_{max}} ED_{dB_i} * dB_i}{d}$	(8)
Traffic noise exposure index (i.e. total noise-based environmental impedance)	$EI = \sum_{i=dB_{min}}^{dB_{max}} ED_{dB_i} * a_{dB_i}$	(9) Similar to environmental impedance function (2) but without noise sensitivity coefficient ( $s = 1$ )
Reduction in traffic noise exposure index (%)	$EI_{diff} = \frac{\Delta EI}{EI_s} * 100 = \frac{EI_q - EI_s}{EI_s} * 100$	(10) Reduction (%) in traffic noise exposure index between short and quiet path
Distance normalized traffic noise exposure index (index)	$EI_n = \frac{EI}{EI_{max}} = \frac{EI}{a_{max} * d} = \frac{EI}{a_{75dB} * d}$	(11) $EI$ of the path normalized by dividing it with maximum theoretical $EI$ for a path of same distance

$dB_i = 5$  dB range with  $dB_i$  as the lower value (e.g. 55 dB refers to noise range of 55–60 dB)

$ED_{dB_i}$  = total contaminated distance with noise level of  $dB_i$  (e.g. 14 m of 55–60 dB noise)

$a_{dB_i}$  = dB-specific noise cost coefficient (

$$a_{dB_i} = 10^{\frac{0.3 * dB_i}{10}} \quad (4)$$

where  $dB_i$  is the lower limit of a 5-dB interval and the minimum  $dB_i$  is 40. Respective noise cost coefficients for  $dB_i$  values from 45 dB to 75 dB are presented in **Error! Not a valid bookmark self-reference.** and in Figure 13. Applicability of the Stevens' power law is limited in this context due to

varying tone (and frequency distribution) of traffic noise at different distances from the sources as well as the related fact that it was not designed to work with A-weighted sound pressure levels (but with simple intensity metrics).

Equation (4) was selected for calculating the noise cost coefficients. The power law doubles the cost (loudness) roughly at every 10-dB increase, hence giving significantly higher costs to the highest noise levels. This is the most desired feature of the function, as the highest noise levels ( $> 65$  dB) are known to be the most harmful to people. The power function may also be partially supported by interpretation of the nonlinear HA%/L<sub>den</sub> curves in Figure 2 (Guski et al., 2017): a majority of the annoyance/SPL curves took the form “J” instead of a straight line, suggesting that an increase in SPL at a higher noise level may have a bigger effect on the perceived annoyance (and possibly loudness) compared to an equivalent increase in SPL at a lower noise level.

However, when both functions for noise cost coefficient were tested in developing the quiet path routing application, almost identical quiet paths were got in most cases. It may be that the sensitivity index and overall availability of quiet path options (between an OD-pair) override the effect of the small differences between the noise cost functions. The uncertainties in noise/annoyance/loudness relationships are considered further in the discussion (chapter 5.2).

Table 3)

$a_{max}$  = highest noise cost coefficient (

$$a_{dB_i} = 10^{\frac{0.3 * dB_i}{10}} \quad (4)$$

where  $dB_i$  is the lower limit of a 5-dB interval and the minimum  $dB_i$  is 40. Respective noise cost coefficients for  $dB_i$  values from 45 dB to 75 dB are presented in **Error! Not a valid bookmark self-reference.** and in Figure 13. Applicability of the Stevens’ power law is limited in this context due to varying tone (and frequency distribution) of traffic noise at different distances from the sources as well as the related fact that it was not designed to work with A-weighted sound pressure levels (but with simple intensity metrics).

Equation (4) was selected for calculating the noise cost coefficients. The power law doubles the cost (loudness) roughly at every 10-dB increase, hence giving significantly higher costs to the highest noise levels. This is the most desired feature of the function, as the highest noise levels ( $> 65$  dB) are known to be the most harmful to people. The power function may also be partially supported by interpretation of the nonlinear HA%/L<sub>den</sub> curves in Figure 2 (Guski et al., 2017): a majority of the

annoyance/SPL curves took the form “J” instead of a straight line, suggesting that an increase in SPL at a higher noise level may have a bigger effect on the perceived annoyance (and possibly loudness) compared to an equivalent increase in SPL at a lower noise level.

However, when both functions for noise cost coefficient were tested in developing the quiet path routing application, almost identical quiet paths were got in most cases. It may be that the sensitivity index and overall availability of quiet path options (between an OD-pair) override the effect of the small differences between the noise cost functions. The uncertainties in noise/annoyance/loudness relationships are considered further in the discussion (chapter 5.2).

Table 3)

$d$  = total path length (m).

### 3.6 Web-based quiet path route planner

A web-based quiet path route planner was developed as a proof of concept to demonstrate the potential utility of the quiet path routing method in practical situations. Also, it accelerated developing and adjusting the quiet path routing method, as different versions of the street network graph and environmental impedance function could be easily tested.

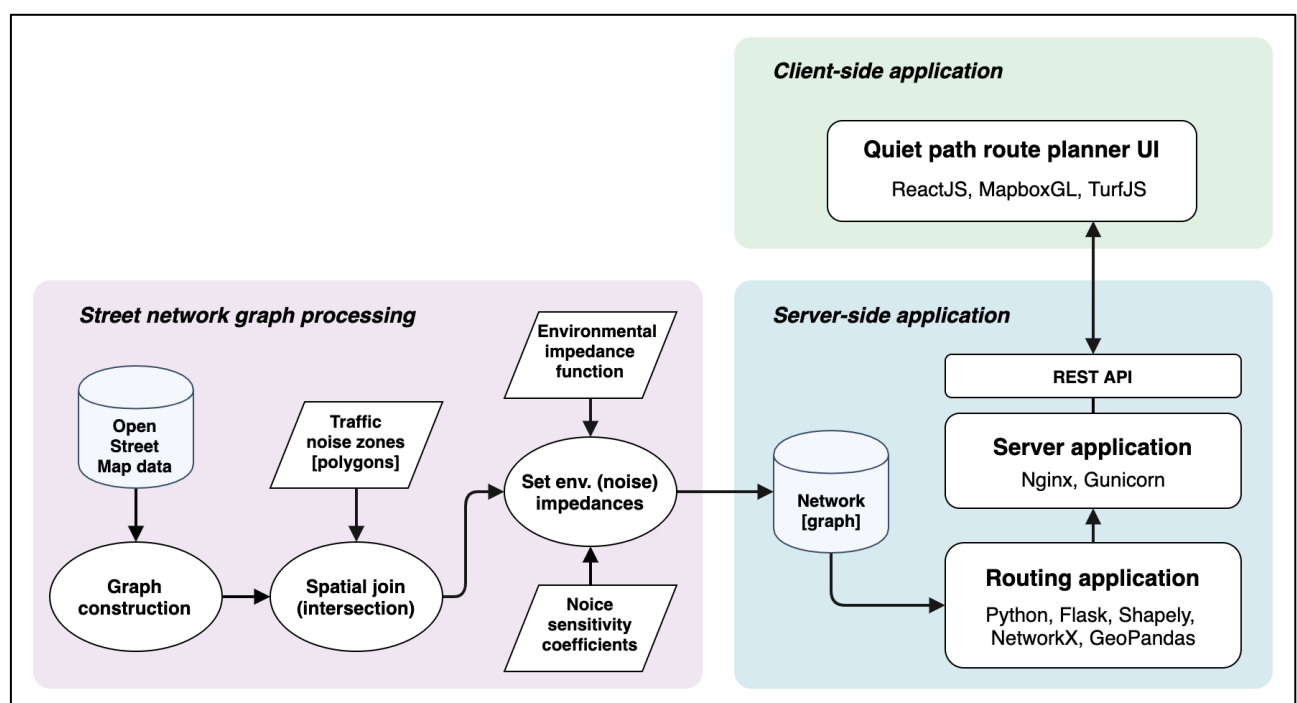


Figure 18. Technical architecture of the quiet path route planner web application.

The technical implementation of the quiet path route planner is composed of three components: 1) graph construction for quiet path routing, 2) server-side quiet path routing application and 3) client-side route planner user interface (Figure 18). The interface between the graph processing scripts and the routing application is a static graph file (in GraphML format). The client-side web application communicates with the routing application via a RESTful API (exposed by the server application). The quiet path routing API is documented in more detail in the chapter (x.x.).

A virtual machine was acquired for hosting the quiet path routing application as a stateless web service. The machine was provided by CSC (CSC - IT Center for Science, Finland) and it came with Ubuntu 18.04 operating system preinstalled. Again, the required Python environment was installed with Conda package manager to match the environment that was used in developing the application. In addition to the initial Python environment, the library Flask was installed to enable exposing the main functionality of the routing application to RESTful web requests. Since Flask is not recommended for production environments, the Python library Gunicorn (ref.), was configured to run the Python-Flask application in more efficient and secure manner. In practice this meant running several instances of the application in parallel to be able to handle multiple simultaneous routing requests. The web server Nginx (ref.) was installed and configured as a reverse proxy to handle all incoming and outgoing connections to the machine. Finally, the quiet path application (wrapped with Gunicorn) was configured as a system service and started.

An interactive web map application was developed to serve as a user interface for the quiet path routing service. It was implemented with ReactJS (ref.) as a single page application (SPA). Mapbox GL (ref.) was chosen as the web mapping library due to its great support for visualizing vector data interactively. This technical setup enabled building highly customized route planner interface for the purpose. Communication between the web map application and the routing service was implemented with asynchronous requests; after the routing request is sent from the client, a callback function (at the client) is invoked once the paths are returned from the routing service. The user-interface and features of the web-based route planner are described in more detail in the results chapter (x.x.).

During the making of this thesis, the web-based quiet path routing application, especially the user interface, was developed iteratively based on the comments and suggestions from a small group of test users. Closer to the end of the thesis project, the focus in developing of the routing application was guided also by the HOPE project. Thus, a support for assessing and minimizing exposure to also real-time air pollution was implemented in the routing application. Also, to enable significantly faster routing analysis for longer O-D distances, the routing analysis was migrated to utilize routing library

igraph (ref.) (instead of NetworkX). The links to the source-codes and further documentation of both versions of the routing application can be found in the results chapter (x.x).

## **3.7 Assessment of pedestrians' exposure to traffic noise at a neighborhood level**

### **3.7.1 Overview of the analysis**

In the following chapters, the word origin is used to refer to origins of commutes (i.e. home locations).

The assessment of pedestrians' exposure to traffic noise was implemented in two parts:

- 1) Identification of origin – PT stop (or commuting destination) walks and estimation of their utilization rates (Figure 19).
- 2) Assessment of pedestrians' exposure to traffic noise along the walks from homes to local PT stops (or commuting destinations) (Figure 20).

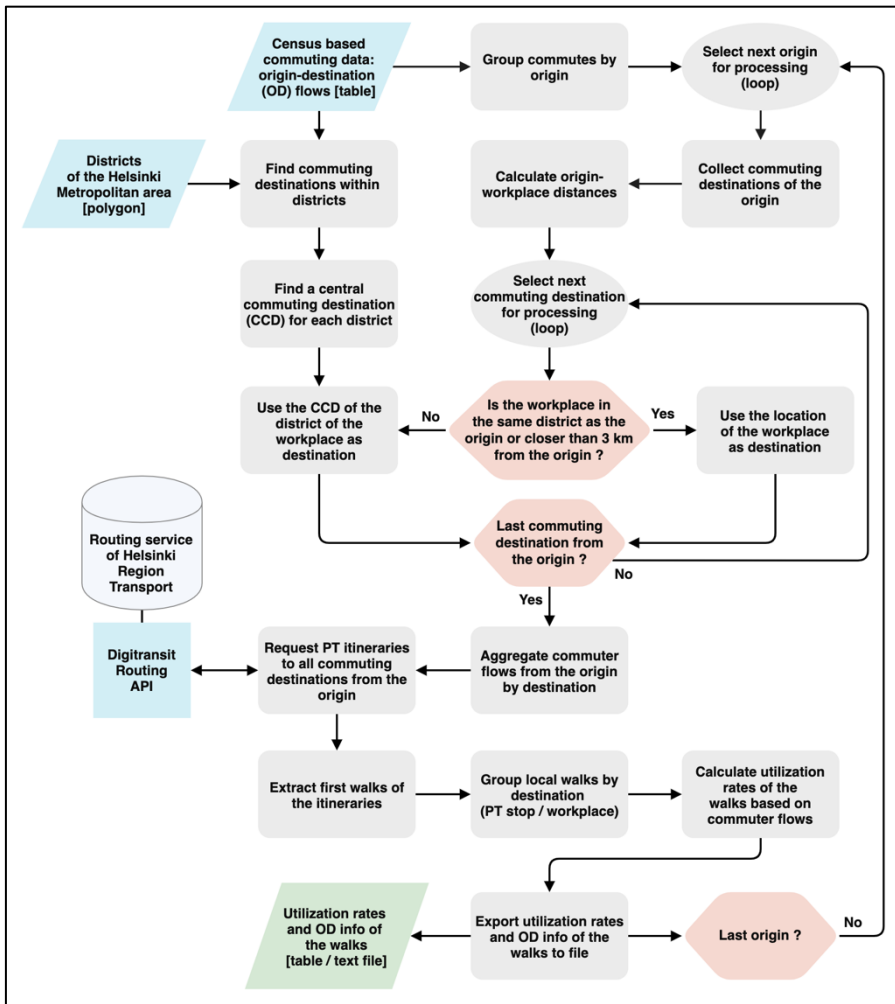


Figure 19. Workflow of the analysis for identifying origin – PT stop (or commuting destination) walks and estimating of their utilization rates based on commuter flows.

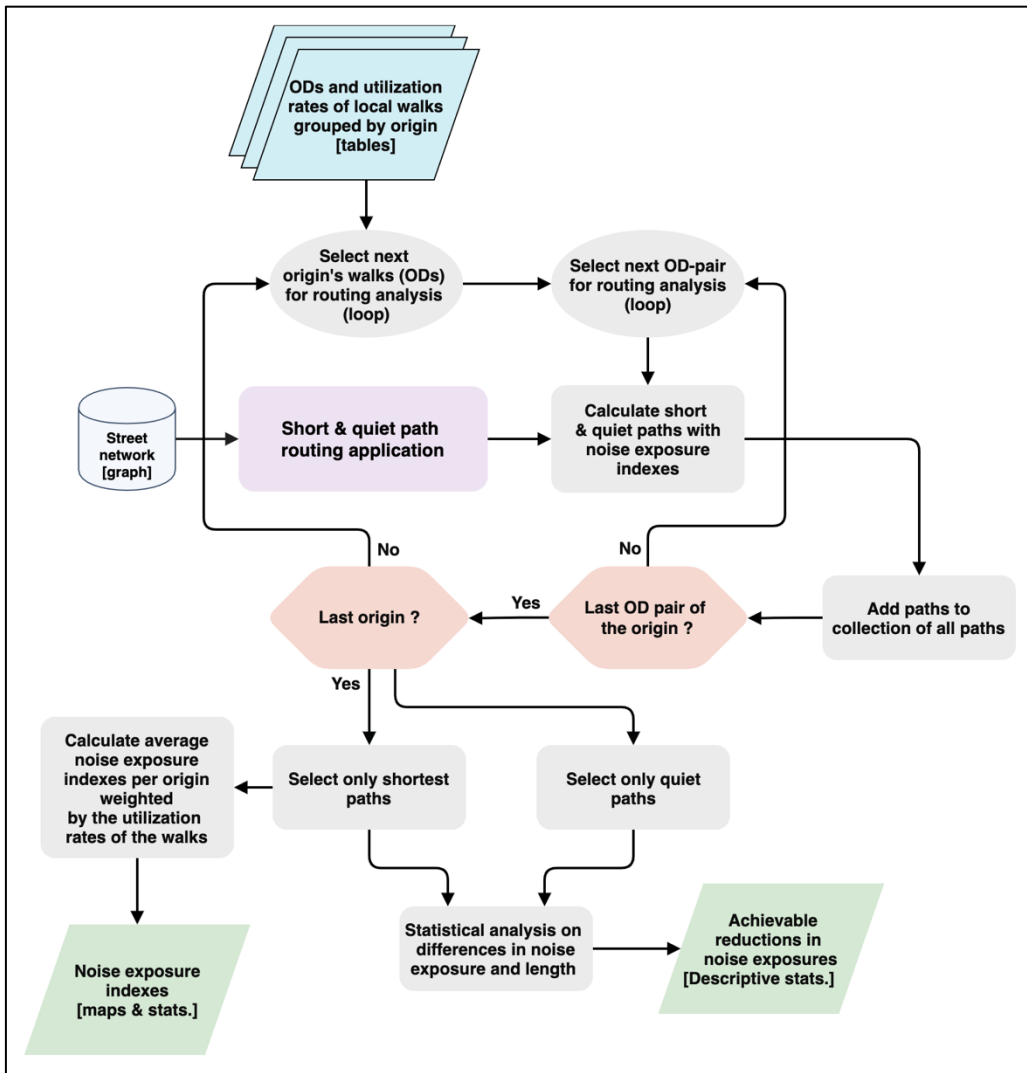


Figure 20. Workflow of the analysis for 1) calculating short and quiet paths by ODs of the local walks, 2) assessing exposures to traffic noise on the paths and 3) assessing achievable reductions in traffic noise exposure by taking quiet paths.

### 3.7.2 Estimation of local walks by commutes

Local walks to public transport stops (PT stops) or commuting destinations were identified as a result of an extensive routing analysis (Figure 19). Before the analysis, all commutes with origin in Helsinki were extracted from the YKR commuting data.

In this chapter, the steps of the analysis required for determining commuting destinations from one origin are described. The iteration of the analysis for the full set of origins is illustrated in the flowchart (Figure 19). The commuting destinations of the YKR data were used as destinations for all workplaces closer than 3 km from the origin. In order to limit the number of routing requests (to

Digitransit API) per origin, distant commuting destinations (farther than 3 km from the origin) were aggregated by their city district. The centers of the districts were used as the commuting destinations for the distant workplaces. The following sequence of GIS analysis was used to adjust the centers of the districts to better represent central workplace locations:

- 1) Create convex hull polygon around the commuting destinations within the district.
- 2) Calculate center of gravity for the convex hull polygon.
- 3) Calculate distance from commuting destinations (within the district) to the center of gravity.
- 4) Select the location of the commuting destination closest to the center of gravity.

For each origin-destination pair (commuter flow), three public transport itineraries were requested from Digitransit routing API. The (open) API is provided by the local public transport authority (Helsinki Region Transport - HRT/HSL). In the routing requests, walking speed was set as 70 m/min (Jäppinen et al., 2013; Toivonen et al., 2014). Default values were used for other routing parameters to match typical user preferences (Table 5). In cases where the routing request did not result any itineraries, origin or target location was slightly adjusted in order to reach the underlying street network.

The resulting itineraries were aggregated by origin. The first walks of the itineraries were extracted and grouped by their destinations. Two kinds of walks were found: 1) walks from origins to PT stops and 2) walks from origins to commuting destinations. Walks from each origin were grouped by their destination and respective utilization rates of the walks were calculated for all unique origin-destination pairs (Figure 21).

Table 5. Parameters used in routing with Digitransit routing API.

Parameter	Value
Origin	Center of the YKR grid cell
Destination	Destination of the commute
Date	Monday 8:30 am, 05/27/2019
Walking speed	70 m/min
Means of transport used	All except city bikes
Transfer safety margin	0 min
Number of itineraries to suggest	3

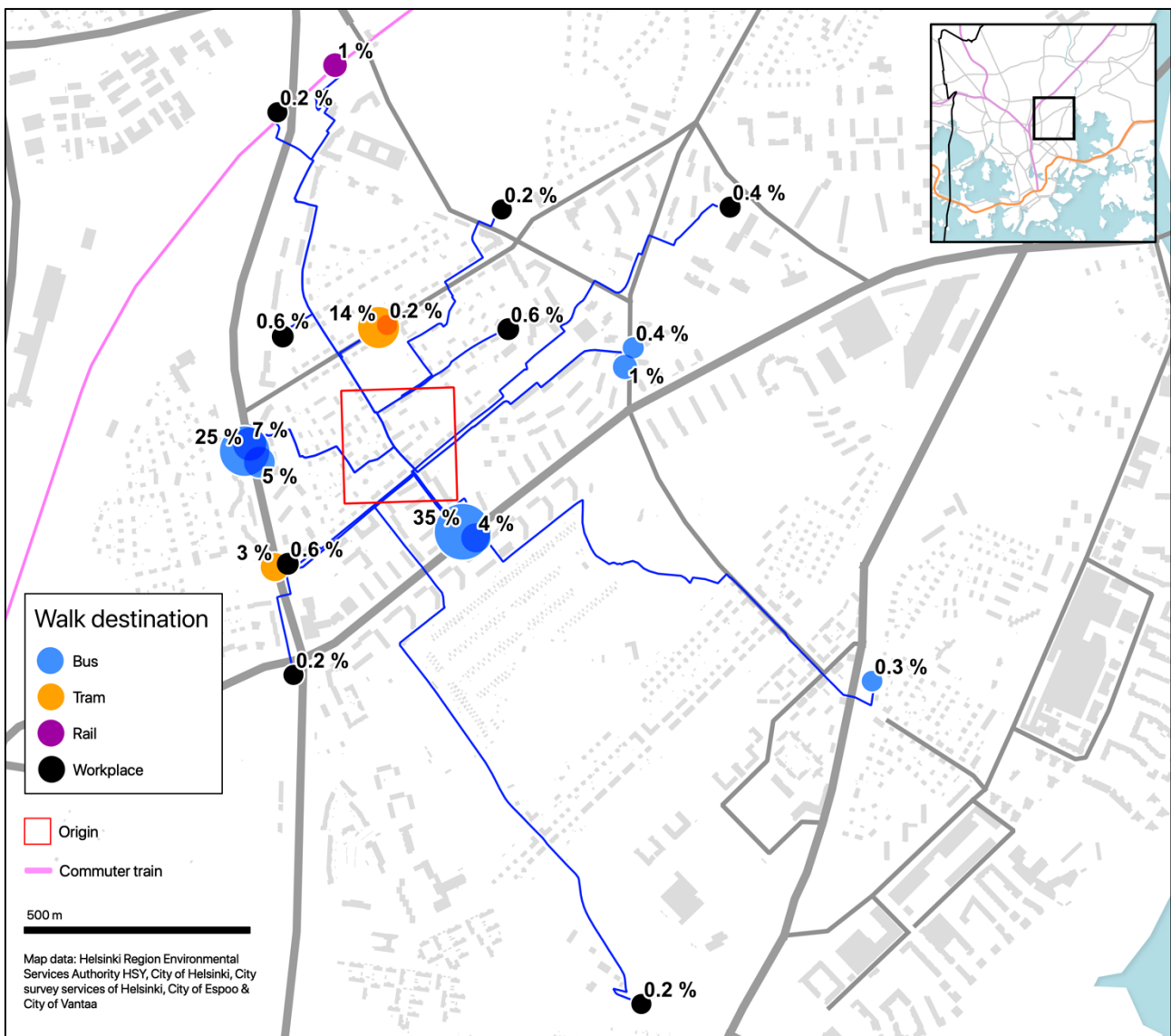


Figure 21. An example of local walks (and utilization ratios) from one origin as a result of the routing analysis. Most of the destinations of the walks are public transport stops.

In order to validate the results of the routing analysis, sums of the utilization rates of the walks were compared to the total flow of commutes for each origin (by the initial YKR commuting data). Of the total number of commutes from the study area (296470), 83% were included in the analysis. The mean inclusion of commutes per origin was 81% with standard deviation of 14%. The routing analysis performed well at most central and residential areas, but considerable share of the commutes from several remote and coastal areas were excluded (Figure 22). Plotting the numbers of commutes against the inclusion of the commutes (in the routing analysis) by origin revealed that the low inclusion of commutes affected mainly origins with fewer commutes (Figure 23). Moreover, by

exploring the origin-level commuting statistics, it was found that of the origins with less than 50% inclusion of commutes (in the routing analysis), none had more than 12 commutes total.

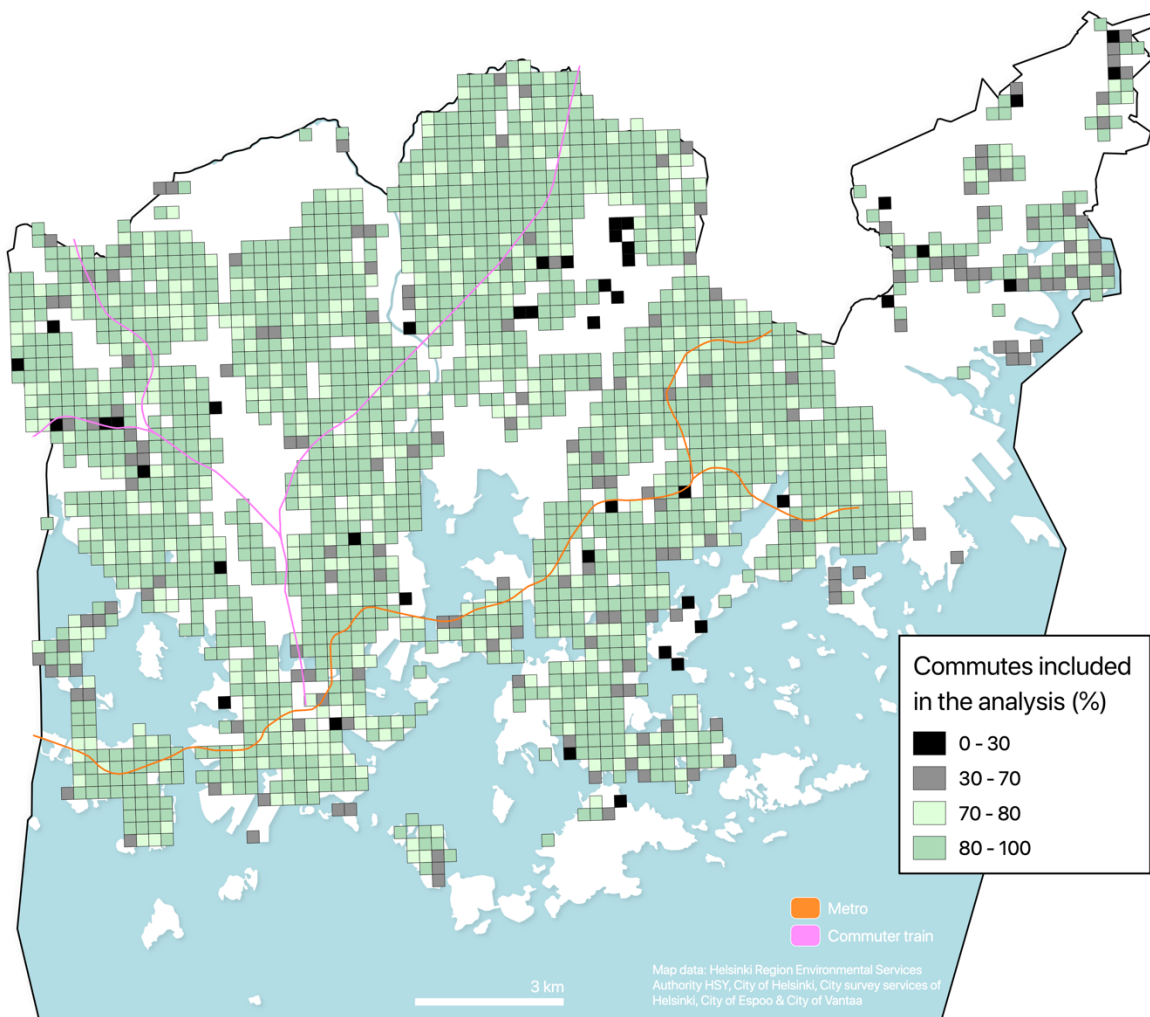


Figure 22. Inclusion (%) of commutes per origin in the analysis for finding local PT stops and walks.

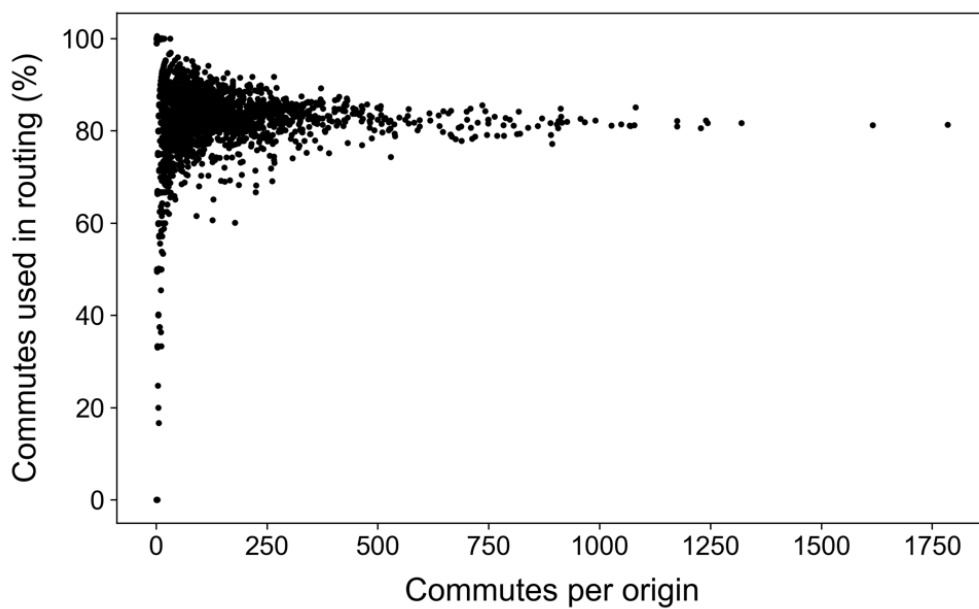


Figure 23. Number of commutes vs. commutes included in the routing analysis (%) per origin.

### 3.7.3 Least cost path calculations: short and quiet paths

Short and set of alternative quiet paths were optimized for all local walks with the quiet path routing application developed in this study. The utilization rate of each walk was inherited as attribute information for the respective short and quiet paths. The noise sensitivity coefficients 0.1, 0.15, 0.25, 0.5, 1, 1.5, 2, 4, 6, 10, 20 and 40 were used in the quiet path routing. This set of noise sensitivity coefficients was found to perform well in quiet path routing, providing appropriate balance between performance and path variability. In most cases, multiple identical or nearly identical quiet paths were found, indicating that adding more sensitivity coefficients would not have provided more quiet path alternatives. Once all paths were processed, descriptive statistics of the lengths of the shortest paths were calculated (Table 6). Figure 24 illustrates the volume of the (shortest) paths at different locations.

Table 6. Descriptive statistics of the length of the shortest paths to PT stops and workplaces (n=31291).

Path length (m)	Mean	Median	SD	p10	p25	p57	p90
All (n=31291)	490	408	338	135	234	669	964
To PT stops (n=18716)	472	396	317	132	229	647	923

To workplaces (n=12575)	882	771	486	332	451	1207	1580
-------------------------	-----	-----	-----	-----	-----	------	------

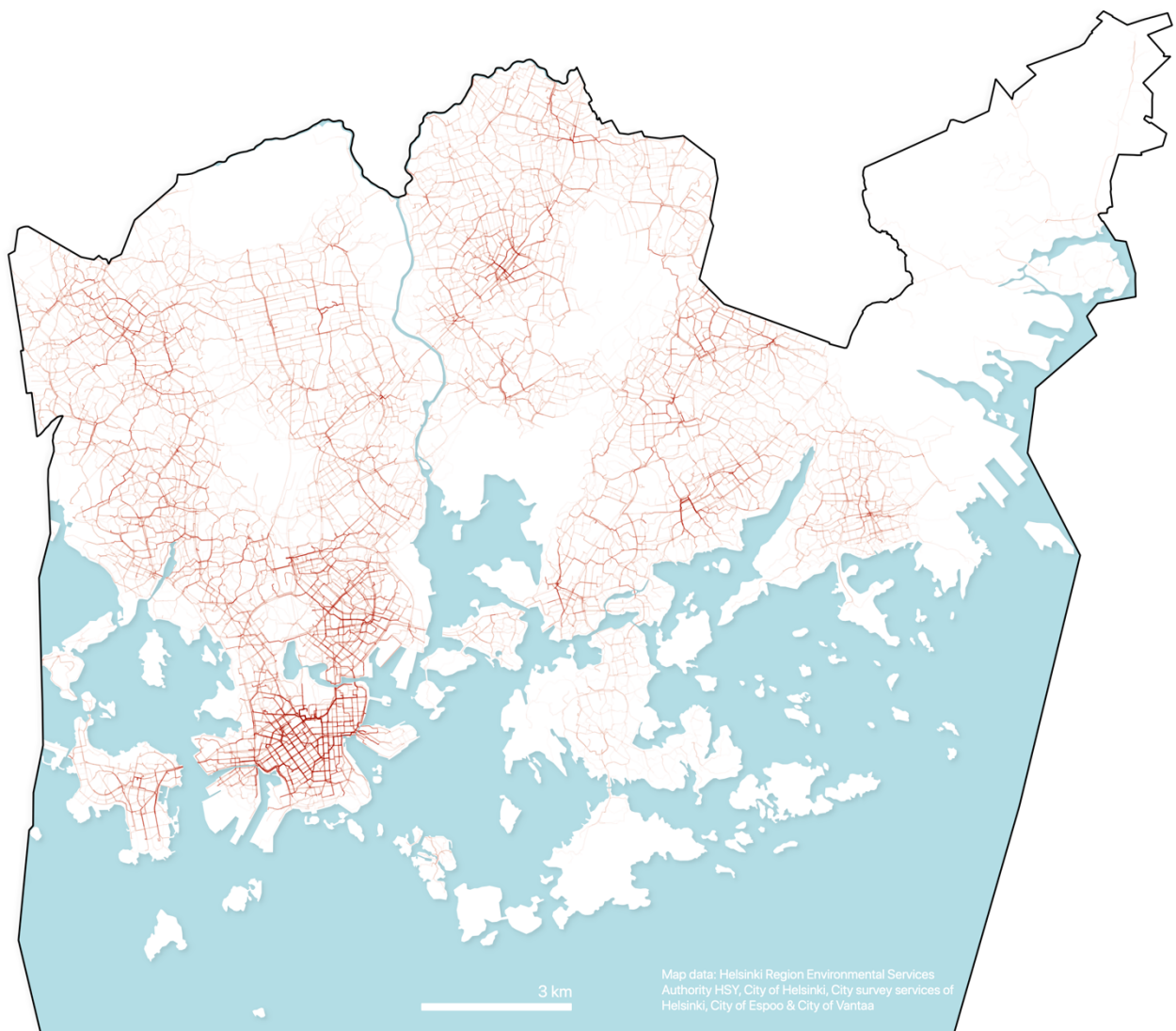


Figure 24. All shortest paths visualized with feature blending method: overlapping paths show darker on the map.

### 3.7.4 Assessment of exposures to traffic noise on the paths

As noise exposure assessment of the paths was already a built-in feature of the short and quiet path routing application, no separate analysis for determining the exposures to traffic noise on the paths was needed. Descriptive statistics of the noise exposure indexes (Table 4) of all paths were calculated and weighted by the utilization rates of the walks. The descriptive statistics were calculated both for all paths and for a subset of only the origin–PT stop paths (excluding origin–workplace paths).

Also, origin-level statistics of noise exposure indexes were calculated to enable exploring possible spatial differences in exposures with map visualizations. In this analysis, only the origin–PT stop paths were included, to assess the noise exposures on the most local walks of each origin. The descriptive statistics were weighted by the utilization rates of the paths (walks). Therefore, the (weighted) mean noise exposure indexes can indicate the expected noise exposure on a random or typical walk from each origin. All paths that were not completely inside the extent of the noise surface data were filtered out in the analysis. The total utilization rates of the paths that were included in the analysis were added up per origin, to assess the statistical significance of the results (per origin).

### **3.7.5 Assessment of achievable reductions in exposure to traffic noise**

A statistical analysis was conducted to assess the achievable reductions in exposure to traffic noise on the quiet paths. The achievable reductions in exposures were calculated at OD pair -level, by comparing the noise exposure indexes of the different quiet paths to the corresponding noise exposure indexes of the shortest paths. The effects of the following properties of the paths were evaluated with respect to the achieved reductions in noise exposures:

- 1) Distance between origin and destination (O-D distance)
- 2) Noise exposure indexes of the shortest path
- 3) Length difference between quiet and shortest path

Two subsets of the paths (grouped by OD) were created to assess the effect of the length of the shortest path (O-D distance) in the magnitudes of the achievable reductions in noise exposure. Paths within the length range from 300 m to 600 m were added to the first set (“paths of short to medium length”) and paths within the length range from 700 m to 1300 m meters to the second set (“long paths”).

The reductions in exposures were measured against a set of thresholds of maximum length differences. The noise exposure indexes of each shortest path were compared to the noise exposure indexes of the corresponding quiet paths with maximum length difference of 100, 200 and 300 meters (respectively). Hence, for each OD-pair, three metrics of achievable reductions in noise exposure indexes were calculated, one for each length difference threshold. Descriptive statistics of reductions in noise exposure indexes with maximum length differences of 100, 200 and 300 meters were calculated per OD pair. In addition, scatterplots of reductions in exposures and length differences were made to explore the relationship between length difference and achievable reductions in noise exposures. Also, the numbers of quiet paths were compared against the lengths of the shortest paths

by scatterplots and boxplots. It was anticipated that more quiet path alternatives were found for longer shortest paths.

Another aggregation of the paths was done by creating several subsets of the OD-level statistics by the exposure indexes of the shortest paths. Thus, the magnitude of the achievable reductions in noise exposures could be assessed also with respect to the initial noise exposures on the shortest paths. Moreover, a simple linear regression analysis was executed between the reductions in the indexes and the initial values of the indexes (on the shortest paths). Here, it was anticipated that for a higher noise exposure on a shortest path, also higher achievable reductions would be found on the respective quiet paths. Finally, the descriptive statistics of the metrics on achievable reductions in noise exposures could then be interpreted as answers to the questions of type “How much reduction in traffic noise exposure was achievable by choosing a quiet path no longer than 100 meters more than to the length of the shortest path”.

## 4 Results

### 4.1 Pedestrians' exposure to traffic noise

Table 7 and Table 8 represent both the typical exposures and variance in exposures to traffic noise on home–PT stop walks (Table 8) and on home–workplace walks, including only shortest paths in these statistics. The noise exposure on the paths was assessed by several noise exposure indexes (defined in chapter 3.5.4). The noise thresholds 60 dB, 65 dB and 70 dB were selected for the exposure indexes in order to assess exposures to the highest traffic noise levels. In Table 8, the direct walks to workplaces are excluded from the statistics. The statistics are weighted by utilization rates of the walks and hence better represent typical exposures to traffic noise. The paths included in Table 8 were shorter than the ones in Table 7 on average, as per the descriptive statistic of path lengths presented in Table 6. Respectively, the unnormalized noise exposure indexes were higher for the longer paths (in Table 7). It can be read from the Table 7, that the higher the threshold of the noise exposure index, the smaller the exposure. On average, almost half (46 %) of the total distance of the walks was exposed to traffic noise levels higher than 60 dB. Reduced mean exposures were found for higher noise levels, yet still considerably high (e.g. mean  $ER_{+65dB}$  of 30 %). However, also great variances in exposure indexes can be seen, indicating highly unequal exposures to traffic noise between different walks.

Table 7. Descriptive statistics of exposure to traffic noise on the first walks of public transport itineraries to workplaces and on direct walks to nearby workplaces (n=31291).

Variable	Mean	Median	SD	p10	p25	p75	p90
EI	100	74	93	15	35	135	221
EI <sub>n</sub>	0.36	0.34	0.22	0.07	0.19	0.53	0.66
dB <sub>mean</sub>	58	57	7	47	52	63	67
ED <sub>+60dB</sub> (m)	210	142	215	13	64	293	497
ED <sub>+65dB</sub> (m)	136	75	176	0	22	179	342
ED <sub>+70dB</sub> (m)	53	8	101	0	0	64	150
ER <sub>+60dB</sub> (%)	46	41	33	4	18	74	100
ER <sub>+65dB</sub> (%)	30	21	30	0	5	47	79

ER <sub>+70dB</sub> (%)	12	2	20	0	0	14	37
-------------------------	----	---	----	---	---	----	----

Table 8. Descriptive statistics of exposure to traffic noise on the first walks of public transport itineraries to workplaces (direct walks to nearby workplaces are filtered out, n=18716).

Variable	Mean	Median	SD	p10	p25	p75	p90
EI	96	72	87	15	35	131	212
EI <sub>n</sub>	0.36	0.34	0.22	0.08	0.19	0.53	0.66
dB <sub>mean</sub>	58	58	7	48	52	63	67
ED <sub>+60dB</sub> (m)	203	140	203	15	64	283	475
ED <sub>+65dB</sub> (m)	130	74	165	0	22	173	330
ED <sub>+70dB</sub> (m)	50	8	94	0	0	63	142
ER <sub>+60dB</sub> (%)	47	41	33	4	19	75	100
ER <sub>+65dB</sub> (%)	30	21	30	0	5	47	80
ER <sub>+70dB</sub> (%)	12	2	20	0	0	14	37

## 4.2 Spatial patterns in pedestrians' exposures to traffic noise

Direct walks to workplaces were excluded in the spatial analysis on pedestrians' exposure to traffic noise. Consequently, the results are based on the noise exposures on the most local walks of each origin. Figure 25 represents a map of average walking distances from origins to PT stops. Figure 26 represents a map of average traffic noise levels (dB<sub>mean</sub>) on the walks from each grid cell. Figure 27 and Figure 28 represent maps of average walking distances in traffic noise levels exceeding noise level thresholds of 65 dB and 70 dB (ED<sub>+65dB</sub> & ED<sub>+70dB</sub>).

The choropleth maps present the average traffic noise exposure indexes weighted with the estimated utilization rates of the walks. Hence, the concepts: 1) *an average local walk*, 2) *a typical local walk* and 3) *an expected local walk* can be used in interpreting the origin-level noise exposure indexes. They aim to consider the spatial and statistical nature of the choropleth maps; as they were weighted with the estimated utilization rates of the walks, they can estimate the traffic noise exposure on an average (commuting-related) walk from each origin.

Some spatial patterns in the noise exposure indexes are clearly visible in the maps. Exposure to the highest  $\text{dB}_{\text{mean}}$  occurs usually (but not always) on the walks from the origins near the major roads of the city. Similarly, the highest average exposures  $\text{ED}_{+65\text{dB}}$  and  $\text{ED}_{+70\text{dB}}$  occur usually near the major roads of the city, but with significant spatial variation. No significant correlation between walking distances from the origins to the respective  $\text{ED}_{+65\text{dB}}$  and  $\text{ED}_{+70\text{dB}}$  values can be seen by visual comparison of the maps. By exploring the maps of average  $\text{ED}_{+65\text{dB}}$  and  $\text{ED}_{+70\text{dB}}$ , it can be said that the highest exposures to the highest noise levels are distributed unequally in the study area. The choropleth maps of average  $\text{ER}_{+65\text{dB}}$  and  $\text{ER}_{+70\text{dB}}$  were not included in the results, as only similar spatial patterns were present in them than already presented for  $\text{dB}_{\text{mean}}$ .

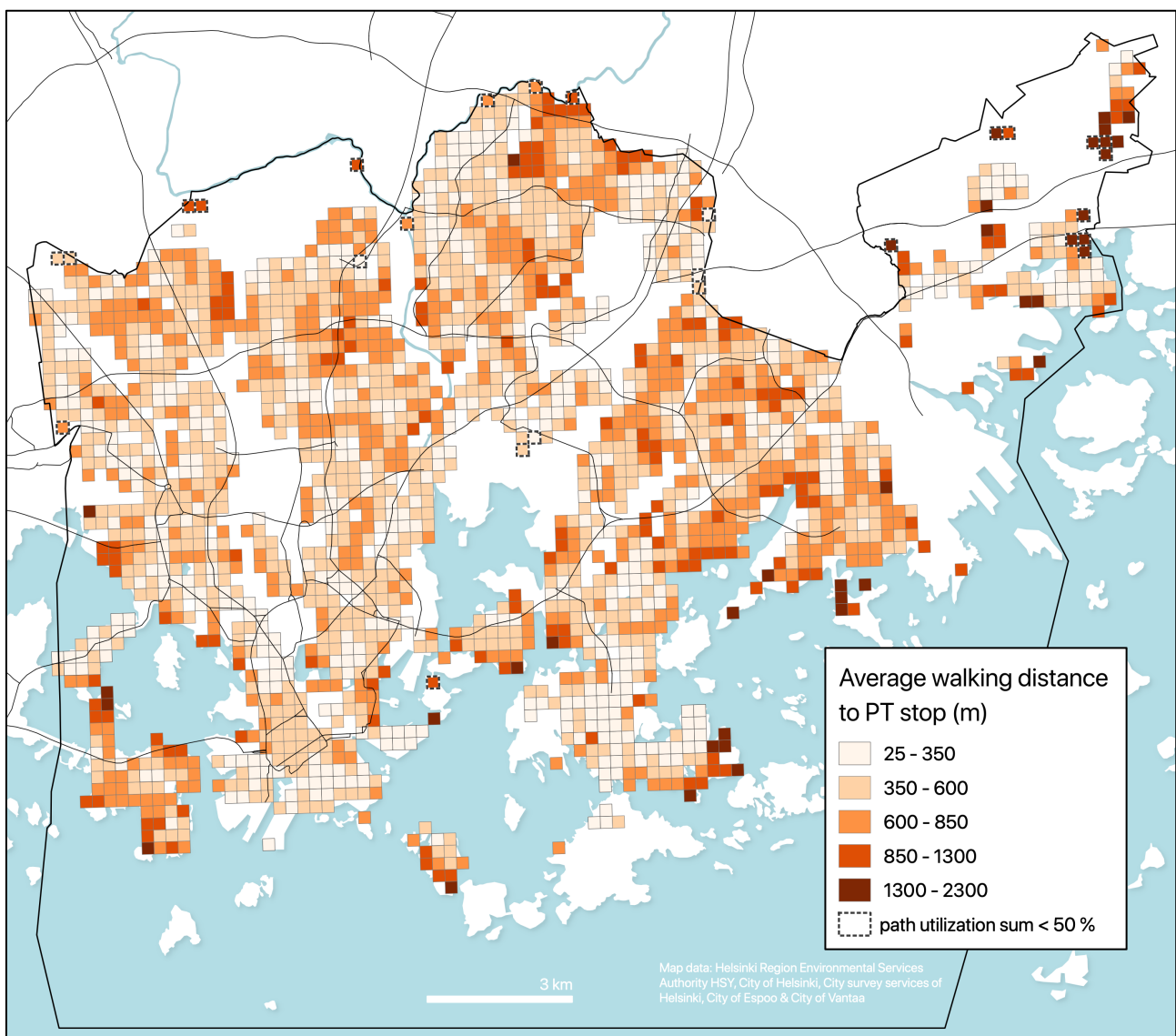


Figure 25. The average walking distance from homes to public transport (PT) stops. The averages are weighted with the estimated utilization rates of the walks based on the total flow of commutes utilizing each PT stop.

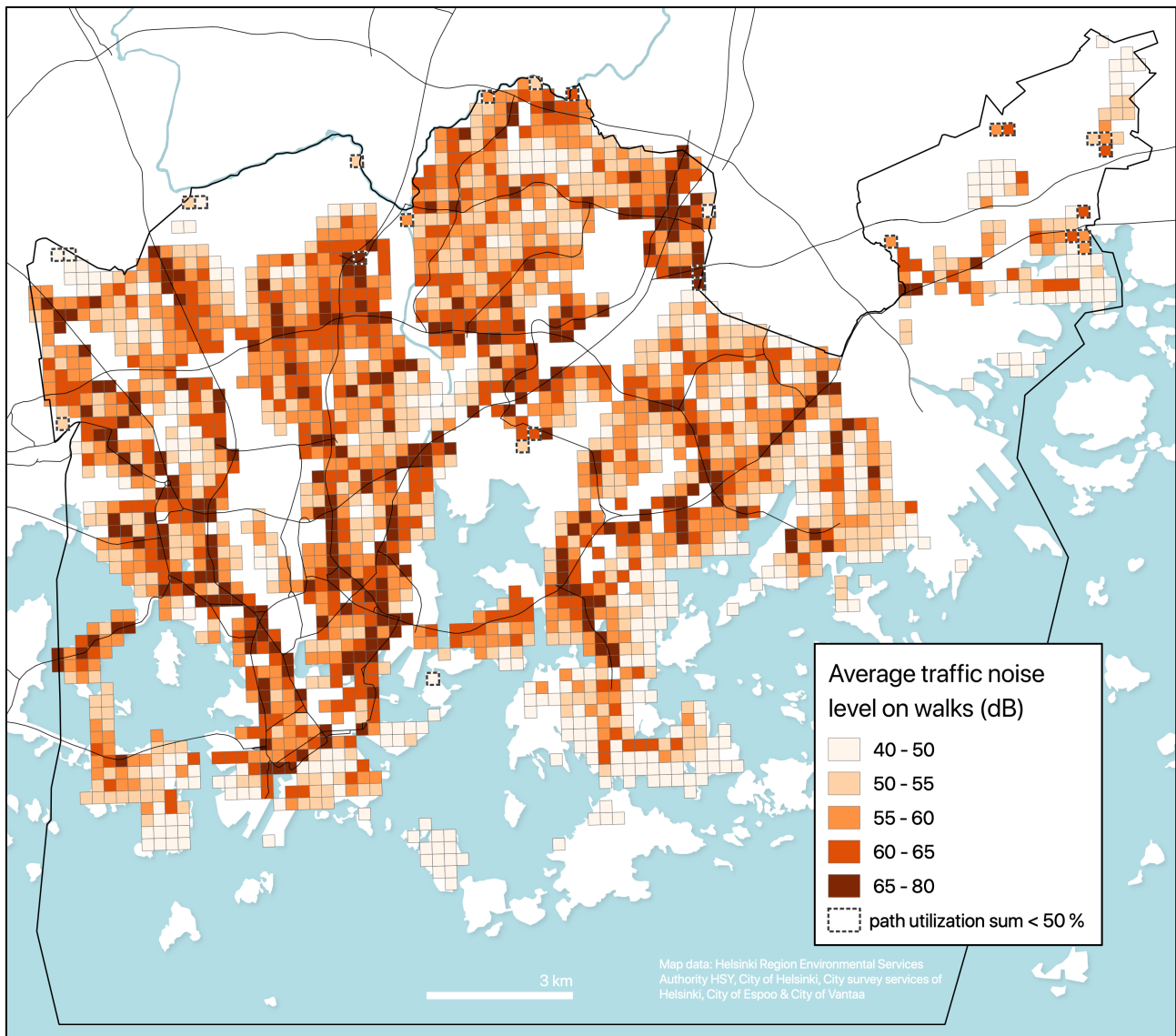


Figure 26. The mean dB on walks from homes to PT stops. The averages are weighted with the estimated utilization rates of the walks based on the total flow of commutes utilizing each PT stop.

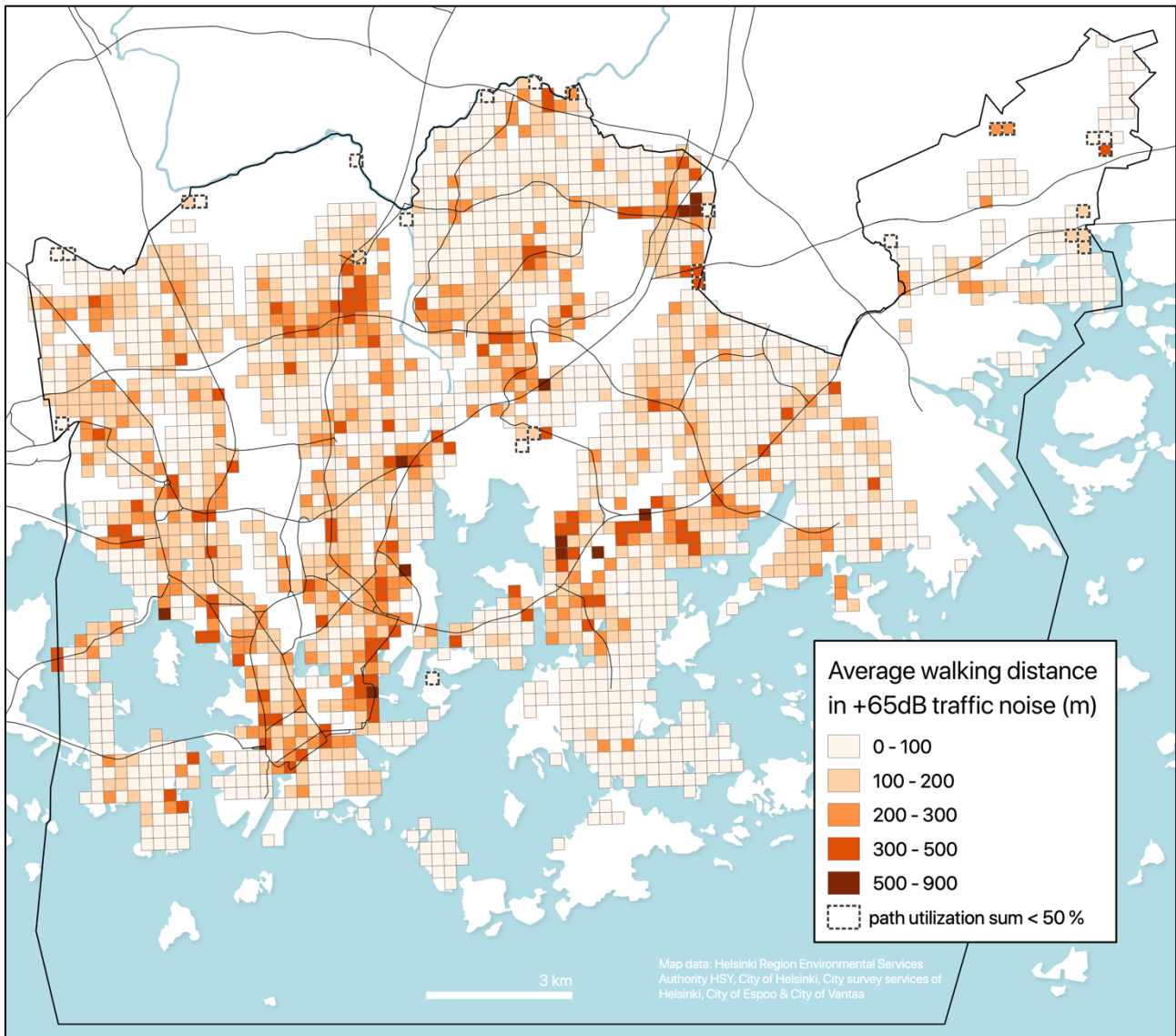


Figure 27. The average walking distance in +65 dB traffic noise level on walks from homes to public transport (PT) stops. The averages are weighted with the estimated utilization rates of the walks based on the total flow of commutes utilizing each PT stop.

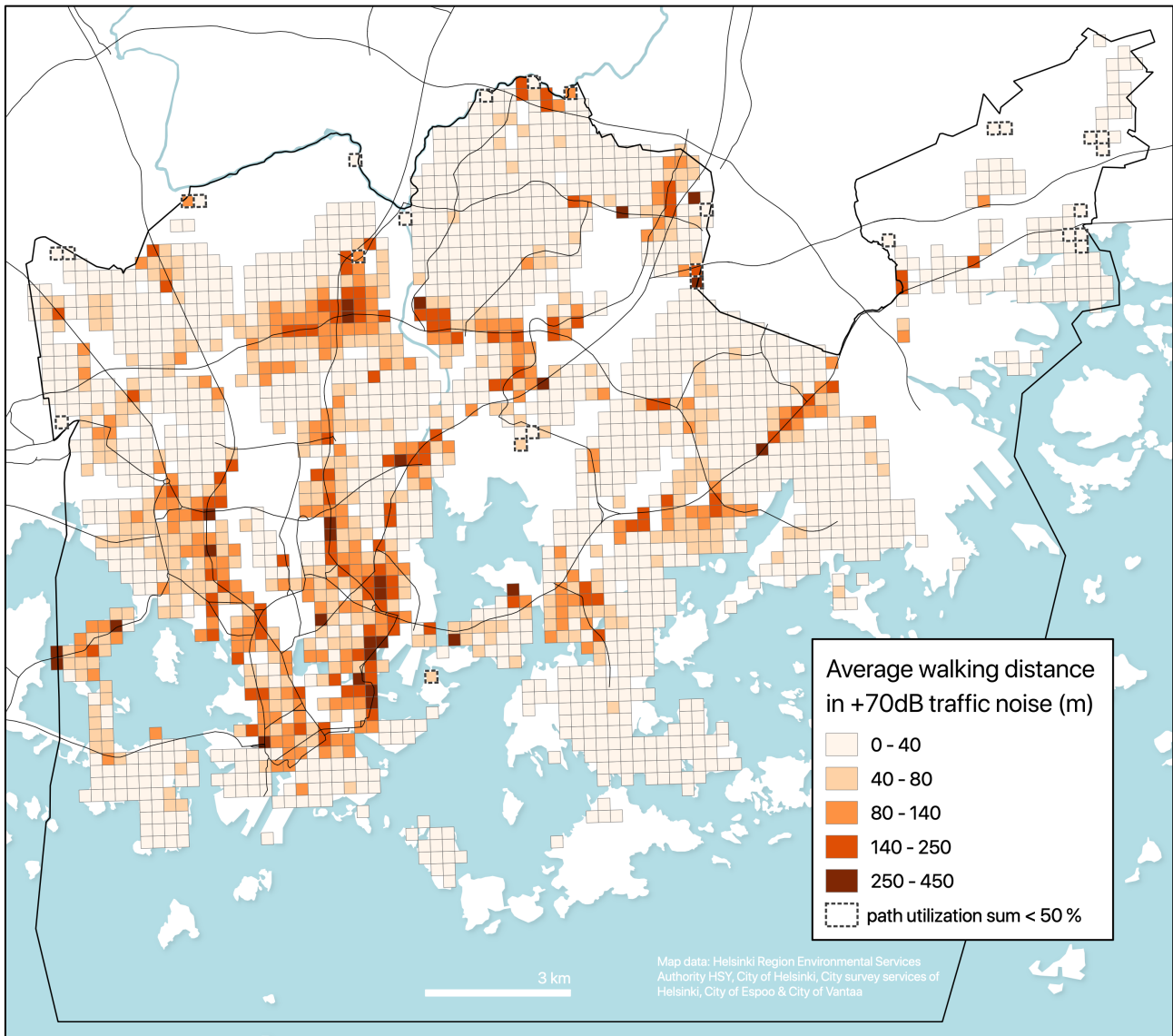


Figure 28. The average walking distance in +70 dB traffic noise level on walks from homes to public transport (PT) stops. The averages are weighted with the estimated utilization rates of the walks based on the total flow of commutes utilizing each PT stop.

### 4.3 Quiet path routing API

- At the time of writing this, the quiet path route planner service exposes an open quiet path routing API.

### 4.4 Quiet path route planner

Figure 29 represents a typical user story of the quiet path route planner application. The user story covers the basic sequence of actions required for getting route suggestions for one OD-pair. Since the main objective of the route planner application was to serve as a proof of concept of the quiet path

routing method, only the necessary functionalities were implemented. Hence, for example, the user can select the origin and destination only by finding them on the map - a sophisticated address geocoding functionality was not implemented in the user-interface due to the limited scope of the thesis project.

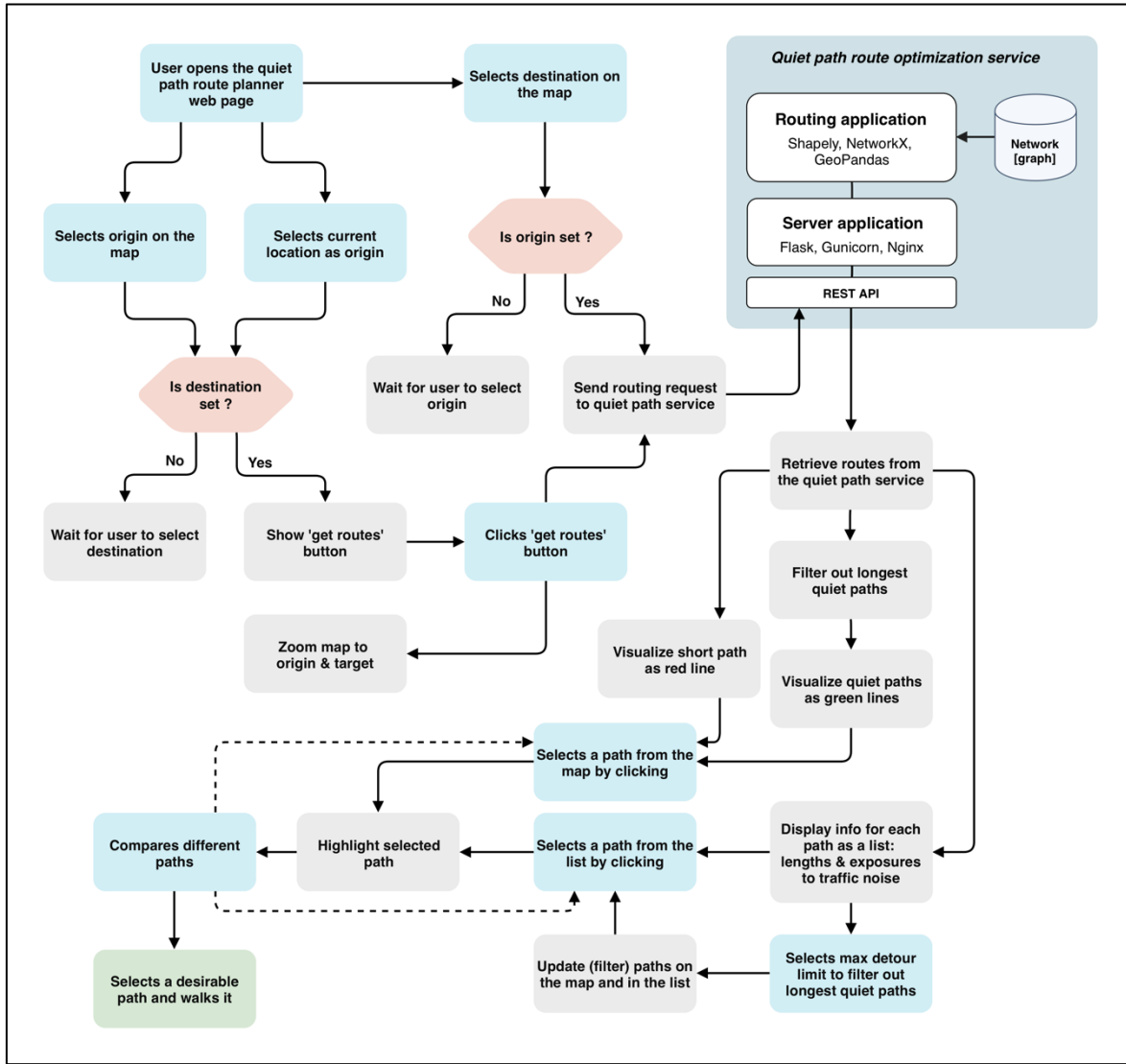


Figure 29. A typical user story demonstrating the basic functionality of the quiet path route planner. (Blue / green = user's actions; grey = actions of the user interface; white = components of the quiet path routing service).

Figure 30. Landing page of the quiet path route planner.

Figure 31. Display of path options and exposures to noise along the alternative paths.

Figure 32. Display of path alternatives.

Figure 33. User-interface of the route planner in a situation where no alternative quiet paths were found.

#### 4.5 Achievable reductions in exposure to traffic noise

A statistical analysis was performed to assess the performance of the quiet path routing in terms of achievable reductions in exposure to traffic noise. In order to assess the effect of O–D distance in the quality of the quiet paths, descriptive statistics were calculated separately for two groups of paths: 1) short paths within the length range from 300 m to 600 m and 2) long paths within the length range from 700 m to 1300 m.

The following four noise exposure indexes were chosen as the metrics by which achievable reductions in traffic noise exposure was assessed:

- 1)  $\text{dB}_{\text{mean}}$  (mean noise level on the path)
- 2)  $\text{ER}_{+60\text{dB}}$  (percentage of exposure to traffic noise levels higher than 60 dB).
- 3)  $\text{ER}_{+65\text{dB}}$  (percentage of exposure to traffic noise levels higher than 65 dB).
- 4) EI (index of total exposure to traffic noise)

In the following chapters, the term *initial noise exposure index* is used to refer to the noise exposure index of a shortest path of a given OD-pair. Figure 34 represents a set of scatterplots of achievable reductions in the above traffic noise exposure indexes against the initial noise exposure indexes for the subset of paths of short O-D distances (300–600 m). For each index, three scatterplots were created by the set of three maximum length additions of the quiet paths (compared to the length of the respective shortest path). In addition, the results of the linear regression analysis are shown in the figure, respectively for each scatterplot. Figure 35 represents the same set of scatterplots and metrics

as Figure 34, but for the longer paths (700–1300 m). Three important observations can be made by assessing the scatterplots and the results of the regression analysis:

- 1) Higher exposure to noise on the shortest path increases the achievable noise reduction (on the quiet paths).
- 2) Greater length addition of the quiet path (compared to the length of the shortest path) seem to predict higher reduction in exposure to noise.
- 3) The statistical relationships between the reductions in noise exposure indexes and the initial noise exposure indexes are stronger for the longer paths (Figure 35 vs. Figure 34).

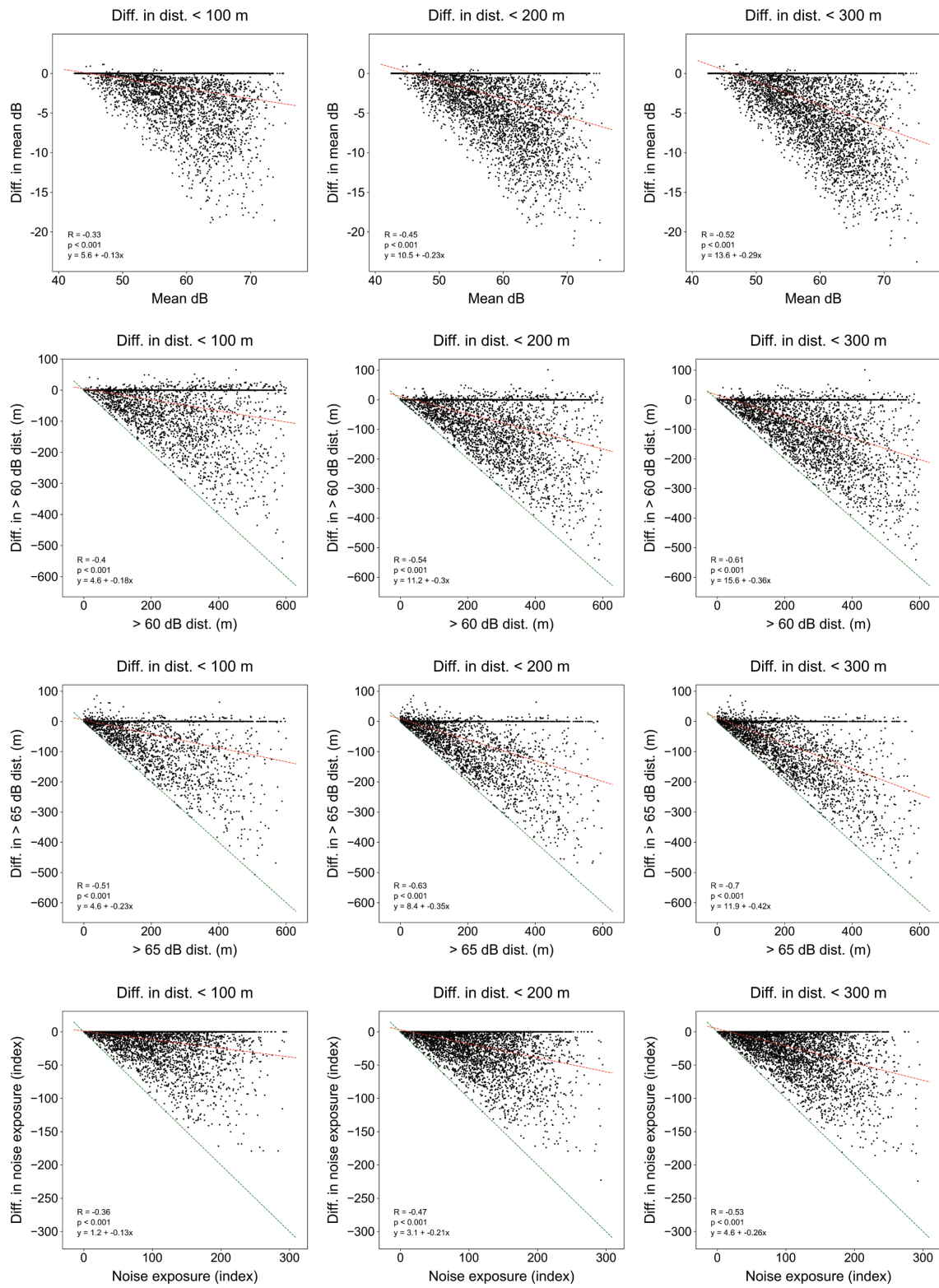


Figure 34. Regression analysis between the reductions in exposures to traffic noise on quiet paths and the traffic noise indexes of the respective shortest paths. Shortest paths within the length range of 300 m to 600 m were selected in the analysis (as well as the respective quiet paths). The red lines represent the regression lines of the regression analysis and the green lines show the theoretical maximum reductions in the noise exposure indexes.

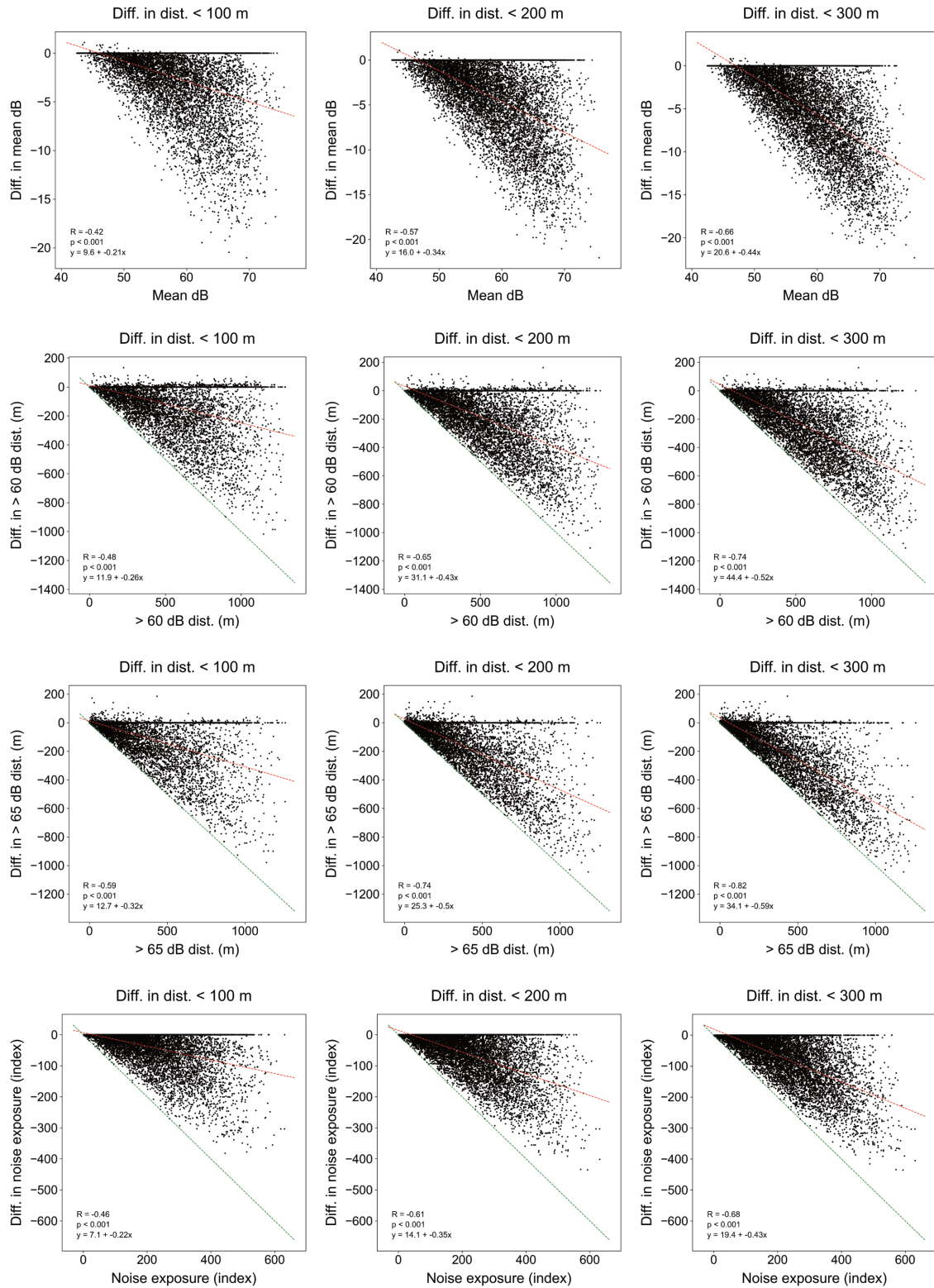


Figure 35. Regression analysis between the reductions in exposures to traffic noise on quiet paths and the traffic noise indexes of the respective shortest paths. Shortest paths within the length range of 700 m to 1300 m were selected in the analysis (as well as the respective quiet paths). The red lines represent the regression lines of the regression analysis and the green lines show the theoretical maximum reductions in the noise exposure indexes.

Table 9 and Table 10 represent the descriptive statistics of the achievable reductions in traffic noise exposure indexes ( $ER_{+65dB}$  and  $dB_{mean}$ ) for different subsets of the paths. At least three observations can be made by exploring the statistics:

- 1) Higher achievable reductions in traffic noise exposure seem to be available for longer (shortest) paths.
- 2) Higher achievable reductions in traffic noise exposure indexes were found for the initially highest noise exposures.
- 3) Higher quiet path length differences (mean and median) were found for longer shortest paths, indicating that more quiet path alternatives were found for longer O-D distances.

Since no quiet paths shorter than the maximum allowed length difference (100, 200 or 300 m) were found in many cases, the average length differences of the quiet paths were substantially lower than the allowed maximum length difference in each group. For this reason, the statistics of the real length differences of the quiet paths were also included in the table (“quiet path length difference”).

The achieved reductions in  $ER_{+65dB}$  were consistently and significantly higher for the longer paths (700–1300 m). Respectively, the mean effect of the quiet paths on  $ER_{+65dB}$  was significantly smaller for the shorter paths (300–600 m). At best, mean  $ER_{+65dB}$  could be reduced by over 50 % by taking a quiet path with length difference of 0–300 m. Similarly, the highest achievable reductions in  $dB_{mean}$  were found for the longer paths.

Table 9. Descriptive statistics of the achievable reductions in noise exposure index  $ER_{+65dB}$  on different subsets of the paths. The subsets were defined by 1) the length of the shortest path, 2) the length difference of the quiet path and 3) the initial  $ER_{+65dB}$ .

Path length (m)	Quiet path length difference (m)	Subset of paths by $ER_{+65dB}$				
		10–40 %	40–70 %	70–100 %	Difference (%) in $ER_{+65dB}$ (mean, median, SD)	
Range	Max	Mean	Median	SD		
300–600	< 100	18	0	28	-12, 0 (26)	-23, -0 (31)
300–600	< 200	44	12	58	-16, -0 (29)	-32, -26 (33)
300–600	< 300	65	21	83	-18, -0, (30)	-36, -36 (34)
700–1300	< 100	30	19	32	-21, 0 (29)	-32, -28 (31)
700–1300	< 200	75	67	63	-29, -20 (32)	-46, -49 (31)

700–1300	< 300	117	107	93	-32, -27, (33)	-53, -59 (29)	-55, -62, (27)
----------	-------	-----	-----	----	----------------	---------------	----------------

Table 10. Descriptive statistics of the achievable reductions in noise exposure index  $\text{dB}_{\text{mean}}$  on different subsets of the paths. The subsets were defined by 1) the length of the shortest path, 2) the length difference of the quiet path and 3) the initial  $\text{dB}_{\text{mean}}$ .

Path length (m)	Quiet path length difference (m)	Subset of paths by $\text{dB}_{\text{mean}}$			
		55–60 $\text{dB}_{\text{mean}}$	60–65 $\text{dB}_{\text{mean}}$	65–80 $\text{dB}_{\text{mean}}$	
Range	Max	Mean	Median	SD	Difference (dB) in $\text{dB}_{\text{mean}}$ (mean, median, SD)
300–600	< 100	19	0	29	-1.6, -0.0 (2.5)    -2.6, -0.0 (3.9)    -2.8, -0.0, (4.0)
300–600	< 200	47	16	59	-2.4, -0.5 (3.1)    -4.3, -3.0 (4.6)    -5.0, -3.6, (5.2)
300–600	< 300	72	32	86	-2.8, -1.2, (3.3)    -5.2, -5.0 (4.9)    -6.4, -5.9, (5.8)
700–1300	< 100	31	21	32	-2.3, -1.3 (2.7)    -3.5, -2.4 (3.9)    -4.5, -3.1, (4.8)
700–1300	< 200	79	75	64	-3.5, -3.0 (3.0)    -5.6, -5.3 (4.3)    -7.5, -7.7, (5.4)
700–1300	< 300	126	122	93	-4.1, -3.9, (3.2)    -6.9, -7.0 (4.3)    -9.4, -10.1, (5.4)

## 4.6 Sharing of the methods and results

All methods developed in the thesis are shared with a permissive MIT license via a public GitHub repository: <https://github.com/hellej/quiet-paths-msc>. Unfortunately, many of the data sources consisted of too big files (e.g. graph data) or had restrictive license (e.g. YKR-commuting data) and hence couldn't be shared with the source-code. However, the script for downloading and processing the OSM street network data for graph construction is included in the repository. Hence, a noise-aware OSM-based walkable street network graph can be easily generated for any area of interest, as long as traffic noise data for the given area is available. After generating a graph for the area of interest, the routing application can be run locally (as opposed to deployment to a remote server). However, before setting up a local instance of the quiet path routing application, considering running the further developed and more comprehensively documented version of it is highly recommended (see next chapter).

During the study, the quiet path routing application was developed further within the HOPE (Healthy Outdoor Premises for Everyone) project. A parallel version of the quiet path routing application was initialized by copying the source-code from: <https://github.com/hellej/quiet-paths-msc> to a new repository under the GitHub community of Digital Geography Lab: <https://github.com/DigitalGeographyLab/hope-green-path-server>. When extending the quiet path routing methods to support also other (and real-time) exposure data, the source code was also heavily refactored and further documented. Also, to enable significantly faster routing analysis for longer O-D distances, the routing analysis was migrated to utilize routing library igraph (ref.) (instead of NetworkX). The name of the concept was changed from *quiet paths* to *green paths*. The source-code for the user interface application matching the routing application is located at: <https://github.com/DigitalGeographyLab/hope-green-path-ui>. Instructions on how to get the application up and running locally were added to the README.md file at the root of the repositories. Both repositories utilize GitHub releases, that enable creating snapshots of the repositories at a specific time. At the time of writing this, the latest release for the hope-green-path-server was v1.3 and for hope-green-path-ui: v1.2. New releases of both projects will be published as they are developed further.

## 5 Discussion

### 5.1 Technical assessment – quality of the shortest paths

- One of the objectives of the thesis was to assess the performance of the quiet path routing method developed as part of the thesis. Since the defined performance of the quiet path routing included comparison of exposure to noise between the shortest and quiet paths, quality of the shortest paths needed to be assessed as well.
- The components of the analysis enabled comparison of shortest path distances to the reference paths calculated with the route planner by Helsinki Region Transport (HRT) (Table 11). Mean and median difference in shortest path distances were little ( $> -1\%$  or  $-9\text{ m}$ ) indicating that a typical shortest path calculated with the routing tool of the thesis was shorter than the corresponding path by the route planner of HRT. The standard deviation of these length differences was as high as  $16\%$  or  $74.8\text{ m}$ , suggesting that the paths calculated by the two routing tools were often significantly different in total distance. However, the  $10^{\text{th}}$  and  $90^{\text{th}}$  percentiles were still moderate,  $-58.2\text{ m}$  ( $-7.1\%$ ) and  $29\text{ m}$  ( $4.2\%$ ), showing that the difference in length was small for majority of the paths. Considering these results, it can be concluded

that the routing tool of the thesis could perform well in most situations, when using the route planner of HRT as a comparison.

- The quality assessment of the shortest path routing enabled efficiently improving the application by exploring the revealed problems in pathfinding. Where higher differences in distance were found, the paths were inspected in GIS software to catch possible faults in the routing application or in the integrated street network graph. By this method, some critical, yet rare, bugs were discovered. These were caused by having unwanted street segments, such as underground service roads, as edges in the graph. Since the few unwanted edges were not highly connected to the rest of the graph, majority of the paths calculated in the routing analysis were unaffected by them. Problems arose in situations where the closest edge to either origin or destination location was one of the unwanted ones. The graph was fixed through an iterative process consisting of the following steps: 1) revising the graph construction script, 2) if necessary, revising the application logic in routing 3) re-running the extensive routing analysis and 4) assessing the shortest path quality (as described above). Two key improvements were made to the application through this process: 1) functionalities for filtering out service tunnels and validating the graph topology were integrated as part of the graph construction script and 2) search radius and logic was adjusted in nearest edge search.

Table 11. Differences in path lengths between the calculated shortest paths and the reference paths (n=31228).

Difference to reference length	meters	%
Mean	-8.7	-0.35
Median	-4.9	-0.66
SD	74.8	16.0
p10	-58.2	-7.1
p90	29.0	4.2

- Also, the paths with length difference greater than 30 m (to a reference path) were inspected manually using GIS software to explore possible faults in shortest and quiet path routing. In some cases, either the origin or destination was matched to a different street segment whereas in other cases the difference was caused by a missing edge between the origin and destination nodes.

The identified reasons for length differences could be classified to three main types:

- 1) A different nearest edge to origin or destination was found and hence the paths differed. This was assessed also statistically by comparing the distances between respective origin and destination points of each path - reference path pair (Table 12). This might have happened due to the little differences in the graphs. Some of these differences originated from the three-dimensional alignments of the edges. Especially in some areas such as eastern Pasila, many sidewalks are located on top of each other – the lower lever having a typical street layout of streets, sidewalks and intersections as opposed to the upper level that features mainly exclusive walkways connected to each other, raised above the cars. Where the nearest edge could be matched to two overlapping walkways, at the same distance, differences between the paths from two different route planners were likely to arise.
- 2) The path took a detour around a private residential area. In HRT's route planner, also the street segments tagged as private are allowed at the start or at the end of a walk – but not as short cuts in the middle of a walk. In the quiet path routing app, all street segments tagged as private were filtered out in graph construction to prevent pathfinding through private residential areas. This is a known limitation in the app and will be fixed in the future.
- 3) The path took a detour around a walkable area. The used graph construction method did not include extraction of virtual walkable street segments from walkable areas (with polygon geometry). This can be considered an additional yet often worthwhile process in order to construct a complete walkable street network graph from OpenStreetMap data. The implementation of importing virtual street segments from walkable areas (with polygon geometry) was left outside the scope of the thesis since the quality of majority of the shortest paths was better than sufficient. Pathfinding was affected by the missing walkable areas only a little and only in some places such as around Helsinki Central Railway Station and other squares.

Table 12. Statistics of offsets (distances) between the origin and destination points of the paths and the origin and destination points of the reference paths.

Offset from reference paths'	origins (m)	destinations (m)
Mean	3.0	3.9
Median	0.5	1.3
SD	9.5	12.0

p5	0.0	0.1
p10	0.1	0.2
p90	4.4	8.5
p95	24.7	15.4

---

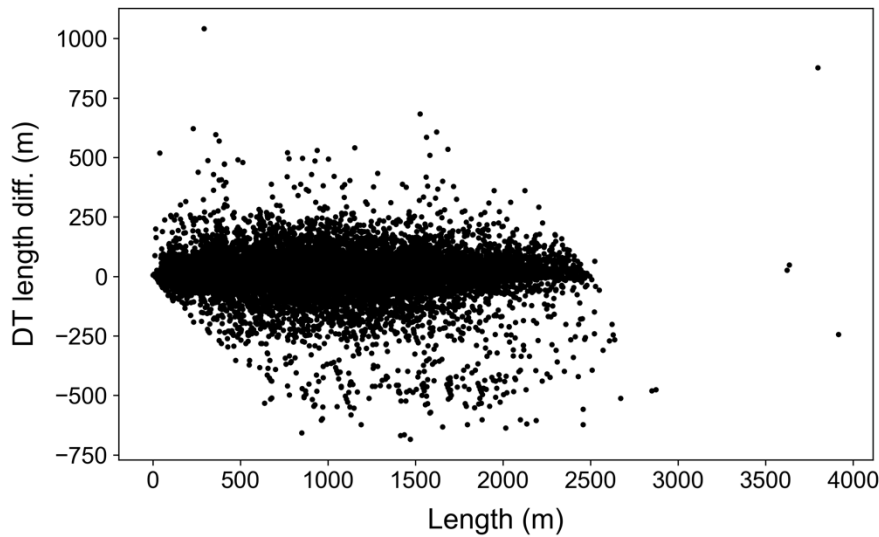


Figure 36. Path length differences (m) to reference path lengths as a function of path length.

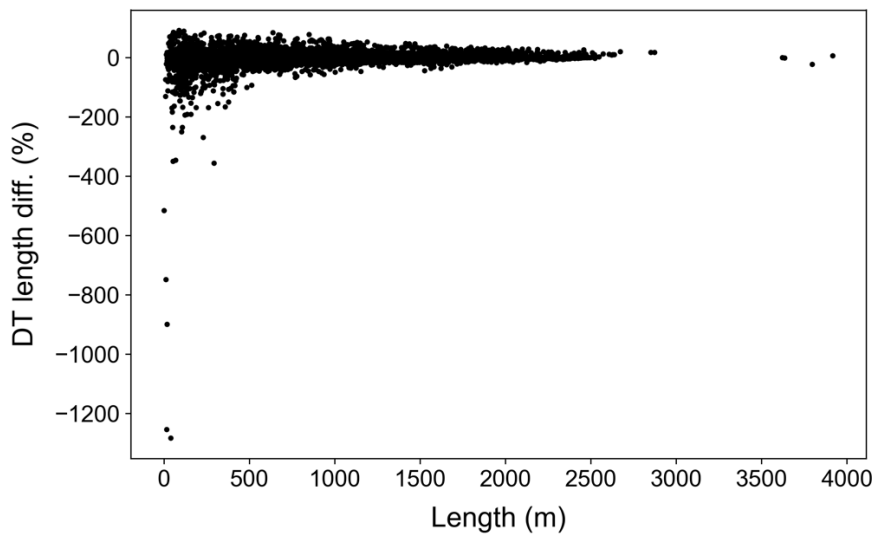


Figure 37. Differences in lengths of the paths (%) to the reference paths as a function of path length.

## 5.2 Indirect large-scale assessment of pedestrians' exposures to traffic noise can reveal unequal walking conditions

- One of the objectives of the thesis was to assess spatial patterns in pedestrians' exposure to traffic noise. As opposed to most of the previous studies where exposure to traffic noise has been assessed as a static variable (depending on home location), a more dynamic assessment was made in this study: exposure to traffic noise was addressed as a function of individuals' daily mobility.

The concept of typical local walk was defined to be the basis of the analysis. The implementation of the complete analysis required several steps:

- 1) Executing extensive public transport itinerary planning by OD commutes data using HRT's route planner public routing API.
- 2) Modeling of utilization rates of local public transport stops based on the flows of commuters and acquired itinerary plans.
- 3) Pathfinding using short & quiet path routing application between origin – PT stop pairs.
- 4) Statistical analysis of exposures to traffic noise on the paths weighted by the utilization rates of the PT stops and aggregated by the origins.

- Unsurprisingly, some distinct areal differences were found when the results were aggregated by origins. The interpretation of origin level results required adopting the concept of a “typical local walk” or an “expected walk”. These concepts were based on weighting origin level statistics of paths by their utilization rates on commutes. Hence, the following question could be answered by interpreting the exposure maps: in which locations the expected exposure to traffic noise is higher than average on a typical local walk?
- Importantly, some areas not directly exposed to high traffic noise levels seem to have highly exposed local walks. This is where the nature of this assessment is most relevant: areas with low traffic noise levels but exposed walks should be considered problematic – as walking is the very activity that exposes residents to environmental pollutants. One could argue that most buildings manage to protect residents from any harmful levels of traffic noise regardless of the prominent traffic noise levels outside. Considering this, modeling residents' daily walks and exposure to traffic noise outside the buildings becomes increasingly important aspect in assessing the health effects of traffic noise to citizens.
- In this study, the modelled local walks were based on commutes and assumption that they were made with public transport. Utilization rates, and subsequently weighted exposures to traffic noise, were assessed for shortest paths between origins and public transport. Using

other than shortest paths in the analysis would have introduced additional complexity to the methods.

- However, as pedestrians do not always take the shortest paths (due to various reasons discussed in the next chapter), the accuracy of the results about exposure to traffic noise may be limited. Due to methodological challenges and limited scope of the thesis, spatial variation in opportunities to choose quieter paths was left unassessed (but analyzed statistically for the whole study area). Yet, the presence of quiet path alternatives at any given area (within the study area) can be easily inspected with the developed quiet path route planner (web application).
- Assessing route choices of pedestrians is a separate, challenging area of research. However, this method ignores the possible arbitrary route choices of individuals: pedestrians' who know the area might actually choose quieter paths based on intuitive decision making. Some observations made in previous studies support this idea, and for an apparent reason: personal route choices (made without use of digital route planner services) tend to optimize least cost path rather than shortest path. Surely, in many cases the personal least cost path happens to be the shortest path, but by the definition it also varies arbitrarily based on individual's preferences. Based on the literature, the differences between e.g. the shortest paths and the ones chosen by cyclists are often significant. Supposedly, similar phenomena apply also to pedestrians - at least to some extent. It could even be that one does not know for sure if the chosen path is the shortest path between the OD pair, but is positive about it being short enough and otherwise reasonable.
- As the results of this thesis show, number of alternative paths increases with the distance between origin and destination. When the number of path alternatives increases, also the probability that some of them have similar total distance increases. As a consequence, choosing the very shortest path of the alternatives gets more difficult (at least if not using a route planner application) and hence other factors might start to play bigger role in the path selection. It could even be, that there is a need for concept of perceived shortness of a path – if a path is e.g. 30 m longer than the actual shortest path, but considerably more walkable, it might feel shorter than the shortest path.

### **5.3 Significant but varying reductions in traffic noise exposure can be achieved with quiet path routing**

- Performance assessment of the quiet path routing indicated that in many cases a substantial share of the total noise exposure on a shortest path could be avoided by taking an alternative quiet path. By comparing exposures to noise on large set of shortest and respective quiet paths, it was possible to quantify the mean and expected effect of the tool on exposure to noise in different situations. The assessment confirmed that the tool indeed has the potential to calculate short yet quiet paths in most situations.

Some general observations could be made by interpreting the results of the assessment:

- 1) The higher the exposure on the shortest path, the higher reduction could be achieved by taking a quiet path.
  - 2) An increased number of quiet path alternatives were found for longer OD distances.
  - 3) Quiet paths for longer OD distances performed at least slightly better (in decreasing exposure to noise) on average when compared to shorter OD distances.
- This can be regarded as the most important result of the thesis, as it reasons the use of the developed quiet path routing tool for optimizing typical walks in Helsinki. However, as benefits from choosing quieter paths are difficult to assess, the potential health effect on the citizens is hard to model. Instead, the significance of the tool can be seen more personal: citizens could choose different quiet paths depending on their individual preferences and sensitivity to noise. The importance of calculating a set of alternative quiet paths (to choose from) is discussed in the following chapter (5.4)

## **5.4 Alternative quiet paths need to be calculated to suit different situations and users with varying preferences**

- One of the key design principles of the quiet path routing tool was to allow the user to make the final decision on which path to choose. Balancing between travel time and noise exposure is a trade-off optimization that depends on both personal preferences and sensitivity to noise and hence cannot be solved using solely application logic.
- Alternative quiet paths were optimized by including a noise sensitivity coefficient in the environmental impedance function. The set of noise sensitivity coefficients used in the method resulted different weights for the noise cost of an edge, ranging from almost zero (0.1) to virtually overriding the effect of the base cost (length) in routing (40).

## 5.5 Uncertainties in exposure-response relationships challenge the environmental impedance function

- Perhaps the unexplained variance in the relationships between highly annoyed (%) and traffic noise level can be explained with dynamic exposure to traffic noise (that is not considered in the noise-annoyance studies)? (Figure 2).
- For this study, only compressed (and modelled)  $L_{Ae}$  data was available. Hence, it was not reasonable to focus much on the uncertainties in how the  $L_{Ae}$  may or may not be sufficient metric to indicate loudness or annoyance.
- Furthermore, as the literature on psychoacoustics suggests, the perceived annoyance of traffic noise is not only affected by loudness but also on various other qualities of sounds. This concerns especially lower intensities where  $L_{Ae}$  alone may be an insufficient metric (Genuit, 1999).
- As already discussed in chapter 3.5.1 , the effective differences between the two alternative noise cost functions were found small when comparing sets of quiet paths calculated with both for the same OD pair. However, if the two noise cost functions were applied in a raster-based LCP analysis, more differences would probably be found between the found quiet paths, as choosing them would not be restricted by the available route options in a graph. In a raster-based LCP model, the paths travel freely between cells of the cost surface (unless restricted areas are present). Hence, the cost surface can be thought as a graph of interconnected cells. If there is enough variance in the cost surface, the effect of the cost function will be a directive factor in pathfinding due to a large number of alternative paths (connections) between OD pairs.
- Ideally, a noise based environmental impedance function (EIF) would reflect the level of annoyance at varying noise levels. Since annoyance is a highly personal factor, defining a generally justified EIF for noise is challenging. In several studies, annoyance to noise have been found to vary significantly among individuals.
- Also, even the A-weighted SPL seem to have some limitations when used as an indicator of loudness or annoyance of sounds (Genuit, 1999; Ouis, 2001; Parmanen, 2007). Naturally, perceived loudness is a highly subjective concept which poses a great challenge in defining an environmental impedance function. Loudness can be seen as a slightly less subjective yet very relevant and was hence applied in this study. In an excellent review by (Ouis, 2001), loudness was assessed in terms of noise levels and perception. As many studies and institutions suggest, loudness can be modeled with a power law that doubles loudness at every

10 dB increase in noise level. This relationship between noise and loudness was applied in the environmental impedance function of quiet path routing method. Hence, the assigned noise costs were increasingly higher for higher decibel levels. Also, a simple linear environmental impedance function was tested as an alternative.

- Not entirely unexpectedly, the quiet paths optimized by using the latter EIF were not significantly different from the ones optimized using the EIF with power law. Instead, the used noise sensitivity coefficients (NSC) had the biggest effect on the optimized set of paths. In this study, a wide range of NSCs were used in order to ensure that enough quiet path alternatives were optimized to suit various preferences and noise sensitivities. For this reason, NSC can be seen as an important component in the EIF for noise. Having length as the base cost in EIF resulted in short paths when using low NSC values. The paths optimized with the lowest NSCs can be seen as the most interesting paths to pedestrians, considering that most of them are willing to minimize travel time as the main “cost”. Mainly two types of quiet paths were optimized with the lowest NSCs: 1) path that were similar to the shortest path to most extent and 2) paths that were almost as short as the shortest paths but considerably different in geometry and exposure to noise (quieter).
- Loudness is related to sound intensity
- Loudness and noisiness refer to perceived, annoying aspect of noise
- Loudness is subjective but annoyance is even more subjective

## **5.6 Exposure-based routing should be developed as a concept to consider multiple pollutants**

- The current quiet path routing method works arguably sufficiently for reducing exposure to one environmental pollutant. However, an interesting possibility would be to incorporate two or more environmental variables into one environmental impedance function (EIF) and thus be able to optimize “composite green paths”. The great challenge in this arises from the need to decide relative weights for different pollutants in the EIF – even if it can be a type of apples to oranges comparison, if they are considered by individuals’ perceptions and opinions (as they probably should). (Naharudin et al., 2017) demonstrated how an analytical network process (ANP) decision model combined with GIS could help determining an overall walkability scores for different parts of a network. In ANP, pairwise comparisons are done between different variables, and a cost matrix is produced to enable cost calculation using different sets and weightings of variables.

- To be able to balance between multiple exposures in routing and comparison, more sound knowledge on the health effects of them should be gained first. However, assessing the health effects of exposures to different levels of traffic noise was left outside the scope of the thesis and the focus was more on both developing the methods for assessing exposure to noise and minimizing it by routing. Negative health effects were assumed to vary from minor to moderate on a decibel range from 45 dB to 80 dB. Also, the effect was assumed to vary depending on individuals' sensitivity to noise. This approach worked well for one environmental pollutant, as the result of the routing was always a set of alternative quiet paths "to choose from". However, if another exposure-based cost was added to (composite) EIF, the relative costs of the two would have to be synchronized somehow. Using the same set of sensitivity coefficients for multiplying the both costs would not solve the issue of initially incompatible EIFs of two different pollutants but the base cost of the two should first be synchronized to reflect the real health effects of the pollutants. When the base costs of exposures to any two environmental pollutants are first synchronized, then (and only then) their relative weights can be adjusted based on set of sensitivity coefficients.
- Ideally, a composite cost function for multiple pollutants would not only consider the relative health effects of its components (e.g. noise and air quality), but also the net health effect of a path. Fundamentally, the net health effect of a walk can be addressed by modeling and comparing the positive health effects from the physical activity and the negative health effects from exposure to environmental pollutants. This problem has been identified in many studies but also regarded as very complex.
- Health effects of environmental pollutants may vary between age and other individual variables, but also temporally. The effects can be seen soon or only after cumulative exposure during e.g. 20 years.
- Furthermore, if the goal in the future is to minimize total exposure to negative health effects of the environmental variables (pollutants), net effect health of the walks should be assessed; i.e. do the positive health effects of physical activity balance out the negative health effects from the exposure to environmental pollutants during the activity? Ideally, EIF would be capable of minimizing exposure to multiple pollutants based on their health effects.

## **5.7 Publishing a green path routing application online can facilitate citizens to choose healthier paths**

- Interactive web map applications have been shown to facilitate rich exchange of information between a service and a user () .
- The goal in developing an online route planner application (based on the quiet path routing method) was to enable individuals to easily find quiet paths between arbitrary OD pairs in Helsinki and thus reduce their exposure to traffic noise.
- The design goal for the user interface of the web application was to facilitate users to both easily query short and quiet paths and compare them in terms of travel time and exposure to traffic noise. To achieve this, several statistics describing exposure to noise are shown for each path and, perhaps more importantly, colors of the paths were set to be based on the respective noise levels. Also, a noise exposure chart was added to the user interface to visualize cumulative exposures to different traffic noise levels on each path.
- Some of the advantages of using travel time to measure accessibility are obvious. Commuters often want to minimize travel time and spend more time at origin or destination. Also, travel time does not need further definition and is hence conceptually simple to use.
- However, in complex urban environments travel time even at its best an oversimplification of the perceived accessibility, especially when considering pedestrians and cyclists. Hence, terms impedance and environmental impedance have been introduced to model perceived accessibility more comprehensively. Depending on the composition, environmental impedance function can incorporate impedances from air pollution, noise pollution and greenery along with travel time.
- It has been proposed that even the concept impedance may be serious oversimplification of, as it implies that the amount of walking should be minimized by default - regardless of the conditions. While there is clearly a need for better consideration of pedestrians' perceived accessibility in accessibility research, there's only a limited number of studies aiming for it.
- While it could be argued that pedestrians (or cyclists) try to minimize their exposure to unhealthy environments, there may still be an “exposure awareness gap” as demonstrated by (Ueberham et al., 2019); people [cyclists] are not necessarily aware of the pollutant exposure on their paths.
- Taking environmental factors into account in solving the routing problem seem to have the potential to generate healthier or in other ways better walking routes (e.g. Lwin & Murayama, 2011, 2013; Quercia, Schifanella, & Aiello, 2014; Ribeiro & Mendes, 2011).

## 6 References

- Agrawal, S., & Gupta, R. D. (2017). Web GIS and its architecture: A review. *Arabian Journal of Geosciences*, 10(23), 518.
- Ahuja, R. K., Mehlhorn, K., Orlin, J., & Tarjan, R. E. (1990). Faster algorithms for the shortest path problem. *Journal of the ACM (JACM)*, 37(2), 213–223. <https://doi.org/10.1145/77600.77615>
- Alam, M. S., Perugu, H., & McNabola, A. (2018). A comparison of route-choice navigation across air pollution exposure, CO<sub>2</sub> emission and traditional travel cost factors. *Transportation Research Part D: Transport and Environment*, 65, 82–100. <https://doi.org/10.1016/j.trd.2018.08.007>
- Apparicio, P., Carrier, M., Gelb, J., Séguin, A.-M., & Kingham, S. (2016). Cyclists' exposure to air pollution and road traffic noise in central city neighbourhoods of Montreal. *Journal of Transport Geography*, 57, 63–69.
- Babisch, W., Beule, B., Schust, M., Kersten, N., & Ising, H. (2005). Traffic noise and risk of myocardial infarction. *Epidemiology*, 33–40.
- Boulos, M. N. K., Warren, J., Gong, J., & Yue, P. (2010). *Web GIS in practice VIII: HTML5 and the canvas element for interactive online mapping*. Springer.
- Brown, A. L., & Van Kamp, I. (2017). WHO environmental noise guidelines for the European region: A systematic review of transport noise interventions and their impacts on health. *International Journal of Environmental Research and Public Health*, 14(8), 873.
- Cole-Hunter, T., Morawska, L., Stewart, I., Jayaratne, R., & Solomon, C. (2012). Inhaled particle counts on bicycle commute routes of low and high proximity to motorised traffic. *Atmospheric Environment*, 61, 197–203. <https://doi.org/10.1016/j.atmosenv.2012.06.041>
- Davies, G., & Whyatt, D. (2009). A least-cost approach to personal exposure reduction. *Transactions in GIS*, 13(2), 229–246.
- Directive 2002/49/EC of the European Parliament and of the Council of 25 June 2002 relating to the assessment and management of environmental noise—Declaration by the Commission in the Conciliation Committee on the Directive relating to the assessment and management of environmental noise.* (2002, July 18). <http://data.europa.eu/eli/dir/2002/49/oj/eng>
- Gaffuri, J. (2012). Toward web mapping with vector data. *International Conference on Geographic Information Science*, 87–101.
- Genuit, K. (1999). The use of psychoacoustic parameters combined with A-weighted SPL in noise description. *INTER-NOISE and NOISE-CON Congress and Conference Proceedings*, 1999, 1887–1892.

- Goldberg, A. V., & Harrelson, C. (2005). Computing the shortest path: A search meets graph theory. *Proceedings of the Sixteenth Annual ACM-SIAM Symposium on Discrete Algorithms*, 156–165.
- Guski, R., Schreckenberg, D., & Schuemer, R. (2017). WHO environmental noise guidelines for the European region: A systematic review on environmental noise and annoyance. *International Journal of Environmental Research and Public Health*, 14(12), 1539.
- Hasenfratz, D., Arn, T., de Concini, I., Saukh, O., & Thiele, L. (2015). Health-optimal routing in urban areas. *Proceedings of the 14th International Conference on Information Processing in Sensor Networks*, 398–399.
- Helsingin kaupungin meluselvitys 2017.* (2017). <https://www.hel.fi/helsinki/fi/asuminen-jaymparisto/ymparistonsuojelu/ilmanlaatu-ja-melu/selvitys/>
- Hertel, O., Hvidberg, M., Ketzel, M., Storm, L., & Stausgaard, L. (2008). A proper choice of route significantly reduces air pollution exposure—A study on bicycle and bus trips in urban streets. *Science of the Total Environment*, 389(1), 58–70. <https://doi.org/10.1016/j.scitotenv.2007.08.058>
- International Standard ISO 226: 1987.* (n.d.). International Organization for Standardization, Geneva, Switzerland.
- Ising, H., Dienel, D., Günther, T., & Markert, B. (1980). Health effects of traffic noise. *International Archives of Occupational and Environmental Health*, 47(2), 179–190.
- Jäppinen, S., Toivonen, T., & Salonen, M. (2013). Modelling the potential effect of shared bicycles on public transport travel times in Greater Helsinki: An open data approach. *Applied Geography*, 43, 13–24. <https://doi.org/10.1016/j.apgeog.2013.05.010>
- Jarno Kokkonen, Kontkanen, O., & Maijala, P. (2016). CNOSSOS-EU Noise Model Implementation in Finland. *ResearchGate*, 38. [https://www.researchgate.net/publication/307907554\\_CNOSSOS-EU\\_Noise\\_Model\\_Implementation\\_in\\_Finland](https://www.researchgate.net/publication/307907554_CNOSSOS-EU_Noise_Model_Implementation_in_Finland)
- Jasika, N., Alispahic, N., Elma, A., Ilvana, K., Elma, L., & Nosovic, N. (2012). Dijkstra's shortest path algorithm serial and parallel execution performance analysis. *2012 Proceedings of the 35th International Convention MIPRO*, 1811–1815.
- Jonasson, H. G., & Storeheier, S. (2001). *Nord 2000. New Nordic prediction method for road traffic noise.*
- Kephalopoulos, S., Paviotti, M., & Anfosso-Lédée, F. (2012). *Common noise assessment methods in Europe (CNOSSOS-EU).*

- Kumar, P., Nigam, S. P., & Kumar, N. (2014). Vehicular traffic noise modeling using artificial neural network approach. *Transportation Research Part C: Emerging Technologies*, 40, 111–122.
- Leaflet*. (n.d.). <https://leafletjs.com/> (accessed on 23 February 2020)
- Lienert, C., Jenny, B., Schnabel, O., & Hurni, L. (2012). Current trends in vector-based Internet mapping: A technical review. In *Online maps with APIs and WebServices* (pp. 23–36). Springer.
- Lu, X. (2005). An investigation on service-oriented architecture for constructing distributed web gis application. *2005 IEEE International Conference on Services Computing (SCC'05) Vol-1*, 1, 191–197.
- Lwin, K. K., & Murayama, Y. (2011). Modelling of urban green space walkability: Eco-friendly walk score calculator. *Computers, Environment and Urban Systems*, 35(5), 408–420. <https://doi.org/10.1016/j.comenvurbsys.2011.05.002>
- Lwin, K. K., & Murayama, Y. (2013). Smart eco-path finder for mobile GIS users. *URISA Journal*, 25(2), 5–14.
- Maghelal, P. K., & Capp, C. J. (2011). Walkability: A Review of Existing Pedestrian Indices. *Journal of the Urban & Regional Information Systems Association*, 23(2).
- Miedema, H. M., & Oudshoorn, C. G. (2001). Annoyance from transportation noise: Relationships with exposure metrics DNL and DENL and their confidence intervals. *Environmental Health Perspectives*, 109(4), 409–416.
- Naharudin, N., Ahamad, M., Sanusi, S., & Sadullah, A. F. M. (2017). OPTIMIZING PEDESTRIAN-FRIENDLY WALKING PATH FOR THE FIRST AND LAST MILE TRANSIT JOURNEY BY USING THE ANALYTICAL NETWORK PROCESS (ANP) DECISION MODEL AND GIS NETWORK ANALYSIS. *International Archives of the Photogrammetry, Remote Sensing & Spatial Information Sciences*, 42.
- Nielsen, H. L. (1997). *Road traffic noise: Nordic prediction method*. Nordic Council of Ministers.
- Noto, M., & Sato, H. (2000). A method for the shortest path search by extended Dijkstra algorithm. *Smc 2000 Conference Proceedings. 2000 Ieee International Conference on Systems, Man and Cybernetics. "cybernetics Evolving to Systems, Humans, Organizations, and Their Complex Interactions" (Cat. No.0, 3, 2316–2320 vol.3.* <https://doi.org/10.1109/ICSMC.2000.886462>
- OpenLayers*. (n.d.). <https://openlayers.org/> (accessed on 23 February 2020)
- Ouis, D. (2001). ANNOYANCE FROM ROAD TRAFFIC NOISE: A REVIEW. *Journal of Environmental Psychology*, 21(1), 101–120. <https://doi.org/10.1006/jevp.2000.0187>

- Parmanen, J. (2007). A-weighted sound pressure level as a loudness/annoyance indicator for environmental sounds – Could it be improved? *Applied Acoustics*, 68(1), 58–70. <https://doi.org/10.1016/j.apacoust.2006.02.004>
- Passchier-Vermeer W, & Passchier W F. (2000). Noise exposure and public health. *Environmental Health Perspectives*, 108(suppl 1), 123–131. <https://doi.org/10.1289/ehp.00108s1123>
- PostGIS*. (n.d.). <https://postgis.net/> (accessed on 23 February 2020)
- Pucher, J., & Buehler, R. (2010). Walking and cycling for healthy cities. *Built Environment*, 36(4), 391–414.
- Qiu, G., & Chen, J. (2018). Web-based 3D map visualization using WebGL. *2018 13th IEEE Conference on Industrial Electronics and Applications (ICIEA)*, 759–763.
- Quercia, D., Schifanella, R., & Aiello, L. M. (2014). The shortest path to happiness: Recommending beautiful, quiet, and happy routes in the city. *Proceedings of the 25th ACM Conference on Hypertext and Social Media*, 116–125.
- Recio, A., Linares, C., Banegas, J. R., & Díaz, J. (2016). Road traffic noise effects on cardiovascular, respiratory, and metabolic health: An integrative model of biological mechanisms. *Environmental Research*, 146, 359–370. <https://doi.org/10.1016/j.envres.2015.12.036>
- Ribeiro, P., & Mendes, J. F. (2011). Route planning for soft modes of transport: Healthy routes. *WIT Transactions on The Built Environment*, 116, 677–688.
- Ribeiro, P., & Mendes, J. F. (2013). Healthy routes for active modes in school journeys. *International Journal of Sustainable Development and Planning*, 8(4), 591–602.
- Sharker, M. H., Karimi, H. A., & Zgibor, J. C. (2012). Health-optimal routing in pedestrian navigation services. *Proceedings of the First ACM SIGSPATIAL International Workshop on Use of GIS in Public Health*, 1–10.
- Sheng, N., & Tang, U. W. (2011). Spatial Analysis of Urban Form and Pedestrian Exposure to Traffic Noise. *International Journal of Environmental Research and Public Health*, 8(6), 1977–1990. <https://doi.org/10.3390/ijerph8061977>
- Stevens, S. S. (1960). The psychophysics of sensory function. *American Scientist*, 48(2), 226–253.
- Su, J. G., Winters, M., Nunes, M., & Brauer, M. (2010). Designing a route planner to facilitate and promote cycling in Metro Vancouver, Canada. *Transportation Research Part A: Policy and Practice*, 44(7), 495–505. <https://doi.org/10.1016/j.tra.2010.03.015>
- Tainio, M., de Nazelle, A. J., Götschi, T., Kahlmeier, S., Rojas-Rueda, D., Nieuwenhuijsen, M. J., de Sá, T. H., Kelly, P., & Woodcock, J. (2016). Can air pollution negate the health benefits of cycling and walking? *Preventive Medicine*, 87, 233–236. <https://doi.org/10.1016/j.ypmed.2016.02.002>

- Toivonen, T., Salonen, M., Tenkanen, H., Saarsalmi, P., Jaakkola, T., & Järvi, J. (2014). Joukkoliikenteellä, autolla ja kävelien: Avoin saavutettavuusaineisto pääkaupunkiseudulta. *Terra* 126 (2014): 3.
- Torija, A. J., & Flindell, I. H. (2015). The subjective effect of low frequency content in road traffic noise. *The Journal of the Acoustical Society of America*, 137(1), 189–198. <https://doi.org/10.1121/1.4904542>
- Ueberham, M., Schlink, U., Dijst, M., & Weiland, U. (2019). Cyclists' Multiple Environmental Urban Exposures—Comparing Subjective and Objective Measurements. *Sustainability*, 11(5), 1412. <https://doi.org/10.3390/su11051412>
- Van Kempen, E., Casas, M., Pershagen, G., & Foraster, M. (2018). WHO environmental noise guidelines for the European region: A systematic review on environmental noise and cardiovascular and metabolic effects: a summary. *International Journal of Environmental Research and Public Health*, 15(2), 379.
- Veenendaal, B., Brovelli, M. A., & Li, S. (2017). Review of web mapping: Eras, trends and directions. *ISPRS International Journal of Geo-Information*, 6(10), 317.
- WHO Europe. (2018). *Environmental noise guidelines for the European Region*. [http://www.euro.who.int/\\_\\_data/assets/pdf\\_file/0008/383921/noise-guidelines-eng.pdf?ua=1](http://www.euro.who.int/__data/assets/pdf_file/0008/383921/noise-guidelines-eng.pdf?ua=1)
- Whyatt, J. D., Pooley, C., Coulton, P., Moser, M., Bamford, W., & Davies, G. (2007). Estimating personal exposure to air pollution on the journey to and from school using GPS, GIS and mobile phone technology. *11th International Conference on Harmonisation within Atmospheric Dispersion Modelling for Regulatory Purposes*, 1, 2–5.

# ACKNOWLEDGEMENTS

I would like to thank all of those who helped me to finish this thesis. To be continued...

# APPENDICES

## Appendix 1

The description of the Python environment as in <https://github.com/hellej/quiet-paths-msc/blob/master/src/env-gis-flask.yml>

```
name: gis-flask
channels:
  - conda-forge
  - defaults
dependencies:
  - python=3.6
  - jupyterlab
  - pylint
  - pytest
  - geopandas
  - osmnx
  - gdal
  - geoplot
  - pysal
  - flask
  - flask-cors
  - flask-testing
  - gunicorn
  - requests
  - pip
  - pip:
    - pycrs
    - polyline
```